Deep–Sea Research I 221 (2025) 104514

Contents lists available at ScienceDirect

Deep-Sea Research Part I

journal homepage: www.elsevier.com/locate/dsri

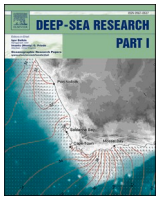

The hanging gardens of Blanes Canyon, Northwestern Mediterranean Sea

Meri Bilan [a,b,*], Jordi Grinyó [c], Cecilia Cabrera [d], Andrea Gori [e,f], Andreu Santín [d,g], Veerle A.I. Huvenne [h], Marie-Claire Fabri [i], Marta Arjona-Camas [j], Sarah Paradis [k], Claudio Lo Iacono [d], Stefano Ambroso [d], Ruth Durán [d], Stefano Piraino [a,l,m], Sergio Rossi [a,n], Pere Puig [d]

[a] Università del Salento, Dipartimento di Scienze e Tecnologie Biologiche e Ambientali, Campus Ecotekne, 73100, Lecce, Italy
[b] Dalhousie University, Department of Oceanography, 1355 Oxford Street, Halifax, NS, B3H 4R2, Canada
[c] NIOZ Royal Netherlands Institute for Sea Research, P.O. Box 53, 1790, AB, Den Burg, the Netherlands
[d] Institut de Ciències del Mar, Consejo Superior de Investigaciones Científicas (ICM-CSIC), Pg. Marítim de la Barceloneta 37-49, 08003, Barcelona, Spain
[e] Universitat de Barcelona (UB), Departament de Biologia Evolutiva, Ecologia i Ciències Ambientals, Av. Diagonal 643, 08028, Barcelona, Spain
[f] Institut de Recerca de la Biodiversitat (IRBio), Universitat de Barcelona (UB), Barcelona, Spain
[g] Centro Interdisciplinar de Investigação Marinha e Ambiental (CIIMAR), Portugal
[h] Ocean BioGeosciences, National Oceanography Centre, European Way, Southampton, SO14 3ZH, United Kingdom
[i] Ifremer, Centre de Méditerranée, La Seyne sur Mer, 83500, France
[j] Universitat de Barcelona, Departament Dinàmica de la Terra i de l'Oceà, Facultat de Ciències de la Terra, C/Martí i Franquès, s/n. 08028 Barcelona, Spain
[k] Environmental Physics, Institute of Biogeochemistry and Pollutant Dynamics, ETH Zurich, Zürich, Switzerland
[l] CoNISMa, Consorzio Nazionale Interuniversitario per le Scienze del Mare, Roma, 00196, Italy
[m] NBFC, National Biodiversity Future Center, 90133, Palermo, Italy
[n] Instituto de Ciências do Mar, LABOMAR, Universidade Federal do Ceará, Fortaleza, 60165-081, Brazil

ARTICLE INFO

Keywords:
Submarine canyons
Cold-water corals
Megabenthic assemblages
Hydrography
Nepheloid layers
Spatial heterogeneity

ABSTRACT

Submarine canyons are ubiquitous geomorphic features found intercepting the continental margins. As such, they provide environmental conditions suitable for many suspension feeding organisms, as they settle on steep rocky canyon walls, whilst taking advantage of increased currents that bring suspended organic matter and food. Additionally, demersal fishing grounds can be found surrounding submarine canyons where it can negatively affect species inhabiting these environments, including vulnerable ecosystems such as cold-water corals (CWCs). In order to understand the impacts of demersal fisheries in CWC communities, we first need to understand their distribution, species composition and vulnerability. Blanes Canyon is an example of a submarine canyon surrounded by demersal fishing grounds, where baseline knowledge on CWCs currently lacks. This study contributes to filling these knowledge gaps by using a dense grid of ROV transects along the canyon, high resolution bathymetry data and CTD surveys, which altogether provide a quantitative description of megabenthic assemblages. Blanes Canyon hosts at least 12 CWC species within 450–1300 m depth range, mainly inhabiting the steep canyon walls. Different assemblages of CWC species were found. *Desmophyllum dianthus* was the most abundant species, found throughout the entire canyon. Colonial scleractinian species (*Desmophyllum pertusum* and *Madrepora oculata*) were found in the canyon head but were lacking in the eastern canyon branch, where octocorals (*Muriceides lepida*) and black corals (*Leiopathes glaberrima*) were prevailing. Detailed CTD survey indicated that nepheloid layers (bottom and intermediate) were found at the same depth range as the megabenthic communities, since they provide suspension feeders with particulate organic matter (POM). Overall, this study confirms Blanes Canyon as a CWC habitat, providing densities and spatial distribution of different megabenthic species, along with information of their environmental niches.

* Corresponding author. Università del Salento, Dipartimento di Scienze e Tecnologie Biologiche e Ambientali, Campus Ecotekne, 73100, Lecce, Italy.
E-mail addresses: meribilan@gmail.com, mbilan@dal.ca (M. Bilan).

https://doi.org/10.1016/j.dsr.2025.104514
Received 19 November 2024; Received in revised form 29 April 2025; Accepted 5 May 2025
Available online 8 May 2025

1. Introduction

Submarine canyons are important features dramatically incising continental margins and oceanic islands (Harris and Whiteway, 2011; Vetter et al., 2010). They are interruptions to the open slope environment, thus changing the local current and sediment dynamics, increasing spatial heterogeneity (Palanques et al., 2005; De Leo et al., 2010, 2014; Puig et al., 2014; Fernandez-Arcaya et al., 2017; Appah et al., 2020). Within canyons, enhanced hydrodynamics such as upwelling/downwelling of water masses as well as internal waves and eddies have been recorded with variable spatial and temporal frequency (Ahumada-Sempoal et al., 2013; Puig et al., 2014; De Leo and Puig, 2018; Pearman et al., 2023). Additionally, the variable sedimentary, hydrodynamic and tectonic settings within canyons provide different substrata. Soft substratum is often found along the canyon axis and gentle canyon flanks, while steeper canyon walls, often coinciding with tectonic lineaments, are composed of a mixture of hard and soft substrata, depending on the steepness and the prevailing sedimentary dynamics (McClain and Barry, 2010). Submarine canyons have been recognized as biodiversity hotspots, as the complex interaction of the above-mentioned environmental conditions increases the variability and diversity of ecological niches, which are populated by different species (De Leo et al., 2010, 2014).

Cold-water corals (CWCs) are recognized as one the most important habitat-forming species inhabiting submarine canyons (Henry and Roberts, 2017; Rueda et al., 2019). The records of presence and extent of CWC distribution on these features are increasing yearly at a worldwide scale, as the widespread use of ROVs (Remoted Operated Vehicles) and other technological advancements allow for an easier access to challenging environments, such as canyon walls (Huvenne et al., 2011; Huvenne and Davies, 2014; Robert et al., 2015, 2019; Fabri et al., 2022; Pearman et al., 2023). CWCs can form dense mono- or multi-specific assemblages, which provide shelter, feeding and/or mating grounds for a myriad of associated taxa, including sponges, molluscs, crustaceans, echinoderms and fish (Mortensen and Buhl-Mortensen, 2005; D'Onghia, 2019; Guilloux et al., 2010; Henry and Roberts, 2017; Corbera et al., 2019; Santín et al., 2021a). CWCs are slow-growing, long--living, and structurally complex animals, making them vulnerable to anthropogenic impacts. They are included in conservation and management schemes, largely because of the official classification of some deep-sea species as indicator species of Vulnerable Marine Ecosystems (VMEs) by the FAO (FAO, 2009, 2016) and regionally relevant General Fisheries Commission for the Mediterranean (GFCM) (General Fisheries Commission for the Mediterranean, 2018), with the aim of protecting ecosystems of high biological and economical value with regards to fisheries (UNGA, 2007; FAO, 2009, 2016; Hall-Spencer and Stehfest, 2009; Christiansen, 2010; CBD, 2014; Otero et al., 2017; Grady et al., 2020).

In the Mediterranean Sea, there has been a significant increase in knowledge on CWCs occurrence and distribution, especially in the last 20 years (Tursi et al., 2004; Orejas and Jiménez, 2019; Taviani et al., 2019; Corbera et al., 2019; Gori et al., 2023). Several areas of their occurrence were identified as CWC provinces, including the submarine canyons of the Gulf of Lion and Catalan margin (Taviani et al., 2005; Gori et al., 2013; Fabri et al., 2014; Lastras et al., 2016; Lo Iacono et al., 2018; Chimienti et al., 2019; Giusti et al., 2019; Puig and Gili, 2019; Aymà et al., 2019; Ciuffardi et al., 2023; Santín et al., 2020, 2021a). Those canyons fall in the North-western Mediterranean Benthic Ecosystems area, which extends over 196,000 km^2 along the coast of NW Mediterranean up to 2500 m depth and is identified as an Ecologically or Biologically Significant Area (EBSA) (CBD, 2014). The area coincides with important fishing grounds, mainly for bottom trawling (Puig et al., 2012; Eigaard et al., 2017). Immediate impact caused by bottom trawling is direct or partial removal of organisms, including untargeted species (Grehan et al., 2004; Althaus et al., 2009; Gorelli et al., 2016). Entangled fishing gears can be either left *in situ* or transported from shallower parts into the canyons (Giusti et al., 2019; Hernandez et al., 2022). Lastly, bottom trawling activities cause the resuspension of bottom sediments, consequently increasing suspended sediment concentrations (SSC), enhancing the formation of bottom and intermediate nepheloid layers and ultimately, the increased SSC can also increase sedimentation rates (Arjona-Camas et al., 2019, 2021; Martín et al., 2014a, 2014b; Paradis et al., 2018, 2021). All these impacts can negatively affect CWCs and associated species. Due to the technological limitations to access deep-sea environments, most canyons still need to be mapped at high resolution, while knowledge of deep-sea assemblage distribution and environmental drivers within canyons still relies on spatially constricted or isolated studies (Harris and Baker, 2020). On the other hand, due to their vulnerability to anthropogenic impacts, there is an urgent need to identify and characterise existing areas of CWC distribution, among other deep-sea ecosystems, in order to understand their role as ecosystem services providers and address appropriate regulation for their conservation including informing spatial management plans (Ragnarsson et al., 2017; Elsler et al., 2022; Gaill et al., 2022; Levin et al., 2022).

Blanes Canyon has been studied from the geological (Lastras et al., 2011; Canals et al., 2013; Durán et al., 2013; Paradis et al., 2018; Cabrera et al., 2024) and oceanographical (Flexas et al., 2008; Zúñiga et al., 2009; Ahumada-Sempoal et al., 2013) perspective, as well as its role harbouring commercial species (Ramirez-Llodra et al., 2010) and meiofauna (Ingels et al., 2013; Román et al., 2019). Sporadic occurrences of CWCs in Blanes Canyon were previously reported (Zabala et al., 1993; Aymà et al., 2019; Santín et al., 2020, 2021b), however their extent, diversity and densities, as well as the factors affecting these, were not addressed until now.

This study provides a more comprehensive knowledge baseline on diversity and distribution of CWC assemblages found on canyon walls of Blanes Canyon. Using a dense grid of ROV transects along the canyon within a depth range of 450–1300 m, along with high-resolution bathymetry and hydrography data, we explored the composition of CWC assemblages and the main environmental drivers of their distribution in Blanes Canyon.

2. Materials and methods

2.1. Study area

Blanes Canyon is located in the North-western Mediterranean Sea, on the Catalan continental margin (Fig. 1). It is oriented mostly in a N-S direction, with 16.2 km incision length (Canals et al., 2013; Cabrera et al., 2024).

Blanes Canyon tip is located only 4 km from shore at 70 m depth from which two canyon flanks separate. The eastern flank has a gentler slope dominated by slides and toe gullies, while the western flank is steeper, characterized by a network of rim gullies (Cabrera et al., 2024). The canyon axis is characterised by soft sediments, mostly silt and clay (Paradis et al., 2018). The main current in the area is the Northern Current (or Liguro-Provencal-Catalan Current) that flows cyclonically along the Northwestern Mediterranean continental margin as a wide band (30–50 km), moving the entire water column (Font et al., 1994; Millot, 1999). Downwelling and upwelling events in the canyon are proposed to be influenced by the meandering of the Northern Current within the canyon (Flexas et al., 2008; Ahumada-Sempoal et al., 2013). These events, along with other processes such as dense shelf water cascading (Canals et al., 2006; Puig et al., 2008) and eastern storms, bring organic matter and sediment to deep waters in the canyon, usually in uneven frequency and intensity (Sanchez-Vidal et al., 2012; Lopez--Fernandez et al., 2013a, 2013b; Pedrosa-Pàmies et al., 2013). However, intense and frequent bottom trawling-induced sediment transport events occurring on the canyon rims and flanks (Palanques et al., 2024) additionally contributes to the sediment dynamics of the canyon by increasing the sedimentation rates in the canyon axis, especially in the

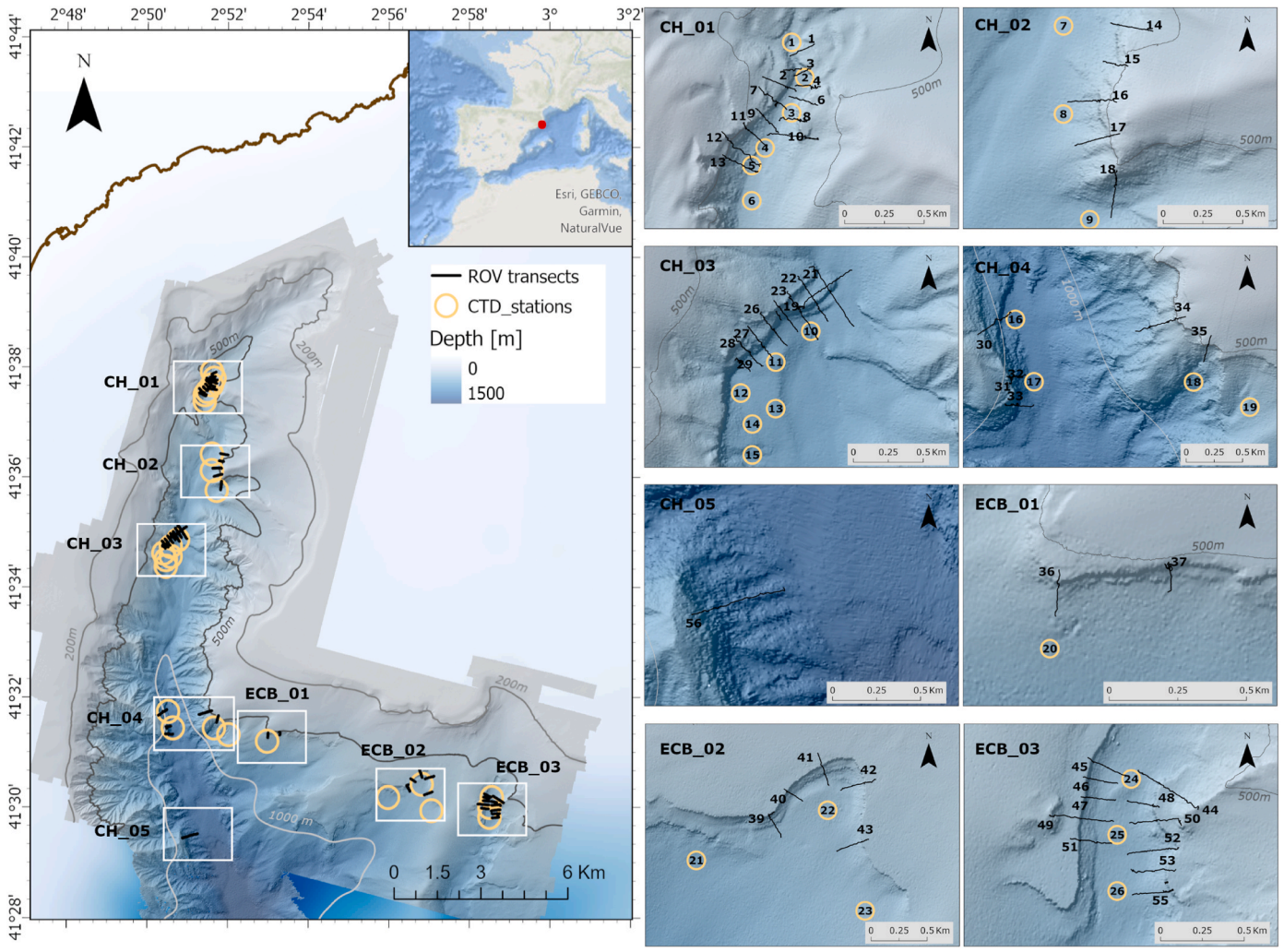

Fig. 1. Blanes Canyon shown with 5-m resolution bathymetry (WGS 84/UTM zone 31N) with ROV transects and CTD stations from ABRIC-1 cruise presented in detail for study sites: CH01, CH02, CH03, CH04, CH05, ECB01, ECB02 and ECB03. Abbreviations: canyon head (CH) and eastern canyon branch (ECB).

upper canyon axis (Paradis et al., 2018), as well as increasing the levels of suspended sediment concentration in the water column and the downward particle fluxes (Lopez-Fernandez et al., 2013b). Additionally, trawling might have smoothened part of the western canyon rim since it coincides with known trawling grounds (Cabrera et al., 2024), similar to the processes described in the fishing grounds of the neighbouring Palamós (or La Fonera) Canyon (Puig et al., 2012).

2.2. Bathymetric survey

A swath bathymetric survey of the upper reaches of Blanes Canyon was acquired during the ABRIC-3 cruise in April–May 2021 on board R/V *Ramón Margalef*. Details regarding equipment used and data processing are described in Cabrera et al. (2024), and the digital elevation model of the section of Blanes Canyon used in this study was gridded to 5-m resolution, while the backscatter data was provided at 10-m resolution.

2.3. ROV survey

A series of video transects were performed during the ABRIC-1 cruise in February 2020, during fishing closure, on board the R/V *Sarmiento de Gamboa* using the ROV *Liropus*. The ROV was equipped with an HD Kongsberg OE14-502A camera, depth and altimeter sensors, compass, two parallel lasers 10 cm apart, two manipulators, one suction system and two bioboxes. ROV positioning was tracked almost every second with a HiPAP 350P Simrad USBL acoustic system and recorded using the HYPACK software.

A total of 56 video transects were successfully recorded covering a depth range from 451 to 1305 m depth (Fig. 1, Table 1). Survey effort was concentrated in three study sites in the canyon characterized by the presence of steep canyon walls, with the aim of collecting high-density video transects, separated ~100 m between them: upper canyon head (CH01) with 13 transects, lower canyon head (CH03) with 11 transects and eastern canyon branch (ECB03) with 12 transects (Fig. 1, Table 1). Additionally, less dense and more spaced video transects were also acquired in other parts of the canyon showing steep terrains along the canyon head: CH02 (5 transects), CH04 (6 transects) and CH05 (1 transect); and along the eastern canyon branch: ECB01 (2 transect) and ECB02 (6 transects), to provide a larger view of the CWC distribution and associated megabenthic assemblages present on canyon walls of Blanes Canyon (Fig. 1, Table 1). All transects started at the foot of the canyon walls, at the deepest point of the transect, and continued upslope, until reaching flat terrain. Length of the transects was calculated as a sum of distances between each second of transect based on x, y and z (WGS 84/UTM 31N). On average 4 transects were performed in a single ROV dive (Table 1).

Table 1
Details on ROV video transects performed during ABRIC 1 cruise in Blanes canyon, in the canyon head (CH) and eastern canyon branch (ECB).

Transect number	Dive start date (dd/mm/yy)	Study site	Centre point latitude	Centre point longitude	Depth range (m)	Duration	Length (m)
1	17/02/20	CH01	41.632	2.861	576–623	37 min	240
2	17/02/20	CH01	41.630	2.860	564–628	48 min	228
3	17/02/20	CH01	41.630	2.861	574–627	28 min	202
4	17/02/20	CH01	41.629	2.861	544–629	58 min	430
5	17/02/20	CH01	41.630	2.859	529–633	58 min	357
6	17/02/20	CH01	41.629	2.861	527–636	50 min	328
7	18/02/20	CH01	41.629	2.859	524–640	53 min	473
8	18/02/20	CH01	41.628	2.860	529–645	59 min	422
9	18/02/20	CH01	41.628	2.858	518–647	1h 12 min	367
10	18/02/20	CH01	41.627	2.860	529–647	1h 31 min	625
11	18/02/20	CH01	41.627	2.857	487–651	1h 3 min	383
12	19/02/20	CH01	41.626	2.856	451–655	1h 3 min	545
13	19/02/20	CH01	41.625	2.856	481–656	1h 17 min	424
14	24/02/20	CH02	41.607	2.865	519–657	45 min	365
15	23/02/20	CH02	41.605	2.864	487–632	1h 11min	332
16	23/02/20	CH02	41.603	2.862	464–697	1h 2 min	543
17	23/02/20	CH02	41.601	2.863	455–656	1h 8 min	420
18	23/02/20	CH02	41.598	2.864	515–716	1h 22 min	645
19	24/02/20	CH03	41.584	2.847	729–866	1h 30 min	597
20	25/02/20	CH03	41.583	2.845	726–758	1h 18 min	476
21	14/02/20	CH03	41.584	2.848	784–867	1h 23 min	810
22	14/02/20	CH03	41.583	2.846	748–864	1h 23 min	629
23	14/02/20	CH03	41.582	2.845	679–870	1h 27 min	721
24	14/02/20	CH03	41.582	2.844	653–843	1h 2 min	586
25	15/02/20	CH03	41.582	2.843	696–770	40 min	228
26	15/02/20	CH03	41.581	2.843	613–830	1h 22 min	615
27	15/02/20	CH03	41.580	2.842	662–829	1h 3 min	584
28	15/02/20	CH03	41.580	2.840	622–828	1h 15 min	637
29	16/02/20	CH03	41.579	2.840	693–826	50 min	469
30	25/02/20	CH04	41.529	2.840	749–1146	2h 22 min	820
31	25/02/20	CH04	41.524	2.842	744–1168	1h 18 min	659
32	28/02/20	CH04	41.524	2.842	792–820	45 min	429
33	28/02/20	CH04	41.522	2.842	828–1190	2h 7 min	785
34	26/02/20	CH04	41.529	2.857	469–874	3h 26 min	1005
35	26/02/20	CH04	41.527	2.862	463–717	48 min	453
36	26/02/20	ECB01	41.522	2.883	516–610	32 min	251
37	27/02/20	ECB01	41.523	2.888	490–591	59 min	418
38	23/02/20	ECB02	41.507	2.941	606–613	23 min	156
39	23/02/20	ECB02	41.506	2.941	605–704	58 min	359
40	22/02/20	ECB02	41.508	2.943	580–654	1h 59 min	364
41	22/02/20	ECB02	41.510	2.947	547–659	49 min	408
42	22/02/20	ECB02	41.509	2.950	570–675	1h 24 min	483
43	22/02/20	ECB02	41.504	2.950	616–699	56 min	385
44	19/02/20	ECB03	41.502	2.979	538–700	1h 52 min	675
45	19/02/20	ECB03	41.504	2.974	621–702	54 min	328
46	19/02/20	ECB03	41.503	2.974	626–703	43 min	268
47	20/02/20	ECB03	41.502	2.973	630–706	49 min	298
48	19/02/20	ECB03	41.502	2.977	633–717	1h 20 min	350
49	20/02/20	ECB03	41.501	2.972	568–721	59 min	523
50	20/02/20	ECB03	41.501	2.979	571–726	2 h 46 min	718
51	20/02/20	ECB03	41.500	2.973	636–734	50 min	388
52	20/02/20	ECB03	41.499	2.978	636–745	55 min	436
53	20/02/20	ECB03	41.498	2.978	640–751	35 min	417
54	21/02/20	ECB03	41.497	2.979	647–687	37 min	230
55	21/02/20	ECB03	41.497	2.978	622–755	51 min	574
56	28/02/20	CH05	41.491	2.850	829–1305	1h 59 min	944

2.4. CTD survey and water sample analyses

2.4.1. CTD casts

After each ROV dive, three CTD casts were performed in the explored study site (Fig. 1, Table 2) using a SeaBird SBE 911 equipped with a fluorometer, turbidity, oxygen, and pH sensor. The CTD was coupled to a SBE 32 Carousel Water Sampler Frame with 24 12-L Niskin bottles. Water sampling was conducted using one CTD cast per day, typically the final cast of the day (Table 2), where water samples were taken at 5, 50, 100 and 200 m above bottom (mab) as well as at the chlorophyll maximum (Chl Max) depth to quantify nutrients, suspended particulate matter (SPM), particulate organic nitrogen (PON), particulate organic carbon (POC), total lipids (TL) (except for the chlorophyll maximum depth) and chlorophyll *a* (Chl a) (only for the chlorophyll maximum depth). CTD casts were processed with SBE Data Processing software following the software manual and *oce* package (Kelley et al., 2022) in R 4.2.2 (R Core Team, 2022). Turbidity measurements, recorded in FTU (Formazine Turbidity Units) were converted to excess suspended sediment concentration (SSC_{exe}, in mg L^{-1}) following Puig et al. (2013), and using the slope of the regression line derived experimentally based on canyon axis sediments from the neighbouring Palamós Canyon (SSC_{exe} = 1.14 FTU (R^2 = 0.99)) (Arjona-Camas et al., 2021).

2.4.2. Water sample chemical analyses

At each sampling depth (see 2.3), 50 ml water sample were filtered to 0.22 μm and taken for quantification of nutrients (ammonium, nitrite, nitrate, phosphate, and silicate), which were stored at −20 °C until analysis. The samples were thawed before processing with Continuous-

Table 2
Details on CTD casts performed during ABRIC 1 cruise.

CTD cast number	Date (dd/mm/yy)	Study site	Latitude	Longitude	Max depth (m)	Water sampling
1	18/02/20	CH01	41.632	2.860	611	
2	18/02/20	CH01	41.630	2.861	622	
3	18/02/20	CH01	41.628	2.860	633	x
4	19/02/20	CH01	41.626	2.858	643	
5	19/02/20	CH01	41.625	2.857	648	
6	19/02/20	CH01	41.623	2.857	651	x
7	25/02/20	CH02	41.607	2.860	712	x
8	25/02/20	CH02	41.602	2.860	708	
9	25/02/20	CH02	41.596	2.862	721	
10	15/02/20	CH03	41.581	2.846	857	x
11	15/02/20	CH03	41.579	2.843	823	
12	15/02/20	CH03	41.577	2.840	831	
13	16/02/20	CH03	41.576	2.843	844	
14	16/02/20	CH03	41.575	2.841	832	x
15	16/02/20	CH03	41.573	2.841	858	
16	26/02/20	CH04	41.529	2.842	1152	
17	26/02/20	CH04	41.524	2.844	1174	x
18	28/02/20	CH04	41.524	2.861	883	
19	28/02/20	CH04	41.522	2.867	712	x
20	28/02/20	ECB01	41.520	2.883	657	
21	23/02/20	ECB02	41.503	2.933	783	
22	23/02/20	ECB02	41.507	2.947	663	x
23	23/02/20	ECB02	41.499	2.951	685	
24	20/02/20	ECB03	41.503	2.976	694	
25	20/02/20	ECB03	41.500	2.975	722	x
26	20/02/20	ECB03	41.497	2.975	749	

Flow Analysis AutoAnalyzer 3 (Seal Analytical).

Collected water was filtered on board onto pre-weighted 47 mm GF/F filters, rinsed with Milli-Q to remove salts, and afterwards immediately frozen at −20 °C until analysis. At each sampling depth, water samples were collected and filtered through three different filters for specific analysis: SPM, POC, PON were measured using the first filter; TL were analysed with the second filter; Chl a was determined using the third filter. For each of these analyses, triplicate samples were collected to ensure reliability and statistical significance of the results. Volumes filtered varied based on designated analysis, so for SPM and subsequent elemental analysis (POC and PON) 8.0 ± 0.85 L (mean ± SD) were filtered, for TL 7.8 ± 0.45 L and for Chl a 5 L were filtered. These volumes were chosen to minimize the effort while ensuring sufficient material for analysis. SPM was quantified for all samples by subtracting the initial weight of the filter before filtration, from the weight measured after drying the filters in an oven at 36 °C for 48h. Before elemental analysis, filters underwent acidification through fumigation according to Yamamuro and Kayanne (1995) and Kiriakoulakis et al. (2011). The filters were stored during 24 h at room temperature in a tight-shut chamber containing a 10 ml beaker with 12N HCl, which produced an acid-fumed atmosphere to remove carbonates. After removing the filters from the acid atmosphere, they were kept in a fume hood during 6 h and transferred to an oven at 36 °C where they were kept for 48 h before being shipped for elemental analysis in sterile 2.5 ml Eppendorf vials. Carbon and nitrogen were quantified with a FlashEA1112 elemental analyser (ThermoFinnigan), equipped with a MAS200R autosampler, based on ¼ of a filter. The values obtained were corrected for the whole filter based on dried filter weight after filtration.

Total lipids were quantified by leaving the filters in 6 ml of chloroform–methanol (2:1) overnight followed by spectrophotometric quantification using cholesterol as a standard (Barnes and Blackstock, 1973). Chl a content was measured with a sensitive fluorometer following extraction with 85 % acetone (Yentsch and Menzel, 1963).

Data from filtered seawater (Chl a, SPM, PON, POC and TL) was standardized based on the volume used. Additionally, PON and POC concentrations were converted to molar by dividing with their respective elemental molar mass, to obtain C/N molar ratio.

2.5. Video analysis

Quantitative video analysis applied in this study followed the methodology by Gori et al. (2011) and Grinyó et al. (2018). The video transects were analysed in continuity with video annotation performed in Adobe Premiere Pro (2020). The analysis was constrained to a 1 m wide strip of seabed which was in line with, centred around and measured with the ROV mounted lasers located 10 cm apart. To facilitate annotation within that 1 m strip, A Ruler for Windows (version 3.4) was used simultaneously with the video. Following data was annotated for each second of the video: morphospecies and number of individuals, substrata type category, video sequence category, number of trawl marks, litter and number of litter items and type of interaction with fauna (e.g., attachment, entanglement). Video sequence category was annotated in order to identify segments of the video that will not be useful for megafaunal analysis such as bad visibility (too far away from the seabed or very high turbidity), stopped ROV (either at bottom or midwater, including sampling) or ROV moving sideways, opposed to segments of the video that will be used (referred as good sequence), where the ROV is moving at a uniform velocity, close to the seabed with good visibility.

2.5.1. Benthic morphospecies

To aid morphospecies annotations, an identification guide was assembled for recognizable (>3 cm) megafauna, which were identified to the lowest possible taxonomic level (Supplementary Material S1). For some morphospecies, where only the phylum level could be identified, descriptive morphospecies names were used. Photo grabs were taken along entire transects for *Desmophyllum dianthus* (Esper, 1794) to accurately count the individuals in ImageJ (version 1.53) since it could reach high densities, and it was difficult to distinguish live and dead individuals in constant video annotation (highlighted in Fig. 2A and B). Photo grabs were also taken for *Desmophyllum pertusum* (Linnaeus, 1758) and *Madrepora oculata* Linnaeus, 1758 to determine colony size and orientation following Gori et al. (2013). Colony sizes were estimated using the diameter of the colony and classified in one of four categories: small (<10 cm), medium (10–20 cm), large (20–40 cm) and very large (>40 cm) (Gori et al., 2013). Additionally, colony direction was estimated based on where the living part of the colony was facing and classified in one of four categories: facing upwards (0°), facing horizontally (90°), facing at downward angle (135°), facing downwards (180°) (Gori et al., 2013). Instances where the living part of the colony was facing all possible directions, facing upwards category was assigned.

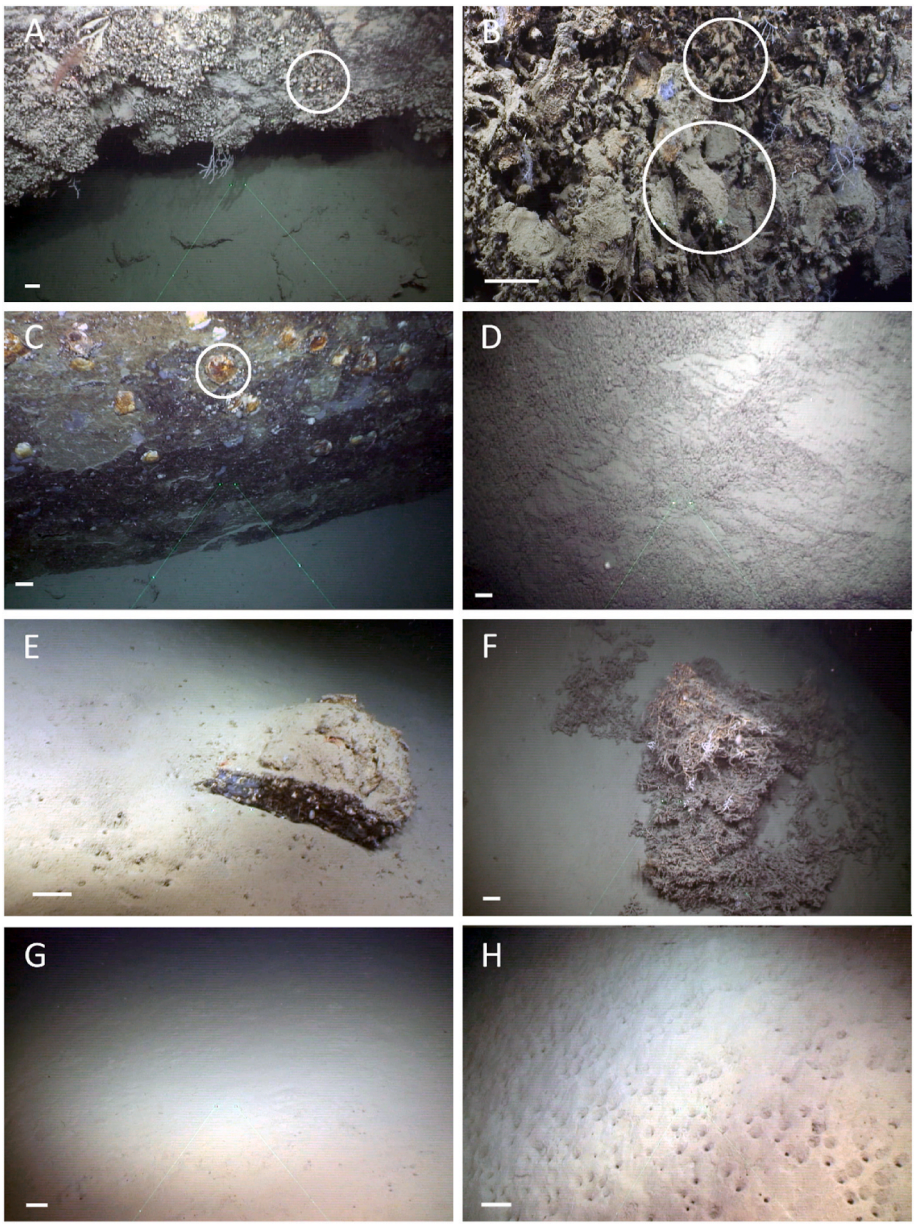

Fig. 2. Seabed substrata types in Blanes Canyon: (A) rocky overhang (RO) with live *D. dianthus* highlighted in circle; (B) biogenic-covered vertical wall (BCVW) with dead *D. dianthus* and *N. zibrowii* highlighted in circles; (C) bare rock vertical wall (BRVW) with live *N. zibrowii* highlighted in circle; (D) mud-draped vertical wall (MDVW); (E) boulders (Bould); (F) coral rubble (CR); (G, H) mud (Mud). Scale: 10 cm (white bars).

2.5.2. Substrata

Seabed substrata was categorized in 7 classes based on CATAMI Classification Scheme with some modifications applied for this study (Althaus et al., 2015) (Table 3); rocky overhang (RO) (no equivalent in CATAMI Classification Scheme) (Fig. 2A); biogenic-covered vertical wall (BCVW) (no equivalent in CATAMI Classification Scheme) (Fig. 2B); bare rock vertical wall (BRVW) (equivalent to *Consolidated (hard): Rock* (SCR– 82001002)) (Fig. 2C); mud-draped vertical wall (MDVW) (equivalent to *Consolidated (hard): Rock* veneer (SCR–82001002 veneer)) (Fig. 2D); boulders (Bould) (equivalent to *Consolidated (hard): Boulders* (SCB–82001003)) (Fig. 2E); coral rubble (CR) (equivalent to *Unconsolidated (soft): Pebble/gravel: Biologenic: Coral rubble* (SUPBR–82001009)) (Fig. 2F); mud (Mud) (equivalent to *Unconsolidated (soft): Sand/mud* (<2 mm*): Mud/silt* (<64μm) (SUSM–82001016)) (Fig. 2G and H).

The distinction was made between bare rock vertical wall and mud-draped vertical wall (Fig. 2C and D), because large part of the hard

Table 3
Substrata classes used in this study with corresponding CATAMI equivalent and code, where applicable.

Substrata class	CATAMI equivalent	CATAMI code
rocky overhang (RO)	NA	
biogenic-covered vertical wall (BCVW)	NA	
bare rock vertical wall (BRVW)	Consolidated (hard): Rock	SCR– 82001002
mud-draped vertical wall (MDVW)	Consolidated (hard): Rock veneer	SCR– 82001002 veneer
boulders (Bould)	Consolidated (hard): Boulders	SCB–82001003
coral rubble (CR)	Unconsolidated (soft): Pebble/gravel: Biologenic: Coral rubble	SUPBR–82001009
mud (Mud)	Unconsolidated (soft): Sand/mud (<2 mm): Mud/silt (<64μm)	SUSM–82001016

substratum was covered with a layer of sediment, which led to the question if this thin layer of sediment affects species presence. Biogenic covered vertical wall was composed of densely packed remaining skeletons of dead *D. dianthus* and/or oyster *Neopycnodonte zibrowii* Gofas, C. Salas and Taviani, 2009, which were often covered with a thick layer of sediment (Fig. 2A and B), unlike the living specimens (Fig. 2C).

2.5.3. Anthropogenic impact

Trawl marks were annotated when the ROV lasers crossed over them. They were easily distinguishable on flat muddy seabed as straight deep gouges in the mud, surrounded by mud clasts. Litter items were categorized based on the Guidance on Monitoring of Marine Litter in European Seas (Directive, S.F., 2013). Type of faunal interaction with litter and species involved were recorded when seen based on Hernandez et al. (2022) and Bruemmer et al. (2023).

2.6. ROV navigation tracks

ROV navigation in each transect was visually inspected and erroneous positions were removed in ArcGIS. Latitude and longitude were projected to WGS 84/UTM zone 31N, which was used for all subsequent calculations. Gaps in navigation data (date, time, latitude (y), longitude (x) and depth (z)) created when removing erroneous positions were filled in R. Firstly, date and time sequence was made based on the logged beginning and ending of the transect. Then, x, y and z were joined to the new date-time sequence, and the gaps were filled based on linear interpolation between gap endpoints using *na.fill* function in *zoo* package (Zeileis and Grothendieck, 2005). Using the *smooth.spline* function in *stats* package in R, a cubic smoothing spline was fit to x, y and z separately in order to reduce the effect of any spatial outlier that was left. Distance between each navigation point was calculated using x, y and z. Accumulated distance and area (1 m x accumulated distance) were calculated based on distance.

2.7. Sampling units

Video annotations were combined with navigation data based on date and time. For each second of the video, number of individuals per morphospecies, number of trawl marks and number of litter items were available as numerical values, while substrata type and video sequence were available as categorical values. Based on the accumulated area, 5 m^2 (5 m length x 1 m width) sampling units (SU) were created using the *cut* function in base R. Data collected for each second of the video was summarized for each SU as follows: numerical values were summed, and categorical values were expressed as percentages. To remove SUs containing video sequences of insufficient quality (see 2.4.) for further analysis, only SUs that had >95 % good sequence were kept.

An SU size of 5 m^2 was used as it partially corresponds to the 5-m bathymetry resolution and similar studies done in the NW Mediterranean also used this SU size (Grinyó et al., 2018; Enrichetti et al., 2019; Dominguez-Carrió et al., 2022). Additionally, species richness, diversity, and evenness did not differ when using larger sampling units (Supplementary Material S2).

2.7.1. Environmental variables assigned to sampling units

Environmental variables include substrata types, hydrography and terrain variables. Each SU was assigned environmental variable values based on the centroid of the SU. Substrata types were annotated during video analysis and were summarized as percentages of all 7 substrata types for each SU.

Hydrography variables from the CTD casts include temperature (°C), salinity, seawater density σ_Θ (kg m^{-3}-1000) and SSC_{exe} (mg L^{-1}). They were attributed to each SU in ArcGIS Pro 3.1.2 based on shortest linear distance, using Near3D tool which considers the shortest distance between points based on x, y and z.

Terrain variables derived from the 5-m bathymetry resolution are: depth, slope, broad-scale bathymetric positioning index (BPI) and fine-scale BPI calculated in ArcGIS Pro 3.1.2, using extension Benthic Terrain Modeler v 3.0 (Wright et al., 2005; Wilson et al., 2007). Broad-scale BPI was calculated based on a 2 pixel (10 m) inner radius and 20 pixels (100 m) outer radius, and fine-scale BPI was based on 1 pixel (5 m) inner radius and 5 pixels (25 m) outer radius (Wright et al., 2005; Wilson et al., 2007). Likewise using the 5-m bathymetry easteness, northness, planform curvature, profile curvature, total curvature, Terrain Ruggedness Index (TRI) and Vector Ruggedness Measure (VRM) were derived in the *spatialECO* package (Evans et al., 2021) in R. Backscatter at 10-m resolution was also used as environmental variable, as well as distance from canyon tip (41°40′3.69"N, 002°54′47.55"E) which was calculated in R using WGS 84/UTM 31N projection.

2.8. Statistical analysis

Principal component analysis (PCA) was used to better visualize if organic components of the water samples (POC, PON and C/N molar ratio) differ between study sites, using *prcomp* in *vegan* package in R (Oksanen et al., 2022). Lipids were excluded from this analysis as they showed high variability in all sampling depth and study sites.

Morphospecies densities per SU were used to identify groups, called megabenthic assemblages. In order to focus the analysis on common benthic morphospecies and reduce the noise produced by rare ones (Poos and Jackson, 2012), benthic morphospecies with less than 5 sightings in the whole study area were excluded. Mobile morphospecies were also removed to avoid overestimating them, i.e., fish, jellyfish, highly mobile crustaceans (belonging to Aristeidae, Penaeidae, Nephropidae, Homolidae, Polybiidae, Geryonidae) and cephalopods.

The data were square root transformed and a Bray-Curtis dissimilarity matrix was generated using *vegdist* function in *vegan* package (Oksanen et al., 2022). Cluster analysis was performed using *hclust* function in *stats* package in R, with Ward's minimum variance method over the square root transformed dissimilarity matrix. A 40 % similarity threshold was employed to define the groups which were determined as significantly different using a PERMANOVA analysis (*adonis* function) from the *vegan* package (Oksanen et al., 2022) Representative morphospecies of each group were identified using the *indval* function from the *labdsv* package (Roberts and Roberts, 2016) in R.

In order to remove correlated environmental variables, Spearman correlation coefficient was calculated between them using *cor* function in *stats* package in R (Supplementary Material S3). All variables that had >60 % correlation were removed from further analysis, leaving depth, slope, backscatter, eastness, northness, total curvature, VRM, broad-scale BPI, percentages of coral rubble, boulder, biogenic-covered vertical wall, bare rock vertical wall, mud-draped vertical wall and rocky overhang, σ_Θ and SSC_{exe}. To quantify the effect of retained environmental variables on the distribution of the megabenthic assemblages, distance-based redundancy analysis (dbRDA) was performed using the *capscale* function in *vegan* package (Oksanen et al., 2022), which included a square root transformation of the Bray-Curtis dissimilarity matrix. An ANOVA like permutation test (*anova.cca* function in vegan package) was used to assess the significance of the constrains (i.e., environmental variables).

Differences in study areas (canyon head – CH and east canyon branch – ECB) were assessed based on environmental variables from the same subset of SUs as used in the dbRDA. Firstly, the data were visualized with a PCA using *prcomp* in *vegan* package in R (Oksanen et al., 2022). Based on the scree plot, first 4 principal components were used in a linear discriminant analysis (LDA) that would determine how the environmental variables contribute to the differences between two study areas (Supplementary Material S8). This was performed using *lda* function in MASS package in R (Venables and Ripley, 2002).

Size and orientation classes were determined for *D. pertusum* and *M. oculata* found in the SUs used in the rest of the analysis. Number of colonies per colony size class and orientation class for *D. pertusum* and

M. oculata were presented as percentages per study site. Density of litter items were presented using descriptive statistics (mean ± SD). Maps were produced in ArcGIS Pro 3.1.2. based on SU geographical positions, whereas plots were made using *ggplot2* package (Wickham, 2016) in R.

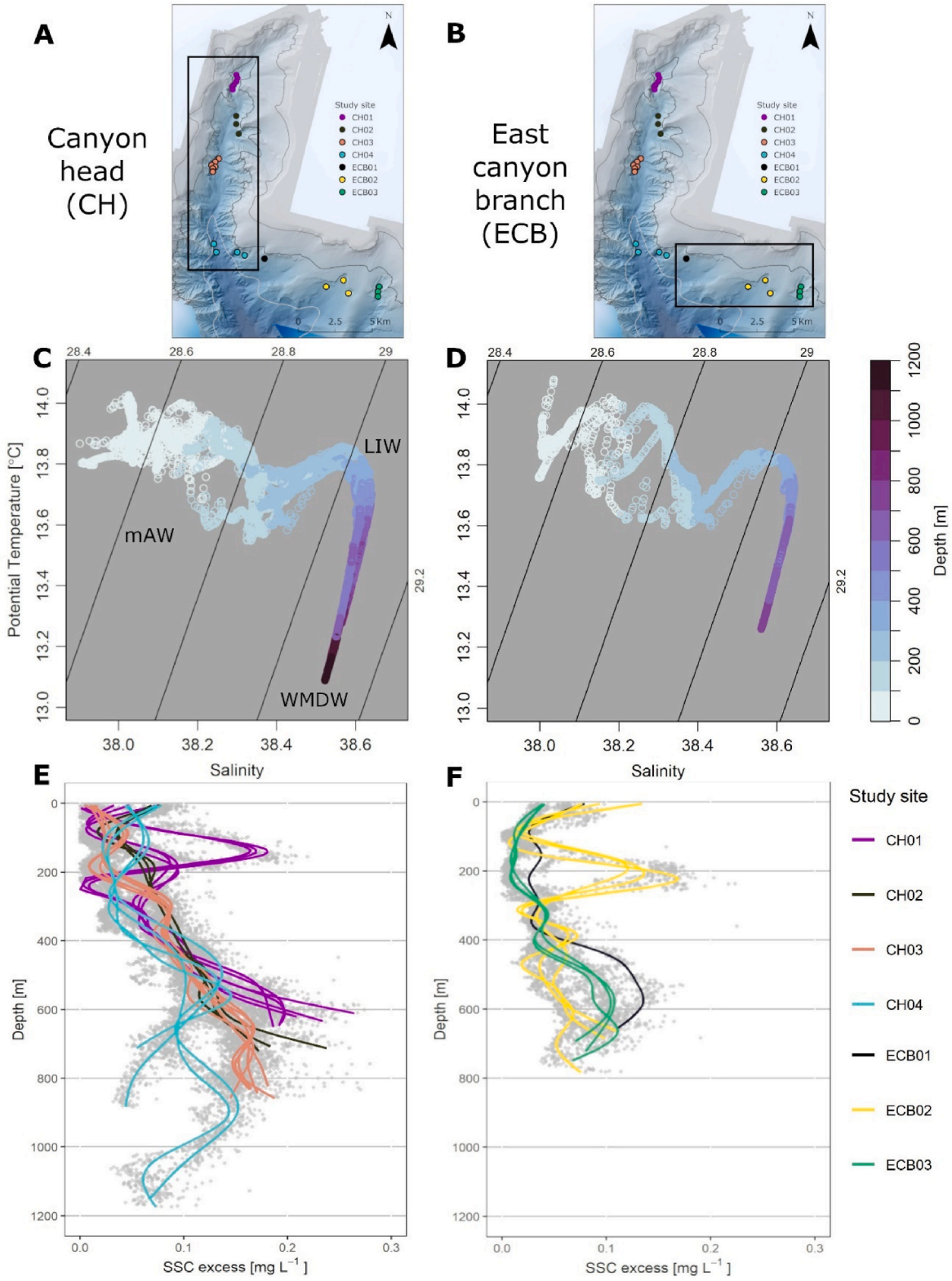

Fig. 3. CTD casts along the study areas canyon head (A) and eastern canyon branch (B); TS diagrams with diagonal isopycnals from the CTD casts along the canyon head (C) and eastern canyon branch (D); SSC excess depth profile based on CTD casts along the canyon head (E) and eastern canyon branch (F). Grey dots in panels E and F represent raw SSC excess data.

3. Results

3.1. Water masses in Blanes Canyon

Water masses were identified based on 26 CTD casts performed in Blanes Canyon (Fig. 3A and B). The Temperature-Salinity (TS) diagrams were typical of the North-western Mediterranean (Fig. 3C and D). The top 200 m was occupied by modified Atlantic Water (mAW) ($T > 13.8$ °C, $S < 38.1$). Below, between 200 and 600 m depth, the Levantine Intermediate Water (LIW) ($T > 13.6$ °C, $S > 38.6$) was found, with the core located at 300–400 m depth. At depths greater than 600 m, the Western Mediterranean Deep Water (WMDW) ($T < 13.2$ °C, $S < 38.6$) was detected (Fig. 3C and D).

Excess suspended sediment concentrations (SSC) were high (>0.1 mg L^{-1}) in all stations, with maximum values reached at 600–800 m depth (Fig. 3E and F). In stations along the canyon head (Fig. 3E), the enhanced SSC was found at shelf break depths (~150 m), as intermediate nepheloid layers, especially pronounced in the study site closest to the coast (CH01). Additionally, near the seabed, bottom nepheloid layers with excess SSC of 0.15–0.25 mg L^{-1} were observed (Fig. 3E). At the deepest study site (CH04), an intermediate nepheloid layer with excess SSC of 0.14 mg L^{-1} was found at ~900 m (Fig. 3E). Similarly, CTD casts at ECB02 study site (Fig. 3F), showed a pronounced intermediate nepheloid layer at shelf break depth (~200 m; ~0.2 mg L^{-1}), while bottom nepheloid layer was more pronounced at study sites ECB01 and EBC03 (~600 m; ~0.19 mg L^{-1}) (Fig. 3F).

3.2. Water samples

Out of 26 CTD casts, 9 were used for water sampling. A total of 45 water samples were analysed for dissolved nutrients, 97 samples for TL, 26 samples for Chl a concentration measured at the chlorophyll maximum depth and 127 samples were analysed for SPM, POC and PON. Chlorophyll maximum was found at 31.1 ± 10.2 m depth with mean Chl-a concentration of 0.27 ± 0.09 mg Chl a L^{-1}. Nitrate, phosphate, and silicate measured in the chlorophyll maximum had lowest concentrations of 1.33 ± 0.84 μmol L^{-1}, 0.03 ± 0.01 μmol L^{-1}, 1.35 ± 0.28 μmol L^{-1}, respectively, while nitrite had highest concentrations of 0.28 ± 0.06 μmol L^{-1} (Table 4). Ammonium was relatively constant with depth, reaching 0.07 ± 0.12 μmol L^{-1} overall. Sampling stations below the chlorophyll maximum (200–5 mab) ranged between 431 and 1173 m depth. Nitrate, phosphate, and silicate were found to be increasing with depth, reaching their maximum at 5 mab with 8.67 ± 1.00 μmol L^{-1}, 0.39 ± 0.02 μmol L^{-1} and 6.11 ± 0.42 μmol L^{-1}, respectively, while nitrite was found to decrease with depth, reaching 0.01 ± 0.005 μmol L^{-1} at 5 mab (Table 4).

SPM did not show a pronounced depth profile, reaching an average value 0.65 ± 0.15 mg L^{-1} among all sampling depths (Table 4, Fig. 4A and B). POC and PON had higher values in the Chl_{Max} sampling depth with mean value 69.85 ± 33.22 μg L^{-1} and 14.17 ± 4.74 μg L^{-1}, respectively (Table 4, Fig. 4A and B). Among the deeper sampling depths (200–5 mab), POC and PON reached highest values at 5 mab, 27.70 ± 10.43 and 6.01 ± 2.39 μg L^{-1}, respectively (Table 4, Fig. 4A and B). Molar C/N ratio was 5.68 ± 1.27 at the Chl_{Max} sampling depth, with higher values found at deeper depths (Table 4, Fig. 4A and B). Total lipids were only measured at deeper sampling depths (200-5 mab), showing high variability and average value at 15.48 ± 7.99 μg L^{-1} (Table 4, Fig. 4A and B).

Differences between study sites in POC, PON and molar C/N ratio were clearer when concentrating on deeper sampling depths (200–5 mab) (Fig. 4A and B). POC was relatively similar between study sites, while PON values were found higher at study sites CH01, CH02 and shallower cast at CH04 (CTD cast 19, Table 2) (Fig. 4A and B). CTD casts of deeper study sites (CH03 and CH04) and along the ECB showed lower PON values (Fig. 4A and B). This discrepancy was also found in the molar C/N values, as casts with lower PON values yielded higher C/N (Fig. 4A and B). The principal components analysis (Fig. 4C) indicates that the first two axes explain 98.94 % of the variation, with PC1 highly influenced by POC and PON and PC2 by molar C/N. The Chl_{Max} values are separated from the deeper sampling stations, as they are scattered in the direction of higher POC, along the first principal component (Fig. 4C–Supplementary Material S4).

3.3. Video analysis

A total of 65.6 h of video material was recorded covering 26,803 m^2 of explored seafloor. A total of 46,938 specimens were recorded belonging to 94 morphospecies, while 372 litter items were recorded belonging to 19 litter categories with 114 faunal interactions. Porifera, Cnidaria and Chordata (of which only one ascidian) were represented by 22, 20 and 24 morphospecies, respectively, while the other 27 species belonged to Arthropoda (11), Echinodermata (8), Mollusca (5) and Annelida (3).

Dividing the ROV transects into 5 m^2 SU (5394 SU) and removing those SU flagged as bad quality resulted in 2410 SU (44.6 %) of which 1202 SU (22.3 %) did not contain faunal records. The most common substrate type among the 2410 SU was mud (Mud) (72.5 %), followed by mud-draped vertical wall (MDVW) (18.6 %), coral rubble (CR) (3.9 %), boulders (Bould) (2.2 %), biogenic-covered vertical wall (BCVW) (1.6 %), bare rock vertical wall (BRVW) (0.8 %) and rocky overhang (RO) (0.2 %).

3.4. Identification of megabenthic assemblages

Identification of megabenthic assemblages was based on morphospecies densities per SU using a cluster analysis. Selected environmental

Table 4
Results of the water samples analysis reported as mean ± standard deviation, including dissolved inorganic nutrients (ammonium, nitrite, nitrate, phosphate and silicate), total lipids (TL), suspended particulate matter (SPM), particulate organic carbon (POC), particulate organic nitrogen (PON) and molar C/N. Columns represent sampling depths, chlorophyl maximum (Chl_{Max}), 200, 100, 50 and 5 m above bottom (mab), with respective depth shown as mean ± standard deviation.

Analysed material	Sampling depth				
	Chl_{Max}	200 mab	100 mab	50 mab	5 mab
Sampling depth (m)	31.1 ± 10.2	572.3 ± 169.0	672.3 ± 169.0	722.5 ± 168.9	772.1 ± 168.8
Ammonium (μmol L^{-1})	0.107 ± 0.045	0.027 ± 0.011	0.073 ± 0.100	0.120 ± 0.237	0.058 ± 0.052
Nitrite (μmol L^{-1})	0.282 ± 0.065	0.014 ± 0.005	0.011 ± 0.003	0.012 ± 0.003	0.010 ± 0.005
Nitrate (μmol L^{-1})	1.33 ± 0.84	7.67 ± 0.82	7.70 ± 0.92	8.08 ± 1.00	8.674 ± 1.00
Phosphate (μmol L^{-1})	0.038 ± 0.012	0.374 ± 0.022	0.378 ± 0.035	0.387 ± 0.025	0.392 ± 0.024
Silicate (μmol L^{-1})	1.36 ± 0.28	5.29 ± 0.51	5.63 ± 0.53	6.02 ± 0.49	6.12 ± 0.42
SPM (mg L^{-1})	0.59 ± 0.15	0.64 ± 0.15	0.64 ± 0.13	0.64 ± 0.20	0.66 ± 0.17
POC (μg L^{-1})	69.86 ± 33.2	22.0 ± 6.5	21.4 ± 3.7	25.0 ± 5.0	27.7 ± 10.4
PON (μg L^{-1})	14.2 ± 4.7	5.8 ± 2.5	5.4 ± 2.6	5.3 ± 2.5	6.0 ± 2.4
C/N (molar)	5.7 ± 1.3	5.3 ± 2.7	5.9 ± 3.0	6.8 ± 3.2	6.4 ± 3.6
TL (μg L^{-1})	NA	12.59 ± 6.75	15.61 ± 7.88	17.17 ± 8.80	16.60 ± 8.12

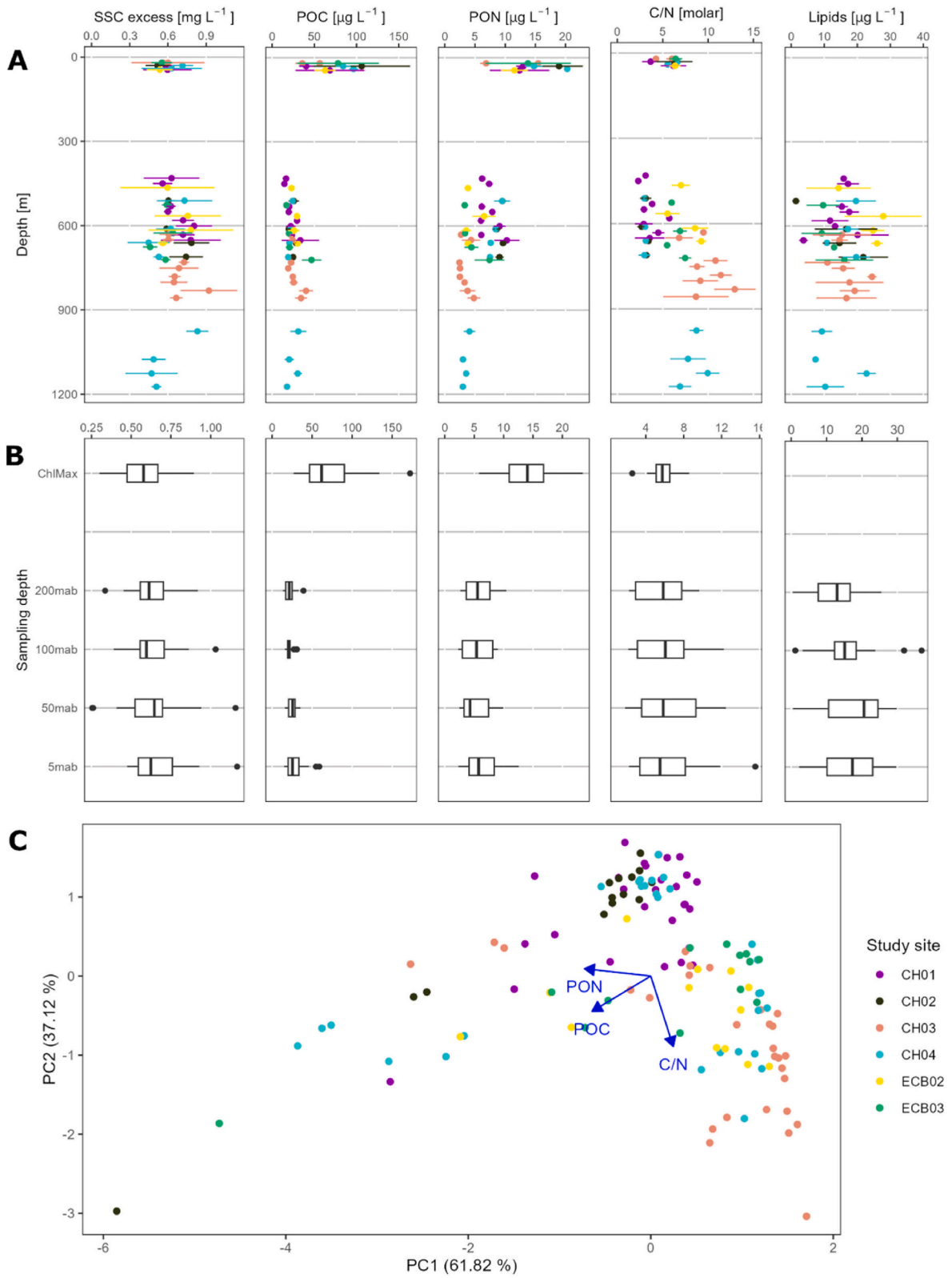

Fig. 4. Vertical profiles of suspended particulate matter (SPM), particulate organic carbon (POC), particulate organic nitrogen (PON), molar C/N and total lipids along depth (A), sampling depths (B) and visualization of principle component analysis (PCA) (C) based on POC, PON and molar C/N. Colours in (A) and (C) represent study sites (abbreviations: CH - canyon head; ECB – east canyon branch). In (A) the values are represented as mean (dot) ± SD (horizontal line) per CTD cast per sampling depth. (For interpretation of the references to colour in this figure legend, the reader is referred to the Web version of this article.)

variables (substrata types, terrain and hydrographic, see 2.8.) were used in dbRDA analysis to identify which environmental conditions best describe the environment where each megabenthic assemblage was found. After removal of rare species, highly mobile species, and SU with no faunal records resulted in 890 SU (16.5 %) suitable for the described analysis. Substrata types in this subset of SUs were mud-draped vertical wall (MDVW) (46.3 %), mud (Mud) (36.5 %), coral rubble (CR) (5.7 %), boulders (Bould) (4.3 %), biogenic-covered vertical wall (BCVW) (4.1 %), bare rock vertical wall (BRVW) (2.2 %) and rocky overhang (RO) (0.7 %). Percentages of each substrata type differed between study sites, where percentage of unconsolidated substrata (Bould, RO, BRVW, BCVW, MDVW) gradually increased along the canyon head, while the study sites in the eastern canyon branch had a larger contribution of consolidated substrata (Mud, CR) (Supplementary Material S5).

Using morphospecies densities from the 890 SU suitable for the analysis, five groups were identified based on a 40 % similarity threshold. Permutation test confirmed that the five groups, named megabenthic assemblages, were significantly different ($Df = 4$, $F = 154.13$, $p < 0.001$) (Fig. 5).

Three assemblages yielded single morphospecies as indicator, unidentified Gastropod for assemblage 1, a single morphospecies from genus *Arachnanthus* for assemblage 2 and a single morphospecies from the genus *Cerianthus* for assemblage 3 (Fig. 5, Table 5). Identification of Gastropod species was not possible with images alone, especially since the Gastropod often exhibited burrowing behaviour. Assemblage 1 was identified in the 4.5 % (40 SU) of the analysed 890 SU, assemblage 2 in 6.2 % (55 SU) and assemblage 3 in 11.8 % (105 SU). All three assemblages were mostly found on flat muddy substratum, with few occurrences found on mixed substrata environments where soft sediment occurred in between boulders and coral rubble (Fig. 6). Such substratum was mainly found below canyon walls or on the canyon floor, although along the canyon walls there were areas dominated by mud (Supplementary Material S6). Assemblage 1 was mainly found in study sites CH01 (Fig. 7A) and ECB03 (Fig. 7D), while assemblage 2 was found throughout the canyon, predominantly in study sites ECB02 and ECB03 (Fig. 7D). Assemblage 3 was also found throughout the canyon, mostly in CH01 (Fig. 7A) followed by CH03 (Fig. 7B) and ECB03 (Fig. 7D). Although all three assemblages were found in similar ranges of environmental settings (Fig. 6), assemblage 3 had higher occurrence in areas of increased SSC (0.16 ± 0.07 mg L^{-1}, mean $\pm$ SD) (Fig. 6H), such as in CH01 (Fig. 7A) and CH03 (Fig. 7B).

Assemblage 4 and assemblage 5 encompass species found on Blanes Canyon vertical walls, sharing 38 morphospecies, with 16 morphospecies mostly attributed to assemblage 4, and 22 morphospecies to assemblage 5. The main difference between the two assemblages is due to stronger affinity of assemblage 5 to rocky substratum and higher slope (Figs. 6 and 7C). Assemblage 4 was found in 42.1 % (375 SU) and assemblage 5 in 35.4 % (315 SU) of analysed 890 SUs. Indicator morphospecies for assemblage 4 are a small unidentified sponge, ascidian *Dicopia antirrhinum* Monniot C., 1972 and spoonworm *Bonelia viridis* Rolando, 1822, while for assemblage 5 indicator morphospecies are corals *D. dianthus*, *M. oculata*, *Muriceides lepida* Carpine and Grasshoff, 1975, *Parantipathes* cf. *tetrasticha* (Pourtalès, 1868) (M. Bo, pers. comm.) and encrusting sponge *Hamacantha* (*Vomerula*) *falcula* (Bowerbank, 1874) (Fig. 5, Table 5). Most coral species (66 %) were attributed to assemblage 5, with exceptions attributed to assemblage 4 as *Javania cailleti* (Duchassaing and Michelotti, 1864) (Fig. 7C), *Swiftia* cf. *dubia* (Thomson, 1929), *Callogorgia verticillata* (Pallas, 1766) and *Acanthogorgia* sp. Gray, 1857. Main sponges attributed to assemblage 5 were *Pachastrella monilifera* Schmidt, 1868, *Tretodictyum reiswigi* Boury-Esnault et al., 2017, *Oopsacas minuta* Topsent, 1927, *Sympagella delauzei* Boury-Esnault et al., 2017, while assemblage 4 contained several unidentified morphospecies of sponges (Supplementary Material S1 and *Phakellia robusta* Bowerbank, 1866. Apart from corals and sponges, giant deep-sea oyster *N. zibrowii* was assigned to assemblage 5 where it was found on bare-rock vertical wall (study site ECB03, 652 m depth) at high density of 7.8 ind m^{-2}.

Both assemblages showed higher occurrence on East facing slopes (eastness values closer to 1, Fig. 6C) and lower σ_Θ (Fig. 6G), while wide range of broad BPI and VRM values indicates areas of rapidly changing slope values and higher variation, such as canyon walls (Fig. 6E and F). Both assemblages were found throughout the canyon, with highest occurrence recorded in study sites ECB03 (Fig. 7D) and CH04 (Fig. 7C) for assemblage 4, and CH04 (Fig. 7C) for assemblage 5.

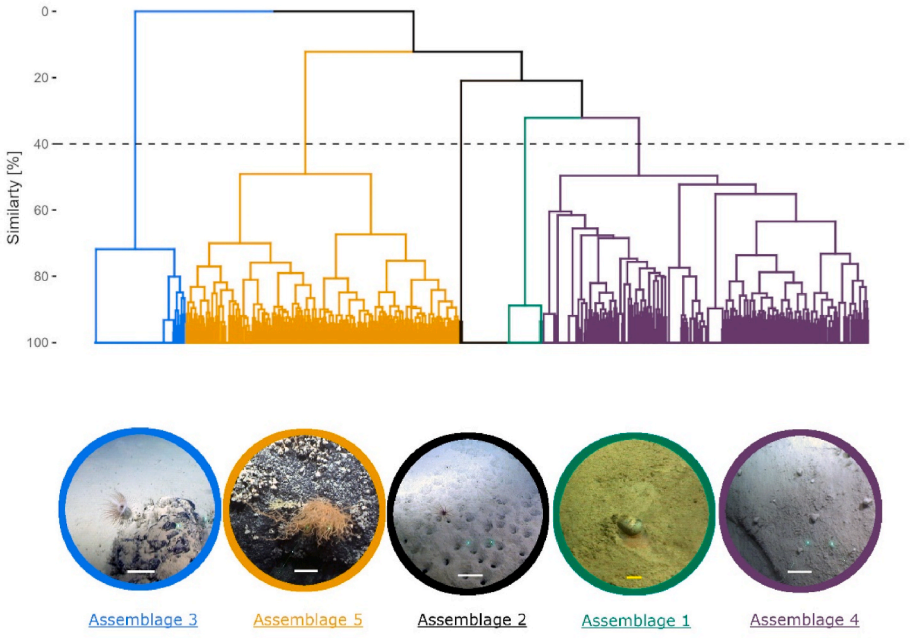

Fig. 5. Cluster analysis based on Bray-Curtis dissimilarity index. Five groups with 40 % similarity are identified, named megabenthic assemblages. From left to right: assemblage 3: *Cerianthus* sp.; assemblage 5: *Antipathes dichotoma* (orange coral) and *Desmophyllum dianthus*. assemblage 2: *Arachnanthus* sp.; assemblage 1: Gastropod; assemblage 4: *Dicopia antirrhinum*. Scale: 10 cm (white bars), 1 cm (yellow bar). (For interpretation of the references to colour in this figure legend, the reader is referred to the Web version of this article.)

Table 5
Summary of megabenthic assemblages identified in Blanes Canyon providing depth (mean ± SD) and indicator morphospecies of each assemblage, including their maximum and mean ± SD density, and indicator value.

Assemblage	Mean depth ± SD [m]	Indicator morphospecies	Max. density [ind/col m^{-2}]	Mean density ± SD [ind/col m^{-2}]	Indicator value
1	681 ± 98	Gastropod	0.4	0.21 ± 0.05	0.9974
2	706 ± 62	*Arachnanthus* sp.	0.4	0.20 ± 0.02	0.9728
3	684 ± 135	*Cerianthus* sp.	1.4	0.24 ± 0.15	0.9187
4	712 ± 167	Porifera sp. 3	4	0.36 ± 0.63	0.2638
		Dicopia antirrhinum	1.8	0.09 ± 0.22	0.1728
		Bonelia viridis	1	0.07 ± 0.14	0.1447
5	726 ± 183	*Desmophyllum dianthus*	130.2	9.67 ± 14.66	0.9455
		Madrepora oculata	2.2	0.15 ± 0.38	0.1818
		Muriceides lepida	6	0.19 ± 0.67	0.1805
		Parantipathes cf. *tetrasticha*	1.4	0.09 ± 0.22	0.1647
		Hamacantha (Hamacantha) falcula	9.6	0.28 ± 0.84	0.1533

Distance-based redundancy analysis (dbRDA) showed that the retained environmental variables (Supplementary Material S3) explained 15.5 % of all variability observed, with the first two components explaining 71 % of constrained variance (Fig. 8).

The ANOVA like permutation test showed that all environmental variables used, except for total curvature, significantly improve the model assembled to explain morphospecies density (Table 6). Specifically, depth, slope, mud-draped vertical wall and biogenic-covered vertical wall explained most of the variation. The dbRDA successfully separated SUs, megabenthic assemblages and morphospecies mostly found on soft substratum (assemblages 1, 2 and 3) from those mostly found hard substratum (assemblages 4 and 5) (Fig. 8A). Assemblages 1, 2 and 3 were associated with higher values of SSC and σ_{Θ} and lower values of slope, which is a proxy for mud as it was excluded from this analysis due to high correlation with slope (Fig. 8A, Supplementary Material S3). Assemblage 4 and 5 overlapped to an extent as they had many more SUs and were mainly driven by presence on boulders and mud-draped vertical walls. However, most of assemblage 5 was driven by different hard substrata, especially biogenic covered vertical wall (Fig. 8A). *Desmophyllum dianthus* was identified as an outlier compared to other species due to its ubiquitousness in Blanes Canyon and high-density values (Fig. 8B–Table 5).

Differences in environmental variables between study areas (CH and ECB) were evaluated using PCA and LDA, where 75 % of SU were found in CH and 25 % in ECB. There was some overlap between the study areas (Fig. 9A), where some study sites were more easily differentiated than others (Supplementary Material S8). The LDA was able to correctly separate 85 ± 19 % of SUs in CH and 60 ± 30 % of SUs in ECB. Environmental variables that were mostly contributing to identification of ECB were seawater density, northness and broad BPI, opposed to backscatter, SSC, eastness and VRM identifying CH (Fig. 9B).

3.5. Biodiversity in Blanes Canyon

Species occurrences and densities were not evenly distributed throughout the canyon (Supplementary Material S9). Some species were common to most study sites, such as corals *D. dianthus* and *P.* cf. *tetrasticha*, sponges Porifera sp. 3, *H. falcula* and *Hexadella* cf. *dedritifera* Topsent, 1913 and ascidian *D. antirrhinum*. Some species showed patchy or study area-specific distribution along the canyon, where *Leiopathes glaberrima* (Esper, 1792), *T. reiswigi, P. monilifera*, and *N. zibrowii* were mostly found on the eastern canyon branch, while *M. oculta*, *D. pertusum*, *C. verticillata, S. deluzei* and *O. minuta* were found along the canyon head (Fig. 10, Supplementary Material S1, S9).

3.5.1. Cold-water corals in Blanes Canyon

The most abundant animal group in Blanes Canyon were corals, found in 452 SU of analysed 890 SUs, making up 79 % (21,413 ind) of all records, where *D. dianthus* accounted for 72 % (15,440 ind) of all records. Besides *D. dianthus*, another 11 coral species were identified (ordered by abundance): *M. lepida* (324 col), *Antipathes dichotoma* Pallas, 1766 (283 col), *M. oculata* (253 col), *P.* cf. *tetrasticha* (220 col), *J. cailleti* (209 ind), *C. verticillata* (84 col), *D. pertusum* (60 col), *S.* cf. *dubia* (36 col), *L. glaberrima* (28 col), *Acanthogorgia* sp. Gray, 1857 (9 col) and *Placogorgia coronata* Carpine and Grasshoff, 1975 (6 col) (Fig. 10).

3.5.1.1. Spatial distribution of cold-water corals in Blanes Canyon. Colonial scleractinian corals (*D. pertusum* and *M. oculata*) were only found in the study sites of the canyon head (CH01-CH04), while *D. perusum* was absent from CH02. The highest densities were reached in study site CH01 (Fig. 11), 1.2 col m^{-2} at 622 m depth for *D. pertusum* and 2.2 col m^{-2} at 548 m depth for *M. oculata*. At study site CH03 (Fig. 11), apart from colonial scleractinian corals, *S.* cf. *dubia* was found reaching 0.6 col m^{-2} at 824 m depth, *A. dichotoma* reaching 1.2 col m^{-2} at 844 m depth and *C. verticillata*, reaching its highest density 3.8 col m^{-2} at 824 m depth (Fig. 12). Study site CH04 (Fig. 11, Fig. 12, Fig. 13) hosted all 12 coral species, some of them reaching their highest densities, such as *J. cailleti* (3.6 ind m^{-2} at 1034 m depth) (Fig. 11), *A. dichotoma* (3 col m^{-2} at 1019 m depth) (Fig. 13) and *L. glaberrima* (1.2 col m^{-2} at 545 m depth) (Fig. 13). This study site had the largest depth range (463–1190 m depth), where deeper mixed coral gardens consisted of *Acanthogorgia* sp., *M. lepida*, *C. verticillata*, *A. dichotoma*, *P.*cf. *tetrasticha*, *J. callieti*, *D. dianthus*, *P. coronata.* The deepest records for *D. pertusum* and *M. oculata* in this study were found at this study site, at 939 and 949 m depth, respectively. Shallower transects at this study site harboured mixed gardens composed of *M. lepida*, *D. dianthus*, *P.*cf. *tetrasticha, M. oculata* and *L. glaberrima*. Eastern canyon branch (ECB) study area was characterized by the absence of colonial scleractinian corals and dominated by *D. dianthus* (Fig. 11), *M. lepida, S.* cf. *dubia* (Fig. 12), *P.* cf. *tetrasticha* and *L. glaberrima* that were mainly found in study site ECB03 530–660 m depth (Fig. 13). *Desmophyllum dianthus*, *P.* cf. *tetrasticha* and *M. lepida* were the only species found in all study sites (Fig. 11, Fig. 12, Fig. 13). Highest densities were found for *D. dianthus* in study sites ECB03 (130.2 ind m^{-2} at 652 m depth) (Fig. 11) and CH01 (74.6 ind m^{-2} at 579 m depth) (Fig. 11), while *P.* cf. *tetrasticha* was found at maximum density of 1.4 col m^{-2} at both CH01 at 545 m depth (Fig. 13) and CH04 at 940 m depth (Fig. 13). *Muriceides lepida* reached maximum 6 col m^{-2} at 623 m depth (ECB02) and 4 col m^{-2} at 568 m depth (CH04) (Fig. 12). While most species, especially octocorals and black corals were found protruding from rocky steep substratum, *D. dianthus* was mainly found facing downwards, growing parallel to the substratum (Fig. 10).

3.5.1.2. Cold-water coral environmental niches. Based on the environmental variables found at SUs containing CWCs we can describe environmental niches that different CWC species occupy in Blanes Canyon (Fig. 14). *Desmophyllum dianthus*, *M. lepida* and *P.* cf. *tetrasticha* were found along the studied depth range explored in this study (Fig. 14, Table 1). We observed *D. pertusum*, *M. oculata*, and *L. glaberrima* at shallower depths, while *J.callieti*, *Acanthogorgia* sp., *C. verticillata* and

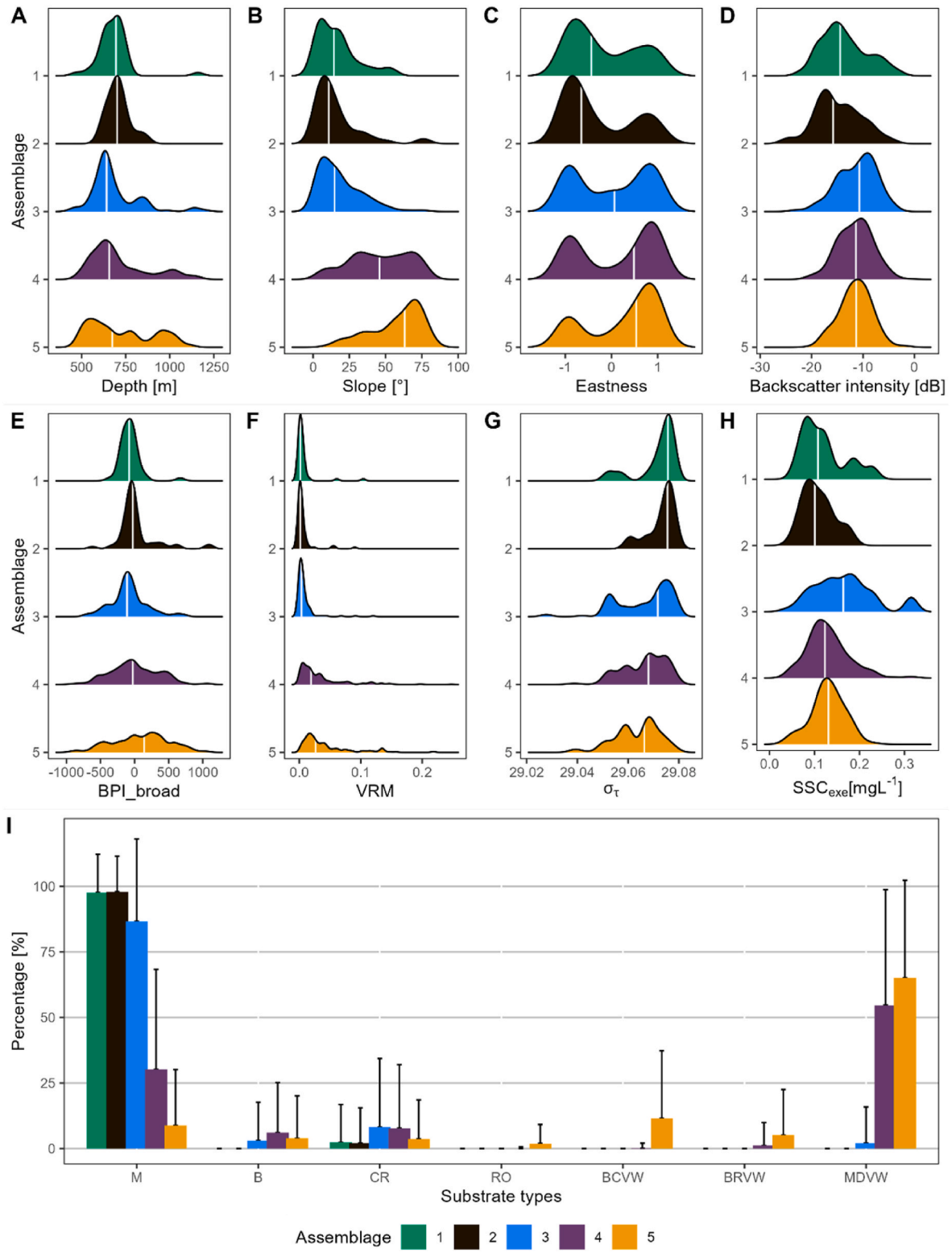

Fig. 6. Environmental variables distribution and substrata types for the five identified megabenthic assemblages in Blanes Canyon: (A) depth, (B) slope, (C) eastness, (D) backscatter intensity, (E) broad BPI, (F) VRM, (G) σ_{Θ}, (H) SSC_{exe} and (I) substrata types (mud (M), boulders (B), coral rubble (CR), rocky overhang (RO), biogenic-covered vertical wall (BCVW), bare rock vertical wall (BRVW), mud-draped vertical wall (MDVW)). White vertical line in (A)–(H) is the median. Substrata types are expressed as mean ± SD of substrata type percentages of each SU within respective assemblage.

A. dichotoma were found deeper (Fig. 14A). Most corals showed higher number of occurrences on East facing canyon walls, except for *L. glaberrima*, which was almost exclusively found on West facing canyon walls (Fig. 14B). Higher temperature and salinity values were found favourable for *D. pertusum, M. oculata* and *L. glaberrima*, while other species were found mostly on the lower end of the temperature-salinity spectrum, except for eurytopic *D. dianthus, M. lepida* and *P.*cf. *tetrasticha* (Fig. 14C and D). Most coral species were found at lower SSC values

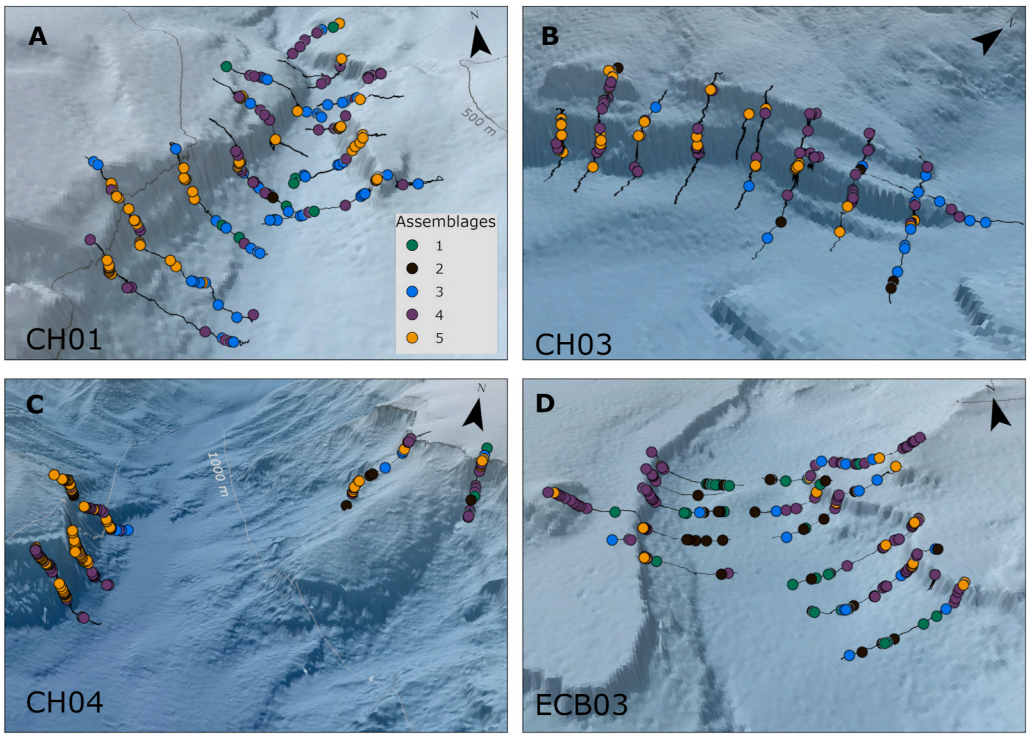

Fig. 7. Spatial distribution of megabenthic assemblages in study sites CH01, CH03, CH04, and ECB03. The rest of the study sites can be found in Supplementary Material S7. Abbreviations: Canyon head (CH), East canyon branch (EBC).

($<$0.1 mg L^{-1}), while *D. pertusum*, *M. oculata* and *S.* cf. *dubia* were found in areas of increased SSC ($>$0.15 mg L^{-1}) (Fig. 14E).

3.5.1.3. Size and orientation of colonial scleractinian corals. Colonial scleractinian corals were mostly growing on canyon walls in Blanes Canyon (Fig. 15A and C), often found partially covered by sediment on the top of their colonies, while the living part of the colony was facing downwards (Fig. 15A). An exception was found at study site CH03 where several *D. pertusum* colonies were found on flat, muddy substratum, where the living part of the colony was oriented perpendicular to the substratum, facing the same direction, presumably towards the prevailing current (Fig. 15B).

We measured a different number of colony sizes and orientations depending on the species and study site. Colonies of *D. pertusum* and *M. oculata* were found to be predominantly very large (⌀ $>$ 40 cm) at all study sites (Fig. 16A), except in case of *D. pertusum* at study sites CH03 and CH04, where medium and small sized colonies prevailed. Small colonies were not found at CH04 for *D. pertusum* and CH02 for *M. oculata* (Fig. 16A).

Desmophyllum pertusum colony direction was mainly facing a downward angle (135°) (62 %) at CH01, while CH03 hosted most colonies growing in a horizontal (90°) (50 %) or upward (0°) (43 %) direction (Fig. 16B). *Madrepora oculata* colonies were mostly found at a downward angle (135°) (65 %) at CH01, while at CH04 colonies were found growing horizontally (90°) (75 % and 33 %) (Fig. 16B).

3.5.2. Mobile and rare species

Mobile fauna included 27 species (mostly belonging to fish and highly mobile crustaceans) that were recorded 546 times in total (Supplementary Material S9). Fish were the most abundant group, where *Notacanthus bonaparte* Risso, 1840 was recorded most frequently (112 ind), followed by *Hoplostethus mediterraneus* Cuvier, 1829 (63 ind), *Nezumia aequalis* (Günther, 1878) (59 ind) and *Lepidion lepidion* (Risso, 1810) (48 ind) (Fig. 10). Majority of fish were found on mud, while *H. mediterraneus* and *L. lepidion* were common on mud-draped vertical walls, with *H. mediterraneus* found shallower (603 ± 80 m, mean ± SD) than *L. lepidion* (919 ± 173 m). Several species of crustaceans were found, hermit crab (59 ind), *Aristeus antennatus* (Risso, 1816) (51 ind), *Bathynectes maravigna* (Prestandrea, 1839) (23 ind) and *Parapenaeus longirostris* (Lucas, 1846) (23 ind). Most crustacean species were found on mud, except for *B. maravigna* which was mostly found on biogenic-covered and mud-draped vertical walls.

This study included 27 rare species, including *Cladorhiza abyssicola Sars, 1872* at ECB03 (646 m), *Protoptilum carpenterii* Kölliker, 1872 at ECB03 (637 m), juvenile *Isidella elongata* (Esper, 1788) at CH03 (750 m), *Acesta excavata* (J. C. Fabricius, 1779) at CH03 (771–822 m) (Fig. 10) and CH04 (830–1051 m) (Bo et al., 2020), *Nephrops norvegicus* (Linnaeus, 1758) at ECB03 (635–754 m), *Paromola cuvieri* (Risso, 1816) at CH01 (525–655 m) and CH05 (926 m), *Plesionika gigliolii* (Senna, 1902) at ECB02 (621–660 m) and ECH03 (660 m), sea spiders (Pycnogonida) at CH01 (552–654 m), *Gaidropsarus granti* (Regan, 1903) at CH01 (474–550 m) and CH02 (586) (Bo et al., 2020), *Etmopterus spinax* (Linnaeus, 1758) at CH01 (607–656 m), *Galeus melastomus* Rafinesque, 1810 at CH01 (640 m) and CH03 (786–838 m) and *Hexanchus griseus* (Bonnaterre, 1788) at ECB03 (714 m).

3.6. Anthropogenic impacts

A total of 218 litter items were observed in Blanes Canyon, while 35 trawl marks were only observed in the canyon axis of study site CH03 (Fig. 17A). In study site CH01 (104 items) 47 % of litter was found, followed by CH02 with 33 %. The most common litter found was related to fishing gear: 151 fishing lines and 18 fishing nets (Fig. 17B, C and D). Other plastic litter included: bottles (Fig. 17F), bags (Fig. 17H), sheets and other plastic objects (Fig. 17G). Metal (Fig. 17I), glass and textile litter items were encountered in forms of carpets, beverage cans and clothing (Table 7). Litter was commonly found on sloping terrain between 522 and 682 m depth (Table 7). The most common animals encountered growing on fishing lines were *M. oculata* (Fig. 17D) followed by *Leptometra celtica* (M'Andrew and Barrett, 1857) and

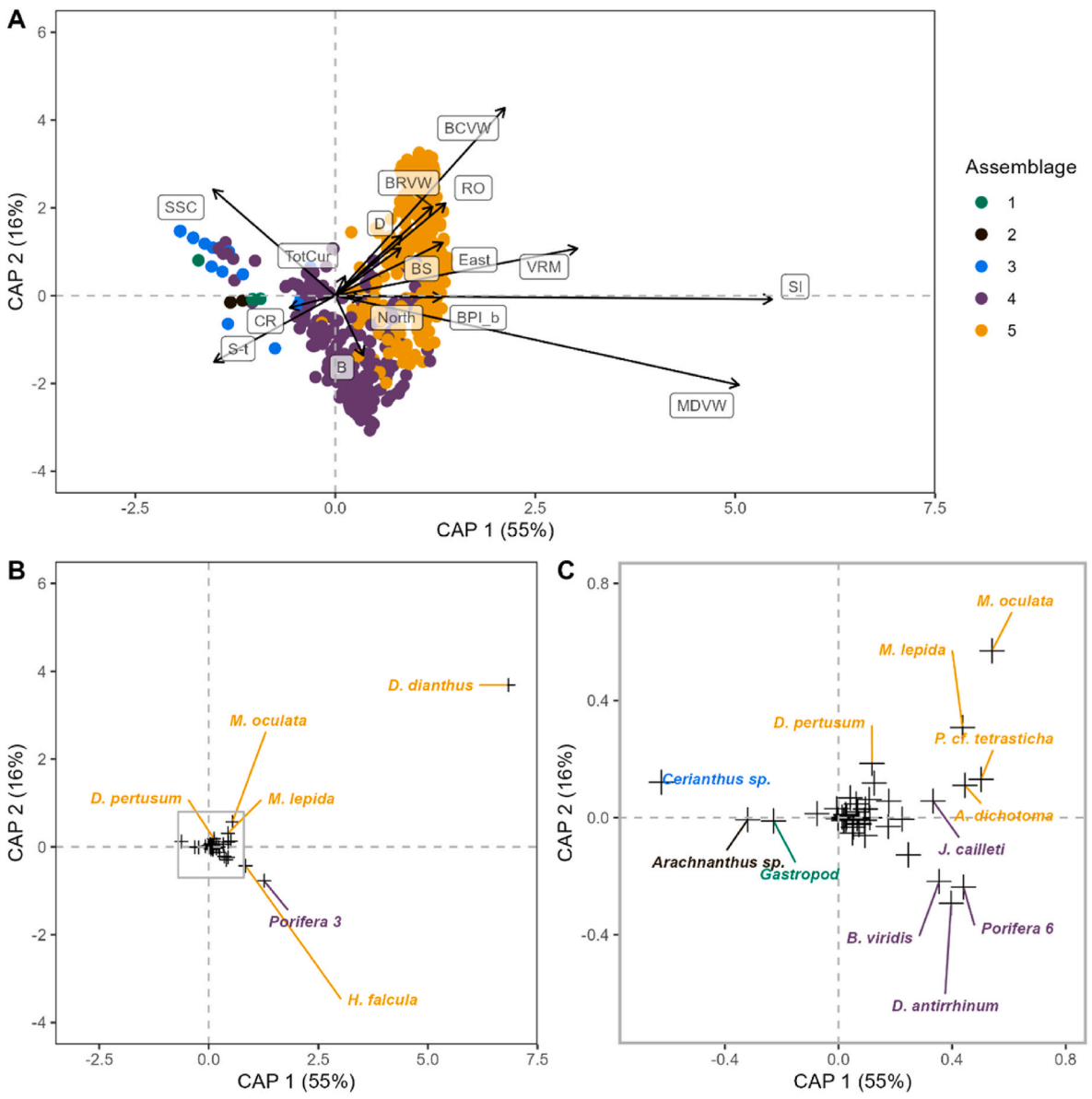

Fig. 8. Distance based redundancy analysis (dbRDA) based on transformed Bray-Curits dissimilarity matrix of morphospecies density per SU constrained with centred environmental variables: (A) Sites scores (SUs) presented as points colored by megabenthic assemblage with environmental variables (arrows) (B) morphospecies scores presented as crosses and colour labelled by megabenthic assemblage. Grey rectangle in (B) is a zoomed detail presented in (C). Abbreviations for environmental variables in (A) can be found in Table 6. (For interpretation of the references to colour in this figure legend, the reader is referred to the Web version of this article.)

D. dianthus, while entanglement was recorded for *M. oculata* (Fig. 17C), *D. pertusum, L. glaberrima* and *Cidaris cidaris* (Linnaeus, 1758) (Table 7).

4. Discussion

The purpose of this study was to provide a detailed description of megabenthic assemblages found on the walls of Blanes Canyon, with a specific focus on CWCs, and the environmental conditions they are found in. Using a dense coverage of ROV transects (26 km) accompanied by CTD casts in several study sites along the shelf-incising canyon head and eastern canyon branch of Blanes Canyon, we provide quantitative evidence that Blanes Canyon is an important CWC habitat, including a variety of associated species.

Five megabenthic assemblages were identified, three on flat soft sediment and two mosaiced on the sloping canyon walls (Fig. 5), without clear geographic or bathymetric separation (Fig. 7). Soft sediment assemblages were characterized, as indicator species, by an unidentified gastropod and tube-dwelling anemones (*Cerianthus* sp. and *Arachnanthus* sp.), which are common inhabitants of such environments worldwide (Davies et al., 2014; Stampar et al., 2015; Cleland et al., 2021) and in the Mediterranean Sea (Pierdomenico et al., 2019; Grinyó et al., 2020; Rueda et al., 2021; Dominguez-Carrió et al., 2022). Canyon wall assemblages mostly included suspension feeders such as corals and sponges, which are commonly reported in submarine canyons (Orejas et al., 2009; Huvenne et al., 2011; Fabri et al., 2014; Santín et al., 2018, 2021a; Quattrini et al., 2015; Pearman et al., 2023). Although the two wall assemblages shared ranges of environmental conditions (Fig. 6), the one characterized by indicator species *D. antirrhinum* and *B. viridis,* was found on areas of the canyon walls that are flatter and more covered with mud, such as terraces, which supports the notion that vertical walls can be highly heterogeneous, thus increasing the number of species they can host (Pearman et al., 2023). In this study we found 12 main CWC species which accounted for 79 % of all faunal records. Previous studies have identified Blanes Canyon as suitable habitat for CWCs (Aymà et al.,

Table 6
Summary of ANOVA like permutation test for distance-based redundancy analysis (dbRDA) used to test the significance of each environmental variable. Abbreviations: Bray Curtis dissimilarity matrix (d1), degrees of freedom (Df), Sums of squares (SS), F-statistic (F), p value (p).

Formula:	d1 ~ D + Sl + BS + East + North + TotCur + VRM + BPI_b + CR + Bould + BRVW + MDVW + BCVW + RO + σΘ + SSCexe			
Variable	Df	SS	F	p
Depth (D)	1	4.72	12.55	0.001
Slope (Sl)	1	21.30	56.69	0.001
Backscatter (BS)	1	2.40	6.39	0.001
Eastness (East)	1	0.91	2.44	0.003
Northness (North)	1	0.92	2.44	<0.001
Total curvature (TotCur)	1	0.34	0.91	0.566
VRM	1	1.59	4.23	0.001
BPI broad (BPIb)	1	1.14	3.03	0.001
Coral rubble (CR)	1	2.28	6.07	0.001
Boulders (Bould)	1	1.62	4.30	0.001
Bare rock vertical wall (BRVW)	1	1.95	5.19	0.001
Mud-draped vertical wall (MDVW)	1	7.98	21.23	0.001
Biogenic-covered vertical wall (BCVW)	1	6.29	16.73	0.001
Rocky overhang (RO)	1	1.84	4.90	0.001
σΘ	1	1.72	4.60	0.001
SSC excess (SSCexe)	1	3.23	8.59	0.001
Residual	872	326.20		

2019; Matos et al., 2021). In the current study we add more detailed insight to within-canyon differences in environmental conditions that could have led to different CWC assemblages in the canyon, including substrata types, water masses and sediment dynamics.

Most CWCs were found on east-facing canyon walls (i.e., west canyon walls) which can be related to the canyon morphology and facing orientation to the prevailing geostrophic current, likely providing organic-rich suspended material (Fig. 14). These walls are steeper and have multiple gullies and exposed overhangs (Lastras et al., 2011; Cabrera et al., 2024) which are suitable for coral settlement and growth (Orejas et al., 2009; Huvenne et al., 2011). Steeper western canyon walls can also contribute to lower sedimentation rates compared to the more depositional eastern canyon wall and eastern canyon branch in Blanes Canyon (Lastras et al., 2011; Durán et al., 2013; Cabrera et al., 2024). Similar pattern of CWC distribution preferring steeper, more erosive canyon walls was documented in submarine canyons of the French and Catalan margin (for *M. oculata* and *D. pertusum*) (Orejas et al., 2009; Fabri et al., 2014; Lastras et al., 2016; Lo Iacono et al., 2018), as well as along the submarine canyons of the Bay of Biscay (van den Beld et al., 2017). Results of the current study additionally provide more fine scale substrata information retrieved from the videos along the vertical walls, highlighting their role in species distribution. For instance, mud-draped vertical walls tend to host the carnivorous ascidian *D. antirrhinum* and sponge species, while biogenic-covered or bare rock vertical walls were more often colonized by CWCs (Figs. 6 and Fig. 8).

CWCs in the Mediterranean Sea are often described associated with LIW water mass (200–600 m depth) (Taviani et al., 2019). This was also the case with some species in the Blanes Canyon, such as *M. oculata*, *D. pertusum* and *L. glaberrima* (Fig. 14). However, in this study we explored deeper (450–1300 m depth) where some species, such as *J. calleti*, *Acanthogorgia* sp., *C. verticillata*, and *A. dichotoma* were found at lower temperatures (<13.4 °C) and salinities (<38.55) (Fig. 14). Thus, our results highlight CWC presence deeper than the LIW core (>600 m) and expand the depth distribution of some CWCs (Fig. 14A), thus emphasising the importance of studying the deeper areas of the Mediterranean Sea (Evans et al., 2016; Sartoretto and Zibrowius, 2018; Taviani et al., 2019; Angeletti et al., 2020; Grinyó et al., 2021).

In this study, nepheloid layers were often found to be within the depth ranges (450–1000 m) of megabenthic assemblages (Fig. 3 and Fig. 6). Bottom and intermediate nepheloid layers were found throughout the canyon, sometimes reaching several hundred meters above seabed, with some differences between study sites (Fig. 3). Formation of nepheloid layers can be challenging to pinpoint to a single mechanism as they are often a result of a complex interplay between local hydrodynamics and seabed topography (Palanques et al., 2005; Zúñiga et al., 2009; Lopez-Fernandez et al., 2013b). In Blanes Canyon, bottom nepheloid layers can be a result of enhanced near-bottom currents during upwelling events (Jorda et al., 2013) and intermediate nepheloid layers can form as detachments from the seabed at canyon rims and shelf break depths, or along a density gradient between LIW and WMDW (600–800 m depth) (Zúñiga et al., 2009) (Fig. 3). These processes can trap POM, zooplankton, and larvae, which are important sources of nutrition for suspension feeders like CWCs (Mienis et al., 2007; Huvenne et al., 2011; Fernandez-Arcaya et al., 2017; Maier et al.,

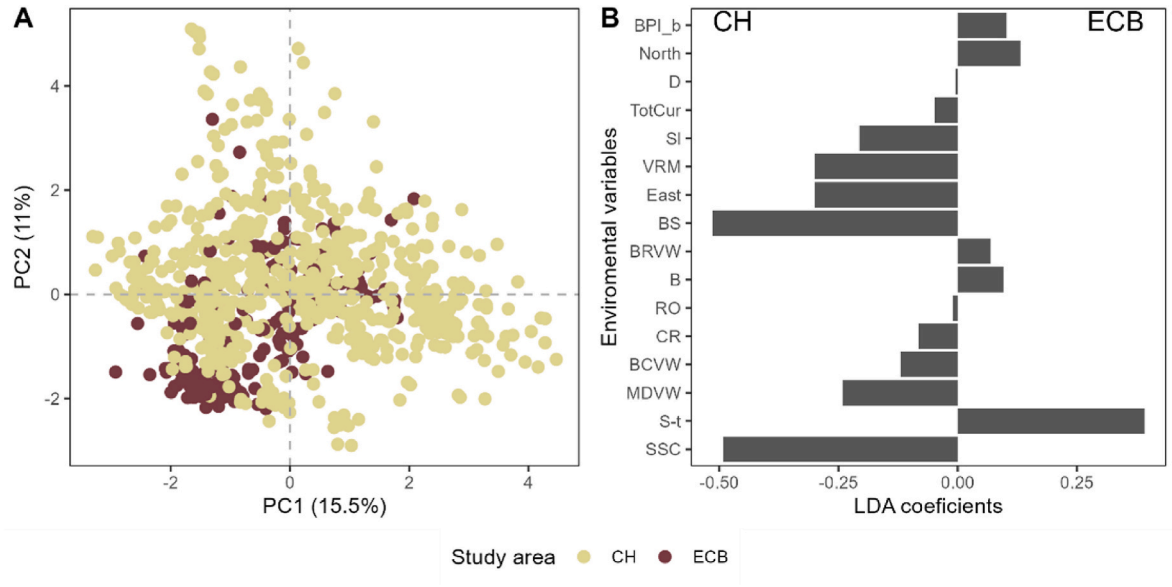

Fig. 9. Differentiation between study areas based on environmental variables: (A) principal component analysis showing SU colored by study area (CH-canyon head; ECB-east canyon branch) (B) linear discriminant analysis coefficients for each environmental variable. Abbreviations for environmental variables in (B) can be found in Table 6.

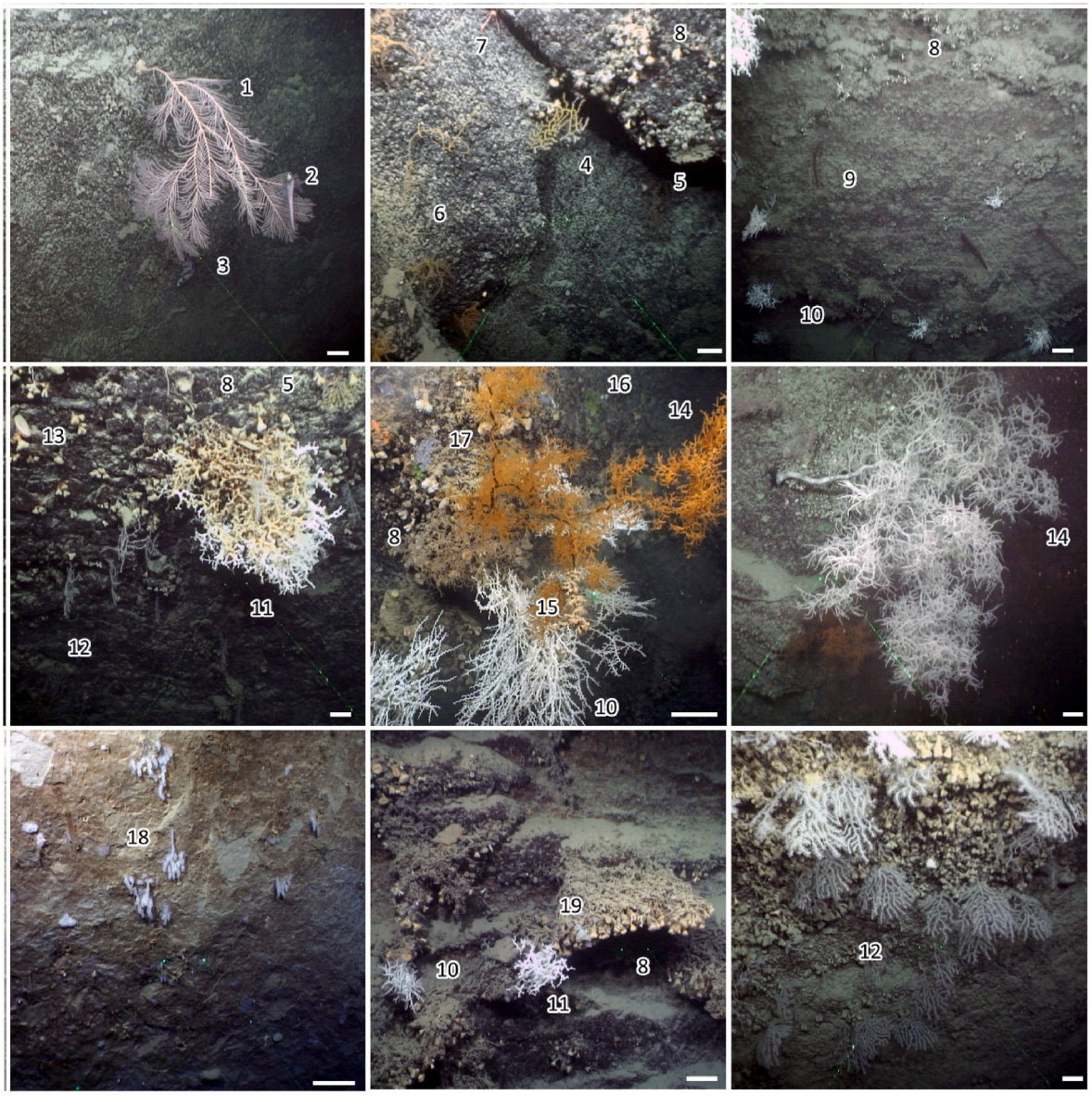

Fig. 10. Selected species from Blanes canyon walls: *Callogorgia verticillata* (1); *Nezumia aequalis* (2); *Lepidion* (3); *Placogorgia coronata* (4), *Acanthogorgia* sp. (5) *Antipathes dichotoma* (6), *Munida* sp. (7), *Desmophyllum dianthus* (8); *Parantipathes* cf. *tetrasticha* (9), *Madrepora oculata* (10), *Desmophyllum pertusum* (11); *Muriceides lepida* (12), *Acesta excavata* (13*), Leiopathes glaberrima* (14), *Epizoanthus* sp.1 (15), *Hexadella* cf. *dedritifera* (16); *Hamacantha falcula* (17), *Tretodictyum reiswigi* (18), *Oopsacas minuta* (19). Scale: 10 cm (white bars).

2023). We sampled POM within 200 m above bottom, at depths that coincided with presence of CWCs, as well as nepheloid layers (Fig. 3 and Fig. 14). In the canyon head, POM was more reactive based on the lower molar C/N (Fig. 4), which can be related to the small distance from the coast (4 km) and local hydrodynamics (enhanced mixing). Interestingly, colonial scleractinian corals (*D. pertusum* and *M. oculata*) were only found in the canyon head (Fig. 11), which might be related to their higher metabolic requirements compared to octocoral and black corals (Fig. 12 and Fig. 13) (Maier et al., 2019, 2023; Rakka et al., 2021; Derviche et al., 2022; Bilan et al., 2023). Additionally, the upper canyon head experiences high energy episodic events, such as eastern winter storms characterized by high current velocities and high turbidity (Sanchez-Vidal et al., 2012; Lopez-Fernandez et al., 2013b). Colonial scleractinian corals are probably better suited to survive these extreme events as they can retract their polyps deep within the calyx, sheltering themselves from high current velocities and large sediment input. The canyon head is also surrounded by fishing grounds, where resuspended sediment from fishing activities settles in the canyon axis (Paradis et al., 2018), but also on the canyon walls and corals, especially colonial scleractinians. Deeper sites in the canyon head (CH03 and one station in CH04) (Fig. 4) were characterized by degraded POM (Fig. 4), based on the molar C/N, which could be due to the retention of nutritive particles by the LIW-WMDW gradient and resuspension of settled particles by the bottom currents (Zúñiga et al., 2009; Jorda et al., 2013). A further potential source can be the fishing ground at study site CH03 (Fig. 17), as fishing grounds have more degraded OM which is resuspended during fishing activity (Kiriakoulakis et al., 2011; Pasqual et al., 2011; Campanyà-Llovet et al., 2018; Paradis et al., 2022). The east canyon branch, which was characterised by degraded POM (Fig. 4), is mainly affected by the along-margin geostrophic current circulation and hemipelagic sedimentation (Ahumada-Sempoal et al., 2013; Jorda et al., 2013), and limited fishing activity (Paradis et al., 2018). At study sites where more degraded POM was found (study sites along the east canyon branch and deep CH04) octocorals and black corals dominated, alongside

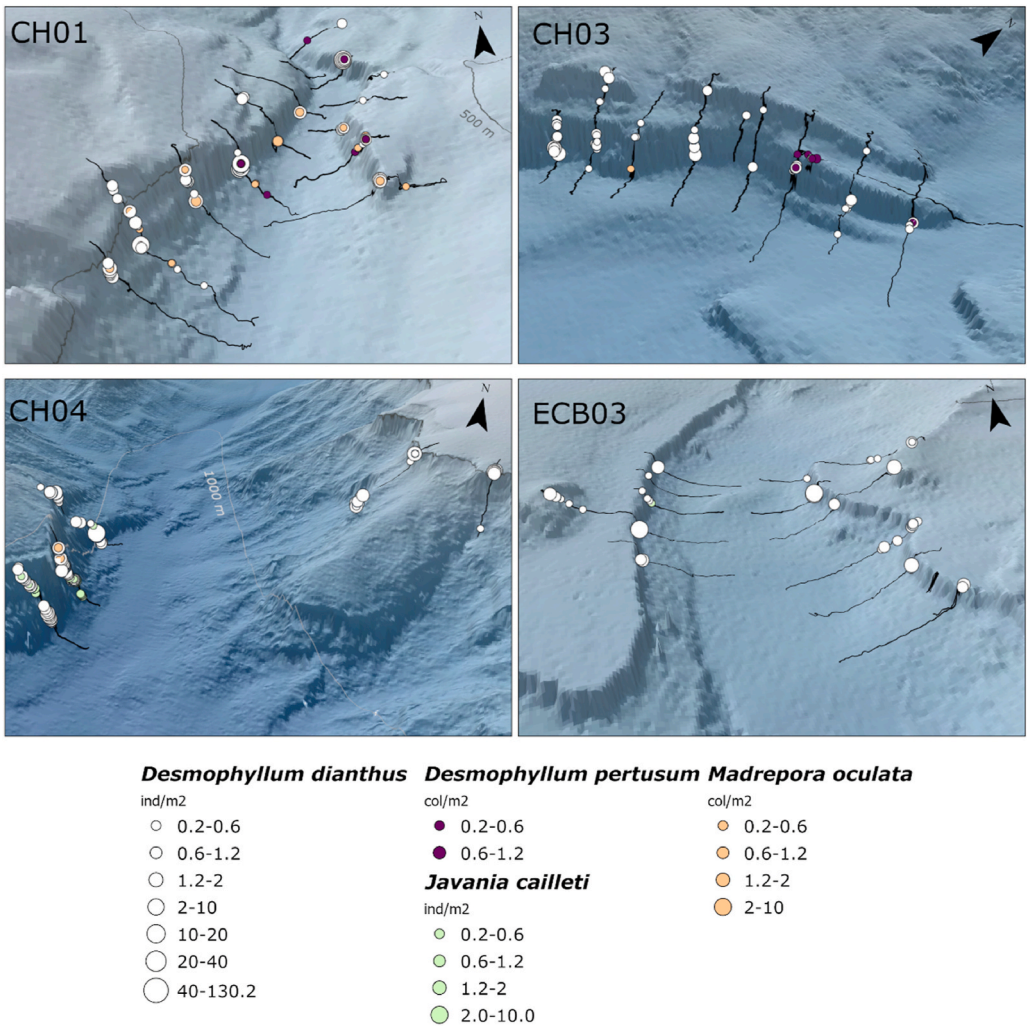

Fig. 11. Spatial distribution and density of scleractinian coral species in Blanes Canyon for selected study sites: CH01, CH03, CH04 and ECH03. Abbreviations: Canyon head (CH); East canyon branch (ECB). The rest of the study sites can be found in Supplementary Material S10.

D. dianthus. However, results from CTD and water samples provide only a snapshot in time in an otherwise dynamic system. Alongside CWCs presence and densities, differences in reproductive strategies, feeding, metabolism, and early life stages of different CWCs should be considered to fully understand their spatial distribution, connectivity and vulnerability.

4.1. Spatial distribution of selected megabenthic species in Blanes Canyon

4.1.1. Frequently encountered species in Blanes Canyon

The most common CWC species in this study was *D. dianthus* which accounted for 72 % of all faunal observations and reaching the highest density of all studied morphospecies (130.2 ind m^{-2}) (Fig. 11). It was found in all study sites, inhabiting a wide range of environmental gradients, including depth, temperature, salinity, and SSC_{exe} (Fig. 14). This species has been frequently recorded along the French and Catalan margin, although no density values were reported (Orejas et al., 2009; Gori et al., 2013; Fabri et al., 2014; Lastras et al., 2016; Dominguez-Carrió et al., 2022). In the Chilean fjords (22–32 m depth) it is found growing downwards, suggested as an avoidance mechanism to high sediment concentrations (Försterra and Häussermann, 2003), which is likely the case of Blanes Canyon population. Its ubiquitous distribution in Blanes Canyon supports its flexibility in terms of ecological and metabolic requirements (Grange et al., 1981; Cairns, 1994; Försterra et al., 2017; Maier et al., 2021; Beck et al., 2022; Bilan et al., 2023). Since this species was occasionally found in very high densities, its framework can resemble the ones built by colonial scleractinian species, which highlights the importance of this species as an ecosystem engineer Fig. 10. Along with *N. zibrowii*, *D. dianthus* was the contributor to the biogenic covered vertical wall substratum type, that was shown to be important for settlement of other CWCs and associated species (Fig. 2). Studies in deeper parts the Corsican margin showcased that *D. dianthus* thanatocoenosis supports high species richness, including crustaceans and sponges (Grinyó et al., 2021).

Two other ubiquitous species were *M. lepida* and *P.* cf. *tetrasticha,* found alongside other CWCs, forming coral gardens, sharing the wide range of environmental gradients, as *D. dianthus* (Fig. 12, Fig. 13, Fig. 14). Several studies in the Mediterranean have observed *M. lepida* in high densities until 550 m depth, such as in the Corsica Channel (Angeletti et al., 2020; Angiolillo et al., 2023) or on the Ligurian seamounts (Bo et al., 2021). To the best of our knowledge, this study extends the depth range of *M. lepida* to 1118 m depth, the deepest record reported in the Mediterranean Sea. Additionally, this is probably the first study in the Mediterranean Sea in which *P.* cf. *tetrasticha* was observed, as most of Mediterranean records are attributed to congeneric species *P. larix* at shallower (100–350 m) depths (Bo et al., 2012b, 2014; Fabri et al., 2014; Moccia et al., 2021). More detailed studies are needed to confirm species identification, which will greatly improve our understanding of Blanes Canyon as a CWC habitat and the distribution of this particular species. Alongside corals, the carnivorous ascidian

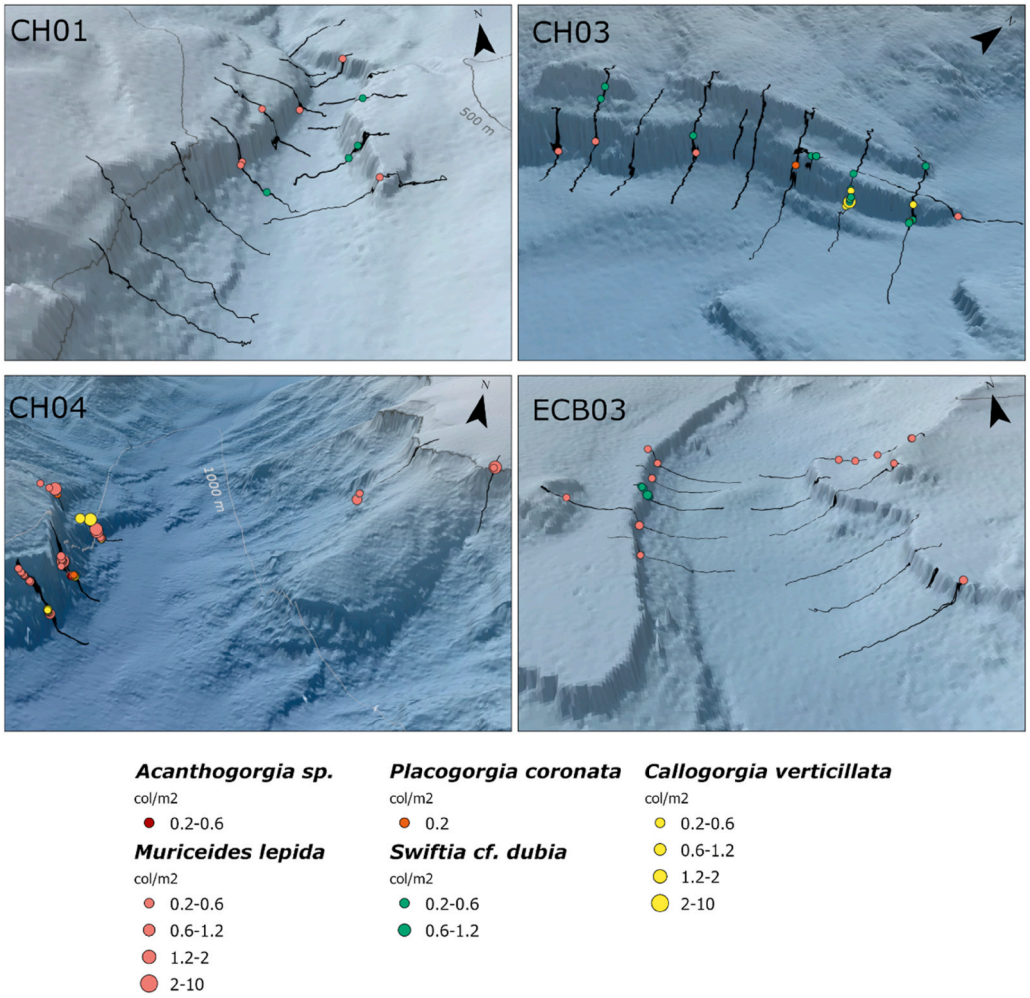

Fig. 12. Spatial distribution and density of octocoral species in Blanes Canyon for selected study sites: CH01, CH03, CH04 and ECH03. Abbreviations: Canyon head (CH); East canyon branch (ECB). The rest of the study sites can be found in Supplementary Material S10.

D. antirrhinum was frequently found along the walls throughout the canyon. It is considered a rare species in the Mediterranean, reported in Palamós (La Fonera) Canyon (5 specimens at ~1100 m depth) (Mecho et al., 2014) and the Aeolian islands (29 specimens at 569–813 m depth) (Mastrototaro et al., 2019), while in this study we recorded 268 specimens at 473–1160 m depth. Additional studies in deeper areas of the Mediterranean Sea might show that this species is in fact not rare, but abundant in non-explored areas.

Among the canyon wall species, we found different morphospecies of sponges. Porifera is a complex phylum, where samples are often required for accurate identification, however they are still amongst the most diverse and abundant associated fauna within and surrounding CWCs, highlighting the role of Mediterranean CWCs as sponge diversity hotspots (Bo et al., 2012a; Bertolino et al., 2019; Santín et al., 2021a). Visually identifiable sponges, *Tretodictyum reiswigi, Poecillastra compressa, Pachastrella monilifera, Sympagella delauzei* and *Oopsacas minuta* (Fig. 10) were found in close relation to CWCs, as reported in submarine canyons of the Catalan margin and the Gulf of Lion (Boury-Esnault et al., 2017; Santín et al., 2018, 2019, 2021a). Previous studies on coral rubble collected from the same area had already highlighted the presence of a diverse poriferan assemblage (confirmed over 60 species) occurring within CWC assemblages in Blanes Canyon (Santín et al., 2020, 2021a, 2021b), which doubles the number of species/morphospecies identified in the present study.

4.1.2. Study site-specific species in Blanes Canyon

Colonial scleractinians (*D. pertusum* and *M. oculata*) were mainly found in the upper canyon head, at higher temperature and salinity values (similar to LIW core) and at the highest SSC values recorded in this study (Figs. 11 and 14). Both species are frequently observed along the canyon heads on the Catalan margin and the canyons of Gulf of Lion, where *M. oculata* is more abundant than *D. pertusum* (Orejas et al., 2009; Gori et al., 2013; Fabri et al., 2014; 2022; Lastras et al., 2016; Lo Iacono et al., 2018). *Madrepora oculata* is more abundant in the Mediterranean Sea, as it thought to better resist higher temperatures (Keller and Os' kina, 2008; Lartaud et al., 2013, 2017) while *D. pertusum* better performs in colder areas such as found in the North Atlantic Ocean (Fosså and Skjoldal, 2009; Naumann et al., 2014). Along the submarine canyons in the Bay of Biscay (Atlantic Ocean) both species are found equally abundant (Khripounoff et al., 2014; Arnaud-Haond et al., 2017; van den Beld et al., 2017). Size distribution of both species in this study showed a population dominated by large colonies. This finding is in accordance with size distributions previously reported for these species in Cap de Creus and Lacaze-Duthiers Canyon, where the same method was used as in this study (Gori et al., 2013). However, Fabri et al. (2022) used a photogrammetric approach to measure colony sizes of *D. pertusum* and *M. oculata* in Lacaze-Duthiers Canyon. That study showed that the population was dominated by smaller colonies (size classes 10–14, 15–19, 20–24 cm), highlighting that larger sample size and photogrammetric approach may provide more accurate estimates of coral sizes. Nevertheless, presence of also small colonies in Blanes Canyon

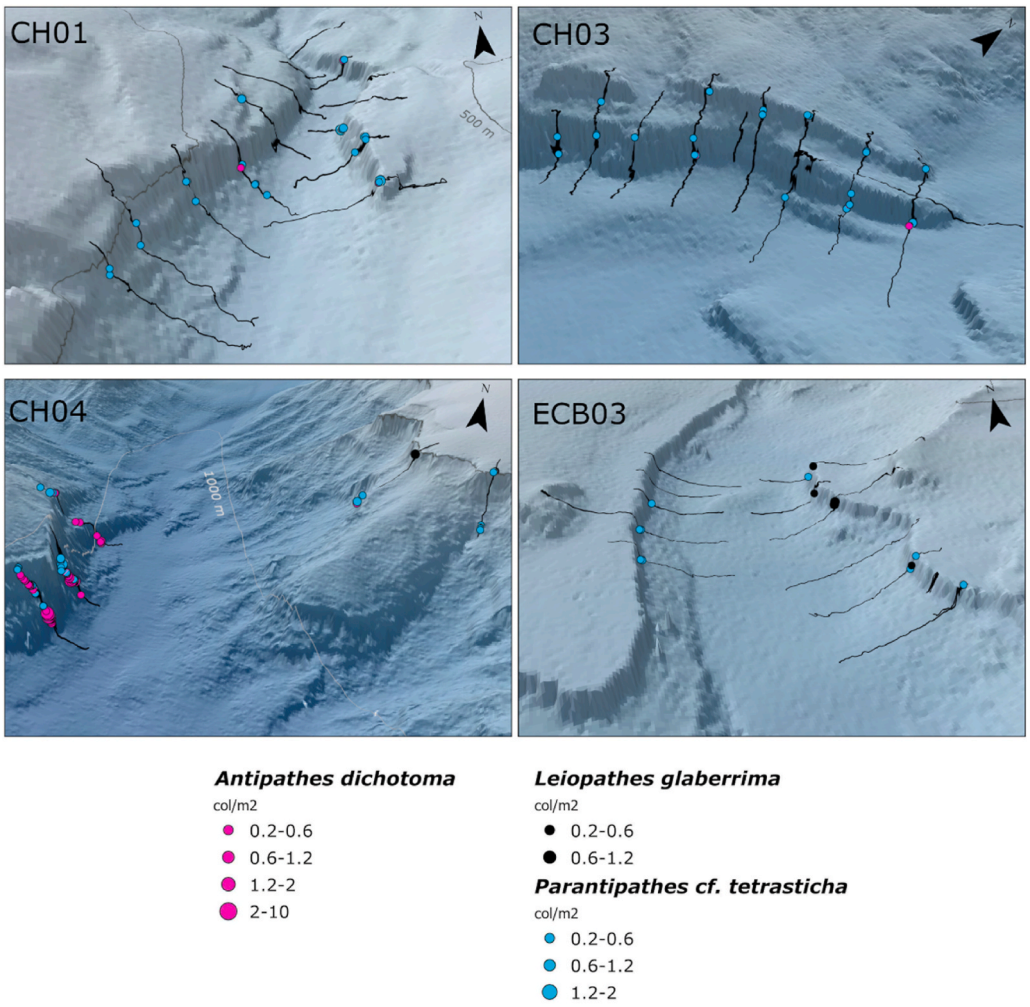

Fig. 13. Spatial distribution and density of antipatharian (black) coral species in Blanes Canyon for selected study sites: CH01, CH03, CH04 and ECH03. Abbreviations: Canyon head (CH); East canyon branch (ECB). The rest of the study sites can be found in Supplementary Material S10.

indicates active recruitment, providing support to the notion that Blanes Canyon is important in maintaining *D. pertusum* populations in the Western Mediterranean Sea (Matos et al., 2024). Colony orientation was recorded, showing that most of the corals were facing downwards, except for the *D. pertusum* found in CH03 where colonies grow on a relatively flat, muddy seabed, facing the prevailing current. On one hand these colonies could be growing from broken pieces delivered from the upper canyon where these species are abundant, or, they can be remains of a more dense patch that was reduced due to repeated fishing at this study site.

Contrary to the upper canyon head, the eastern canyon branch and deeper study sites were dominated by octocorals and black corals, alongside *D. dianthus*, while colonial scleractinians were absent (Figs. 12 and 13). We suggest this spatial distinction is a product of several large scale and occasional processes, characteristics of Blanes Canyon geomorphology and biology of the species. This includes the sediment dynamics where the upper canyon head is likely to receive more resuspended sediment from surrounding fishing grounds, but also fresher POM and likely zooplankton due to smaller distance to shore and enhanced mixing. Hydrodynamics in Blanes Canyon is governed by meandering of the Northern Current through the canyon which can cause local and fine scale differences between study sites as the currents interact with fine scale geomorphological characteristics. Occasional extreme events due to eastern storms can be detrimental for more fragile species, such as black corals and octocorals, which might explain why we find them more frequently in deeper areas and in the east canyon branch. The east canyon branch is characterized by hemipelagic sedimentation processes governed by the along-margin advection of suspended particles by the geostrophic Northern Current (Durán et al., 2013). The implication of a more degraded POM in this area sustaining CWC species with low metabolic rates, such as *L. glaberrima* and *M. lepida* (Bilan et al., 2023), need further research and dedicated studies. Additionally, distribution of species in the canyon is also governed by ecological interactions, such as competition for settlement and food, as well as species specific traits, such as growth.

4.2. Anthropogenic impacts

Trawl marks were only observed at the foot of the western upper canyon axis, at study site CH03 (Fig. 17A), which corresponds to a fishing ground along the canyon axis targeting the deep-sea shrimp *Aristeus antennatus* (Paradis et al., 2018). Bottom trawling causes sediment to be resuspended during fishing activities and transported down canyon, settling along the canyon axis and increasing sedimentation rates (Paradis et al., 2018; Palanques et al., 2024). In this study site (CH03), a few but very large colonies of *D. pertusum* were found on soft bottom (Fig. 15), which might have been an area of more dense coral population, unintentionally decreased during fishing activities in the past. Additionally, *D. pertusum* and *M. oculata* colonies found in the canyon head were covered by mud and showed a predominantly downward orientation (135-180°), while in further offshore canyon environments, the direction of the colonies was more evenly distributed

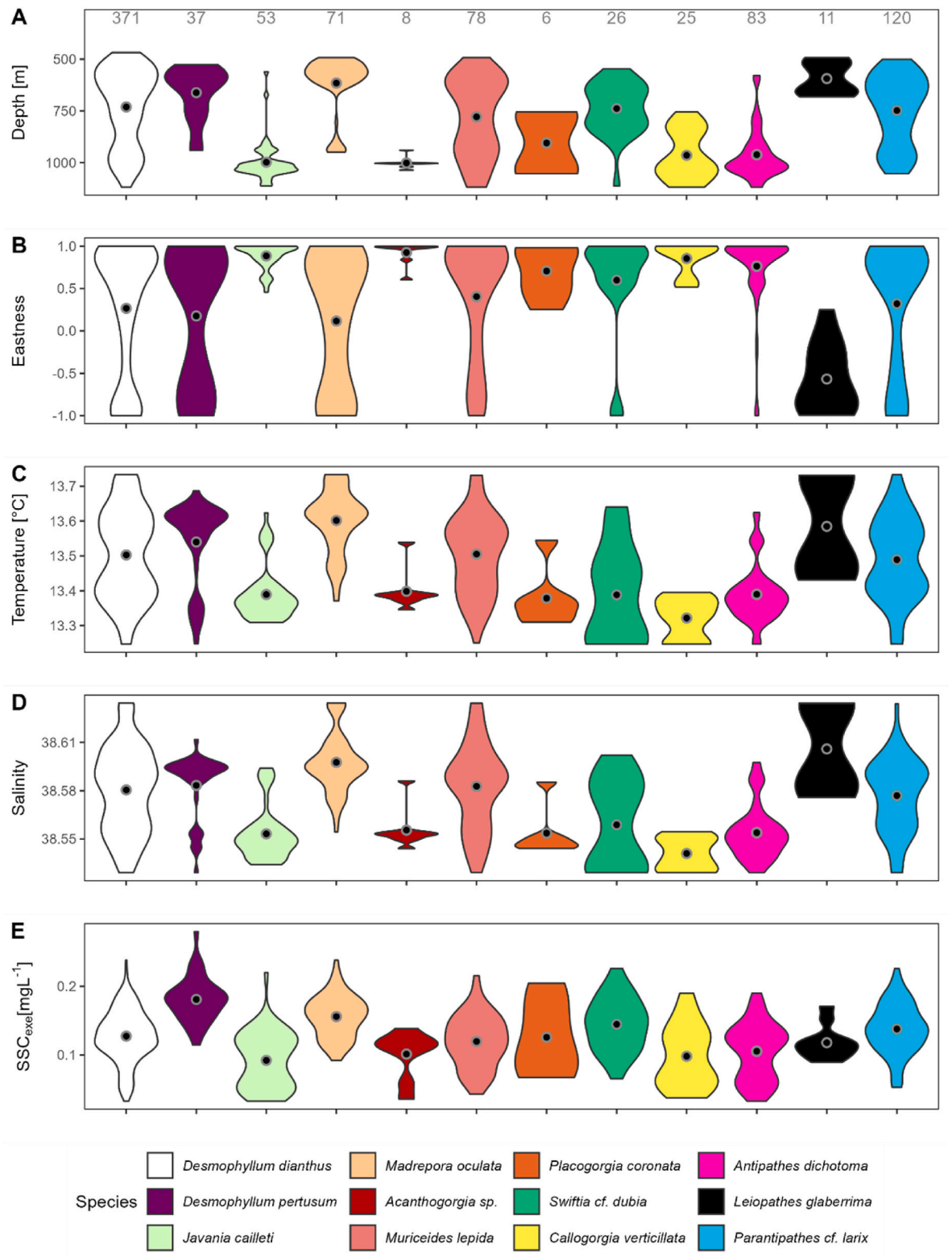

Fig. 14. Coral distribution over selected environmental variables in Blanes Canyon: (A) depth, (B) eastness, (C) temperature, (D) salinity, (E) excess SSC. Numbers grey in (A) are the number of SU used for this figure containing each species. Mean value is represented as a black dot outlined grey, in each violin plot.

between upward (0-90°) and downward orientation (135-180°) (Fig. 16). Colonial scleractinians are the only coral species in Blanes Canyon that have an extensive framework where sediment can settle and cause partial mortality of a colony. Experimental studies showed that when sediment load is too high or too frequent, these corals cannot clean themselves with mucus, which ultimately leads to suffocation (Brooke et al., 2009; Larsson et al., 2013; Bilan et al., 2023). Thus, predominantly downward oriented colonies were also observed in nearby canyons, but at shallower depths, where it was suggested as a compromise between predominant current direction and protection against sediment dumping and/or overload (Gori et al., 2013), which is likely the case for Blanes Canyon populations.

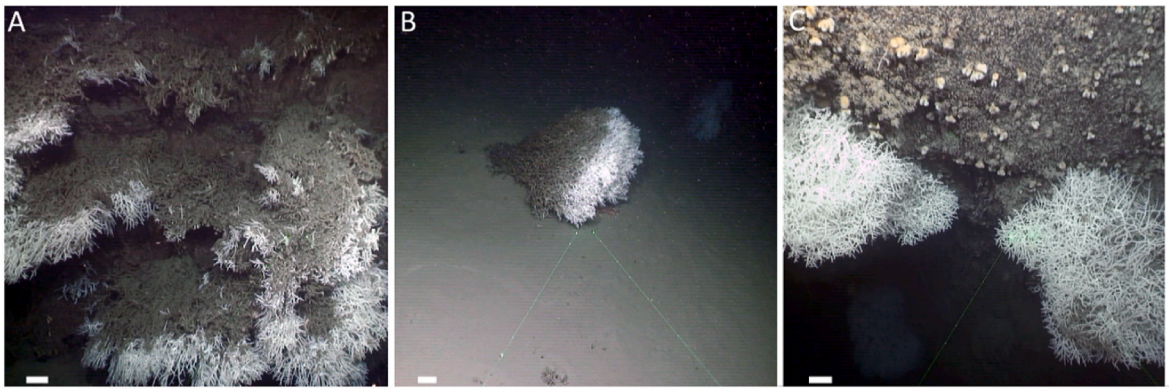

Fig. 15. Colonial scleractinian in Blanes canyon. (A) *Madrepora oculata* colonies from study site CH01, with parts of the colony were heavily covered by sediment and showing an overall downward colony orientation; (B) *Desmophyllum pertusum* at study site CH03 growing on flat muddy substratum, growing the direction of the prevailing current; (C) *Madrepora oculata* colonies growing upwards at study site CH04 canyon wall, with absence of accumulation of sediment on top. Scale: 10 cm (white bars).

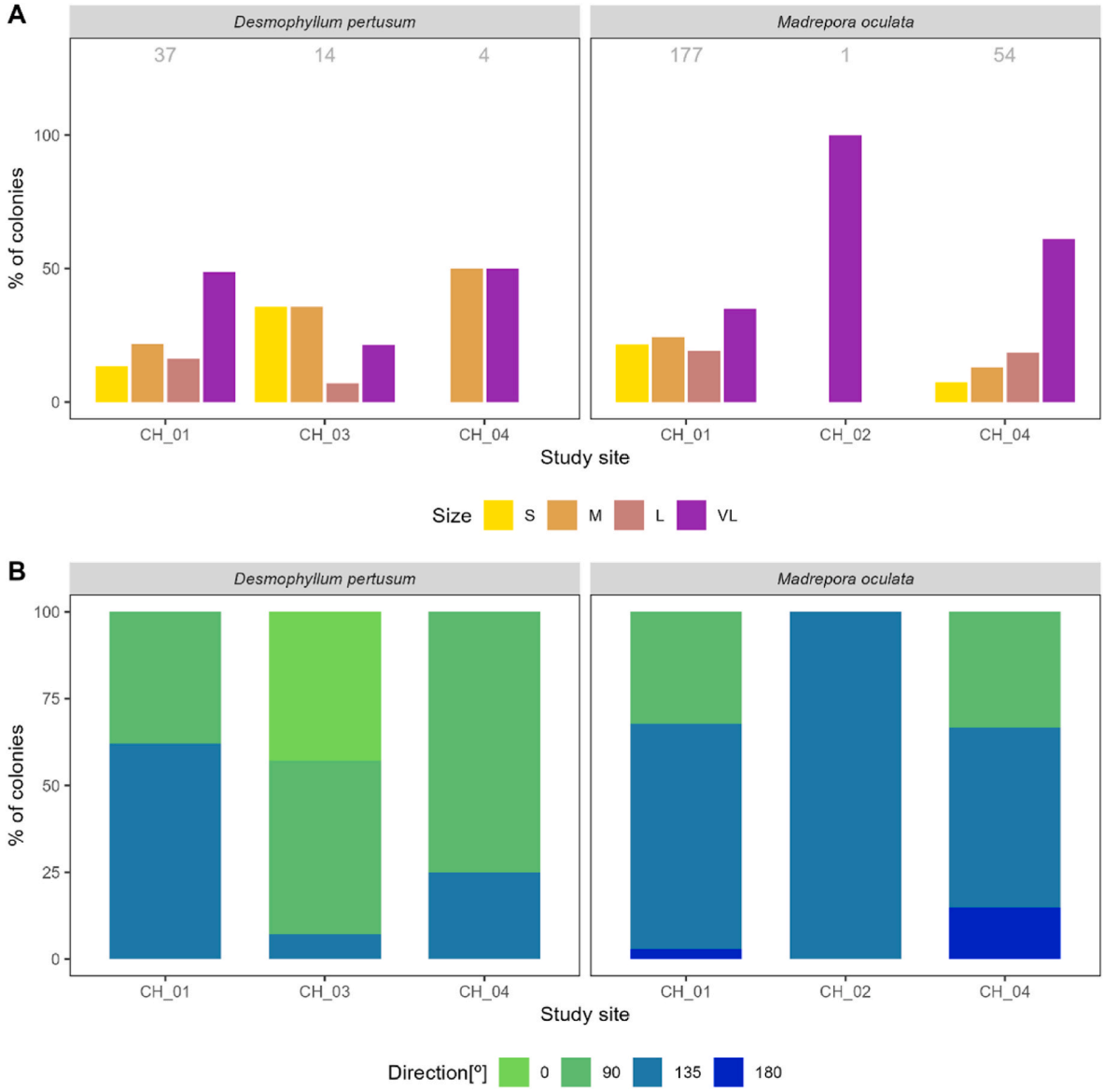

Fig. 16. Colony size and direction for *D. pertusum* and *M. oculata* in study sites in the canyon head of Blanes Canyon: (A) size categories (B) orientation categories. Grey numbers in (A) represent number of colonies measured for size and orientation per study site.

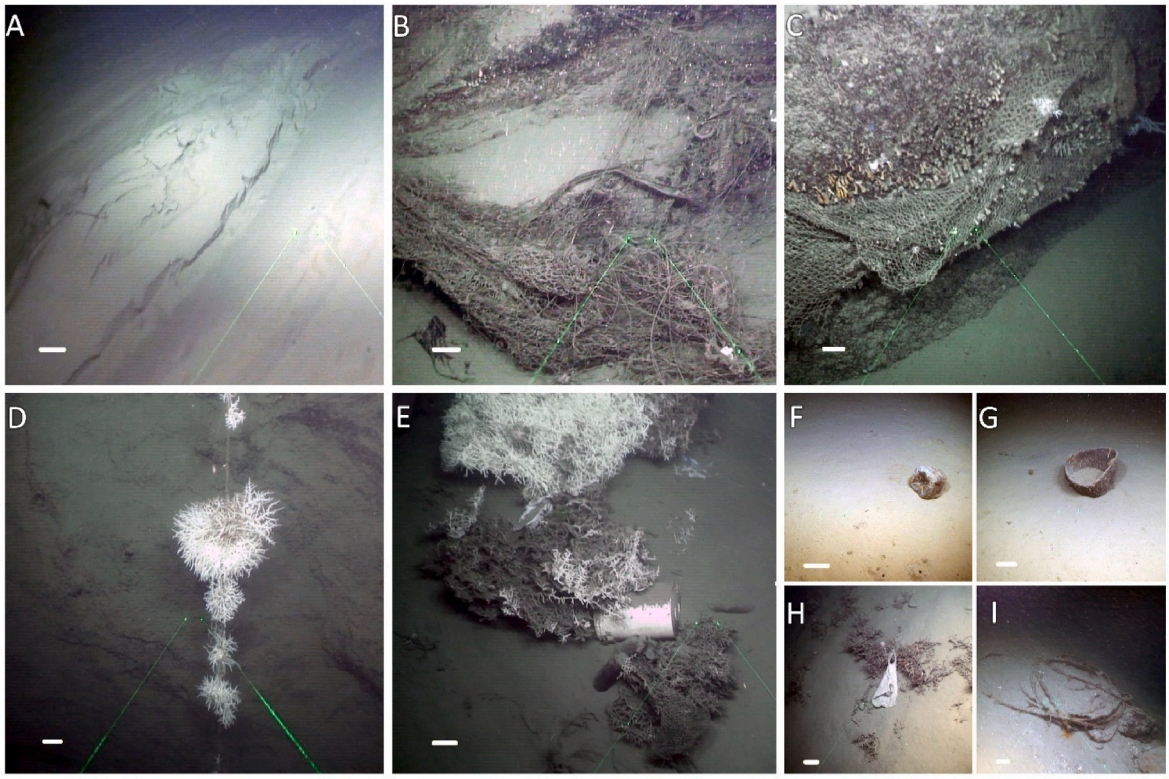

Fig. 17. Anthropogenic impacts found in Blanes Canyon during the current study: (A) Trawl marks, (B) fishing net and fishing lines, (C) fishing net, (D) fishing line with *M. oculata*, (E) mixed items among coral rubble, (F) plastic bottle, (G) bucket, (H) plastic bag, and (I) metal cables. Scale: 10 cm (white bars).

Table 7
Litter categories found in Blanes canyon, showing density, depth and slope and type of interaction with species.

Litter category	Max density [item m^{-2}]	Mean ± SD density [item m^{-2}]	Mean ± SD Depth [m]	Mean ± SD Slope [°]	Type of interaction	Species
A1. Bags	0.4	0.26 ± 0.11	656.09 ± 35.2	11.37 ± 10.36		
A2. Bottles	0.4	0.24 ± 0.09	617.58 ± 56.22	28.01 ± 30.95		
A4. Sheets	0.4	0.21 ± 0.06	665.30 ± 110.53	38.11 ± 22.08		
A5. Other plastic objects	0.2	0.2	671.06 ± 89.37	17.76 ± 14.76		
A6. Fishing nets	1.2	0.32 ± 0.30	599.43 ± 48.81	32.40 ± 22.41	Attachment, Entanglement	*Leptometra celtica, Cidaris cidaris, Desmophyllum pertusum, Madrepora oculata*
A7. Fishing lines	2.0	0.33 ± 0.27	582.97 ± 88.26	44.23 ± 19.44	Attachment	*Desmophyllum dianthus, Gracilechinus acutus, Desmophyllum pertusum, Madrepora oculata, Muriceides lepida, Leiopathes glaberrima, Sympagella delauzei, Tretodictyum reiswigi, Leptometra celtica*
A8. Other fishing related	0.2	0.2	552.15	45.05		
A9. Ropes/ strapping bands	0.2	0.2	573.60 ± 71.94	43.43 ± 18.20		
C1. Beverage cans	0.2	0.2	673.34 ± 37.84	10.77 ± 6.15		
C5. Cables	0.2	0.2	616.71	25.02		
C6. Fishing related	0.2	0.2	522.14 ± 98.37	20.98 ± 19.36		
D1. Bottles	0.2	0.2	552.15	45.05		
E1. Clothing (clothes, shoes)	0.2	0.2	669.59 ± 37.76	19.43 ± 13.95		
E2. Large pieces (carpets, etc.)	0.2	0.2	660.14 ± 69.10	40.38 ± 40.11		
I. Unspecified	0.2	0.2	682.50 ± 122.40	35.96 ± 32.35		

Litter was frequently observed in the canyon, with most found in the CH01 and CH02 study sites. Pham et al. (2014) identified Blanes Canyon as one of the most polluted submarine canyons, where the majority of litter items found on the canyon axis was plastic (Table 7, Fig. 17). However, our results showed that majority of litter belonged to lost fishing gear, including fishing lines and nets entangled in rocky outcrops on the canyon walls. Similar findings are found in studies from the Gulf of Lion and Catalan margin (Orejas et al., 2009; Fabri et al., 2014; Pham et al., 2014; Tubau et al., 2015; Lastras et al., 2016; Santín et al., 2020; Dominguez-Carrió et al., 2020). We also report on entanglement and attachment of megabenthic species, where for some species these are the first records (e.g., *M. lepida, S. delauzei, T. reiswigi*). Using litter as settlement surface has unknown long-term consequences for these organisms. Although they may provide a beneficial position for suspension feeders, it is unknown how long they can support organisms as they grow and potentially more species colonize the surface (Angiolillo et al., 2021; Ragnarsson et al., 2017; Bruemmer et al., 2023). Experimental studies suggest that micro- and macroplastic items can cause disruption in feeding, increased mucus production and decreased growth (Chapron et al., 2018; Mouchi et al., 2019; Pereira et al., 2024). More research is needed on this topic to fully understand the impacts of litter on deep-sea ecosystems, especially in submarine canyons, that due to their topography and hydrodynamics, tend to accumulate litter (Cau et al., 2017; Pierdomenico et al., 2019; Dominguez-Carrió et al., 2020; Hernandez et al., 2022).

4.3. Strengths and limitations of the study

ROV videos and imagery are getting better with advancements in technology, however species identification can be challenging, especially for Porifera (Santín et al., 2021a). One of the limitations of this study is limited sponge species identification and likely underestimation of their diversity in Blanes Canyon. Additionally, stable isotope analysis of coral species in different parts of the canyon could have provided more evidence on their diet and understanding of their spatial distribution. The workflow used for video analysis reduced the number of SU available for megafaunal analysis, which might have provided additional data to support different species distribution in Blanes Canyon. While in this study 55.4 % of all 5 m^2 SU were removed, it is still comparable with studies using the same SU size, where Grinyó et al. (2018) removed 7 % of recorded video, average percentage of not valid SU per transect was 36 % in Enrichetti et al. (2019) and 13 % in Domniguez-Carrió et al. (2022).

One of the main strengths of this study is the detailed spatial and high bathymetric coverage which resulted in broadening of our understanding of several benthic species and determining Blanes Canyon as an important habitat for CWCs. However, offshore and deeper parts of the canyon remain a knowledge gap which should be considered in the future. Additionally, fine scale data on hydrodynamics in the canyon would be beneficial for further discussion on spatial preferences of benthic species.

5. Conclusions

The main result of this study is that Blanes Canyon hosts diverse, extensive, and dense coral gardens on its canyon walls. We identified at least 12 CWC species, carnivorous ascidian and Porifera species as the main contributors to canyon wall assemblages, while the canyon floor assemblages consisted of tube anemones and a burrowing gastropod. However, Blanes Canyon seems to be a CWC dominated canyon, as 79 % of recorded fauna in this study were CWCs. The most abundant and spatially distributed CWC was *D. dianthus*, where it was found to build very dense assemblages (max. 130.2 ind./m^2). Densely packed solitary scleractinian coral areas were recorded providing suitable habitat for other CWC, which grew on top either dead or alive thickets of *D. dianthus* and *N. zibrowii*. Along with *D. dianthus*, *M. lepida* and *P.* cf. *tetrasticha* were the only CWCs to be found throughout the canyon, while other CWCs showed spatial or bathymetric preferences. For example, colonial scleractinian corals (*D. pertusum* and *M. oculata*) were mainly found in the canyon head, while the eastern canyon branch was dominated by *L. glaberrima* and *S.* cf. *dubia.* Different coral gardens emerged along the longest and deepest canyon walls, where in the deepest areas *J. callieti* was abundant, following *C. verticiallata* and *A. dichotoma*. The environmental data collected during this study showed that fine-scale differences in substrata types have an impact on species distribution along the canyon wall; CWCs were found mostly on western canyon wall, which is steeper and more erosive, facing the prevailing geostrophic current; CWCs were found within LIW but also within the depth range of the WMDW, highlighting the importance of exploring deeper areas in the Mediterranean Sea. Finally, bottom and intermediate nepheloid layers may play a significant role in providing POM to suspension feeding organisms on the canyon walls. In addition, this study provides information on the anthropogenic impacts, with trawl tracks found at study site CH03, which corresponds to a known trawling ground that crosses the canyon axis. Fishing lines and fishing nets were the most abundant and frequent litter types, mostly found in the upper canyon head, entangled in coral framework (*D. pertusum* and *M. oculata*) or on rocky outcrops. This study provides a solid baseline on CWCs and other megabenthic species found in Blanes Canyon, which may be helpful in future spatial management of this submarine canyon, as it is not currently included in any legally binding protection framework.

CRediT authorship contribution statement

Meri Bilan: Writing – review & editing, Writing – original draft, Visualization, Methodology, Formal analysis, Data curation, Conceptualization. **Jordi Grinyó:** Writing – review & editing, Visualization, Methodology, Investigation, Conceptualization. **Cecilia Cabrera:** Writing – review & editing, Visualization, Investigation, Data curation. **Andrea Gori:** Writing – review & editing, Writing – original draft, Supervision, Methodology, Conceptualization. **Andreu Santín:** Writing – review & editing, Visualization, Methodology. **Veerle A.I. Huvenne:** Writing – review & editing, Methodology, Investigation. **Marie-Claire Fabri:** Writing – review & editing, Methodology, Investigation. **Marta Arjona-Camas:** Writing – review & editing, Methodology, Investigation. **Sarah Paradis:** Writing – review & editing, Visualization, Methodology, Investigation. **Claudio Lo Iacono:** Writing – review & editing, Investigation. **Stefano Ambroso:** Writing – review & editing, Investigation. **Ruth Durán:** Writing – review & editing, Investigation, Data curation. **Stefano Piraino:** Writing – review & editing, Supervision. **Sergio Rossi:** Writing – review & editing. **Pere Puig:** Writing – review & editing, Writing – original draft, Supervision, Resources, Project administration, Methodology, Investigation, Funding acquisition, Formal analysis, Conceptualization.

Declaration of competing interest

The authors declare that they have no known competing financial interests or personal relationships that could have appeared to influence the work reported in this paper.

Acknowledgements

The authors would like to thank the crew of R/V Sarmiento de Gamboa, crew of ROV Liropus and the scientific team of the ABRIC-1 cruise. Samples were collected and analysed during the ABIDES project (Ref. CTM2015-65142-R) and the ABRIC project (Ref. RTI2018-096434-B-I00), both funded by the Spanish Ministry of Science and Innovation and granted to PP., with the institutional support of the 'Severo Ochoa Centre of Excellence' accreditation (CEX2019-000928-S). V. Huvenne was also funded by the Natural Environment Research Council, through the National Capability programmes CLASS (Grant No

NE/R015953/1) and AtlantiS (Grant No NE/Y005589/1). MB was granted a full Ph.D. fellowship by the University of Salento, Lecce. The authors are grateful to the reviewers for their constructive comments.

Appendix A. Supplementary data

Supplementary data to this article can be found online at https://doi.org/10.1016/j.dsr.2025.104514.

Data availability

Data will be made available on request.

References

Ahumada-Sempoal, M.A., Flexas, M.M., Bernardello, R., Bahamon, N., Cruzado, A., 2013. Northern Current variability and its impact on the Blanes Canyon circulation: a numerical study. Progress in Oceanography, Integrated study of a deep submarine canyon and adjacent open slopes in the Western Mediterranean Sea: an essential habitat 118, 61–70. https://doi.org/10.1016/j.pocean.2013.07.030.

Althaus, F., Williams, A., Schlacher, T.A., Kloser, R.J., Green, M.A., Barker, B.A., Bax, N. J., Brodie, P., Schlacher-Hoenlinger, M.A., 2009. Impacts of bottom trawling on deep-coral ecosystems of seamounts are long-lasting. Mar. Ecol. Prog. Ser. 397, 279–294. https://doi.org/10.3354/meps08248.

Althaus, F., Hill, N., Ferrari, R., Edwards, L., Przeslawski, R., Schönberg, C.H.L., Stuart-Smith, R., Barrett, N., Edgar, G., Colquhoun, J., Tran, M., Jordan, A., Rees, T., Gowlett-Holmes, K., 2015. A standardised vocabulary for identifying benthic biota and substrata from underwater imagery: the CATAMI classification scheme. PLoS One 10, e0141039. https://doi.org/10.1371/journal.pone.0141039.

Angeletti, L., Castellan, G., Montagna, P., Remia, A., Taviani, M., 2020. The "Corsica Channel cold-water coral province" (Mediterranean Sea). Front. Mar. Sci. 7, 661. https://doi.org/10.3389/fmars.2020.00661.

Angiolillo, M., La Mesa, G., Giusti, M., Salvati, E., Di Lorenzo, B., Rossi, L., Canese, S., Tunesi, L., 2021. New records of scleractinian cold-water coral (CWC) assemblages in the southern Tyrrhenian Sea (western Mediterranean Sea): human impacts and conservation prospects. Prog. Oceanogr. 197, 102656. https://doi.org/10.1016/j.pocean.2021.102656.

Angiolillo, M., Bo, M., Toma, M., Giusti, M., Salvati, E., Giova, A., Lagudi, A., Rossi, L., Collina, M., Bruno, F., Canese, S., Tunesi, L., 2023. A baseline for the monitoring of Mediterranean upper bathyal biogenic reefs within the marine strategy framework directive objectives. Deep Sea Res. Oceanogr. Res. Pap. 194, 103963. https://doi.org/10.1016/j.dsr.2023.103963.

Appah, J.K.M., Lim, A., Harris, K., O'Riordan, R., O'Reilly, L., Wheeler, A.J., 2020. Are non-reef habitats as important to benthic diversity and composition as coral reef and rubble habitats in submarine canyons? Analysis of controls on benthic megafauna distribution in the porcupine bank canyon, NE atlantic. Front. Mar. Sci. 7, 571820. https://doi.org/10.3389/fmars.2020.571820.

Arjona-Camas, M., Puig, P., Palanques, A., Emelianov, M., Durán, R., 2019. Evidence of trawling-induced resuspension events in the generation of nepheloid layers in the Foix submarine canyon (NW Mediterranean). J. Mar. Syst. 196, 86–96. https://doi.org/10.1016/J.JMARSYS.2019.05.003.

Arjona-Camas, M., Puig, P., Palanques, A., Durán, R., White, M., Paradis, S., Emelianov, M., 2021. Natural vs. trawling-induced water turbidity and suspended sediment transport variability within the Palamós Canyon (NW Mediterranean). Mar. Geophys. Res. 42. https://doi.org/10.1007/S11001-021-09457-7.

Arnaud-Haond, S., Van den Beld, I.M.J., Becheler, R., Orejas, C., Menot, L., Frank, N., Grehan, A., Bourillet, J.F., 2017. Two "pillars" of cold-water coral reefs along Atlantic European margins: prevalent association of Madrepora oculata with Lophelia pertusa, from reef to colony scale. Deep Sea Research Part II: topical Studies in Oceanography, towards ecosystem based management and monitoring of the deep Mediterranean. North-East Atlantic and Beyond 145, 110–119. https://doi.org/10.1016/j.dsr2.2015.07.013.

Aymà, A., Aguzzi, J., Canals, M., Company, J.B., Lastras, G., Mecho, A., Lo Iacono, C., 2019. 26 occurrence of living cold-water corals at large depths within submarine canyons of the northwestern Mediterranean Sea. In: Orejas, C., Jiménez, C. (Eds.), Mediterranean Cold-Water Corals: Past, Present and Future: Understanding the Deep-Sea Realms of Coral, Coral Reefs of the World. Springer International Publishing, Cham, pp. 271–284. https://doi.org/10.1007/978-3-319-91608-8_26.

Barnes, H., Blackstock, J., 1973. Estimation of lipids in marine animals and tissues: detailed investigation of the sulphophosphovanilun method for 'total' lipids. J. Exp. Mar. Biol. Ecol. 12, 103–118. https://doi.org/10.1016/0022-0981(73)90040-3.

Beck, K.K., Schmidt-Grieb, G.M., Laudien, J., Försterra, G., Häussermann, V., González, H.E., Espinoza, J.P., Richter, C., Wall, M., 2022. Environmental stability and phenotypic plasticity benefit the cold-water coral Desmophyllum dianthus in an acidified fjord. Commun. Biol. 5, 1–12. https://doi.org/10.1038/s42003-022-03622-3.

Bertolino, M., Ricci, S., Canese, S., Cau, A., Bavestrello, G., Pansini, M., Bo, M., 2019. Diversity of the sponge fauna associated with white coral banks from two Sardinian canyons (Mediterranean Sea). J. Mar. Biol. Assoc. U. K. 99, 1735–1751. https://doi.org/10.1017/S0025315419000948.

Bilan, M., Gori, A., Grinyó, J., Biel-Cabanelas, M., Puigcerver-Segarra, X., Santín, A., Piraino, S., Rossi, S., Puig, P., 2023. Vulnerability of six cold-water corals to sediment resuspension from bottom trawling fishing. Mar. Pollut. Bull. 196, 115423. https://doi.org/10.1016/j.marpolbul.2023.115423.

Bo, M., Bertolino, M., Bavestrello, G., Canese, S., Giusti, M., Angiolillo, M., Pansini, M., Taviani, M., 2012a. Role of deep sponge grounds in the Mediterranean Sea: a case study in southern Italy. Hydrobiologia 687, 163–177. https://doi.org/10.1007/s10750-011-0964-1.

Bo, M., Canese, S., Spaggiari, C., Pusceddu, A., Bertolino, M., Angiolillo, M., Giusti, M., Loreto, M.F., Salvati, E., Greco, S., Bavestrello, G., 2012b. Deep coral oases in the south tyrrhenian sea. PLoS One 7, e49870. https://doi.org/10.1371/journal.pone.0049870.

Bo, M., Canese, S., Bavestrello, G., 2014. Discovering mediterranean black coral forests: Parantipathes larix (Anthozoa: Hexacorallia) in the tuscan archipelago, Italy. Ital. J. Zool. 81, 112–125. https://doi.org/10.1080/11250003.2013.859750.

Bo, M., Al Mabruk, S.A., Balistreri, P., Bariche, M., Batjakas, I.E., Betti, F., Bilan, M., Canese, S., Cattaneo-Vietti, R., Corsini-Foka, M., Crocetta, F. New records of rare species in the Mediterranean Sea (October 2020).

Bo, M., Coppari, M., Betti, F., Enrichetti, F., Bertolino, M., Massa, F., Bava, S., Gay, G., Cattaneo-Vietti, R., Bavestrello, G., 2021. The high biodiversity and vulnerability of two Mediterranean bathyal seamounts support the need for creating offshore protected areas. Aquat. Conserv. Mar. Freshw. Ecosyst. 31, 543–566. https://doi.org/10.1002/aqc.3456.

Boury-Esnault, N., Vacelet, J., Dubois, M., Goujard, A., Fourt, M., Perez, T., Chevaldonne, P., 2017. New hexactinellid sponges from deep Mediterranean canyons. Zootaxa 4236, 118–134. https://doi.org/10.11646/zootaxa.4236.1.6.

Brooke, S.D., Holmes, M.W., Young, C.M., 2009. Sediment tolerance of two different morphotypes of the deep-sea coral Lophelia pertusa from the Gulf of Mexico. Mar. Ecol. Prog. Ser. 390, 137–144. https://doi.org/10.3354/meps08191.

Bruemmer, A.L., Dissanayake, A., Davies, J.S., 2023. Marine litter-fauna interactions: a standardised reporting framework and critical review of the current state of research with a focus on submarine canyons. Front. Mar. Sci. 10, 1225114. https://doi.org/10.3389/fmars.2023.1225114.

Cabrera, C., Puig, P., Durán, R., Fabri, M.-C., Guerin, C., Lo Iacono, C., Huvenne, V.A.I., 2024. Geomorphology and evolution of the Blanes Canyon (NW Mediterranean). New insights from high resolution mapping of vertical cliffs. Geomorphology 461, 109290. https://doi.org/10.1016/j.geomorph.2024.109290.

Cairns, S.D., 1994. Scleractinia of the temperate north Pacific. Smithsonian Contrib. Zool. 557. https://doi.org/10.5479/si.00810282.557.i.

Campanyà-Llovet, N., Snelgrove, P.V.R., De Leo, F.C., 2018. Food quantity and quality in Barkley Canyon (NE Pacific) and its influence on macroinfaunal community structure. Progress in Oceanography, Bridging the gap between the shallow and deep oceans: The key role of submarine canyons 169, 106–119. https://doi.org/10.1016/j.pocean.2018.04.003.

Canals, M., Puig, P., Durrieu De Madron, X., Heussner, S., Palanques, A., Joan, F., 2006. Flushing submarine canyons. Nature 444, 354–357. https://doi.org/10.1038/nature05271.

Canals, M., Company, J.B., Martín, D., Sànchez-Vidal, A., Ramírez-Llodrà, E., 2013. Integrated study of Mediterranean deep canyons: Novel results and future challenges. Progress in Oceanography, Integrated study of a deep submarine canyon and adjacent open slopes in the Western Mediterranean Sea: an essential habitat 118, 1–27. https://doi.org/10.1016/j.pocean.2013.09.004.

Cau, A., Alvito, A., Moccia, D., Canese, S., Pusceddu, A., Rita, C., Angiolillo, M., Follesa, M.C., 2017. Submarine canyons along the upper Sardinian slope (Central Western Mediterranean) as repositories for derelict fishing gears. Mar. Pollut. Bull. 123, 357–364. https://doi.org/10.1016/j.marpolbul.2017.09.010.

CBD, 2014. Mediterranean regional workshop to facilitate the description of ecologically or biologically significant marine areas (EBSAs). Convention on Biological Diversity, Málaga, Spain.CBD, 2016. Voluntary Specific Workplan on Biodiversity in Cold Water Areas within the Jurisdictional Scope of the Convention (No. CBD/COP/DEC/XIII/11). Convention on Biological Diversity. Cancun, Mexico. No. UNEP/CBD/EBSA/WS/2014/3/4).

Chapron, L., Peru, E., Engler, A., Ghiglione, J.F., Meistertzheim, A.L., Pruski, A.M., Purser, A., Vétion, G., Galand, P.E., Lartaud, F., 2018. Macro- and microplastics affect cold-water corals growth, feeding and behaviour. Sci. Rep. 8, 15299. https://doi.org/10.1038/s41598-018-33683-6.

Chimienti, G., Bo, M., Taviani, M., Mastrototaro, F., 2019. 19 occurrence and biogeography of mediterranean cold-water corals. In: Orejas, C., Jiménez, C. (Eds.), Mediterranean Cold-Water Corals: Past, Present and Future: Understanding the Deep-Sea Realms of Coral, Coral Reefs of the World. Springer International Publishing, Cham, pp. 213–243. https://doi.org/10.1007/978-3-319-91608-8_19.

Christiansen, S., 2010. Background document for coral gardens. OSPAR Commission.

Ciuffardi, T., Kokkini, Z., Berta, M., Locritani, M., Bordone, A., Delbono, I., Borghini, M., Demarte, M., Ivaldi, R., Pannacciulli, F., 2023. Deep water hydrodynamic observations around a cold-water coral habitat in a submarine canyon in the eastern Ligurian sea (Mediterranean Sea). Earth Syst. Sci. Data Discuss. 1–22. https://doi.org/10.5194/essd-15-1933-2023.

Cleland, J., Kazanidis, G., Roberts, J.M., Ross, S.W., 2021. Distribution of megabenthic communities under contrasting settings in deep-sea cold seeps near Northwest Atlantic canyons. Front. Mar. Sci. 8, 692851. https://doi.org/10.3389/fmars.2021.692851.

Corbera, G., Lo Iacono, C., Gràcia, E., Grinyó, J., Pierdomenico, M., Huvenne, V.A.I., Aguilar, R., Gili, J.M., 2019. Ecological characterisation of a mediterranean cold-water coral reef: cabliers coral mound province (Alboran sea, western mediterranean). Prog. Oceanogr. 175, 245–262. https://doi.org/10.1016/j.pocean.2019.04.010.

Davies, J.S., Howell, K.L., Stewart, H.A., Guinan, J., Golding, N., 2014. Defining biological assemblages (biotopes) of conservation interest in the submarine canyons

of the South West Approaches (offshore United Kingdom) for use in marine habitat mapping. Deep-Sea Res. Part II: Topical Studies in Oceanography, Submarine Canyons: Complex Deep-Sea Environments Unravelled by Multidisciplinary Research 104, 208–229. https://doi.org/10.1016/j.dsr2.2014.02.001.

De Leo, F.C., Puig, P., 2018. Bridging the gap between the shallow and deep oceans: the key role of submarine canyons. Prog. Oceanogr. 169, 1–5. https://doi.org/10.1016/j.pocean.2018.08.006.

De Leo, F.C., Smith, C.R., Rowden, A.A., Bowden, D.A., Clark, M.R., 2010. Submarine canyons: hotspots of benthic biomass and productivity in the deep sea. Proc. Biol. Sci. 277, 2783–2792. https://doi.org/10.1098/rspb.2010.0462.

De Leo, F.C., Vetter, E.W., Smith, C.R., Rowden, A.A., McGranaghan, M., 2014. Spatial scale-dependent habitat heterogeneity influences submarine canyon macrofaunal abundance and diversity off the Main and Northwest Hawaiian Islands. Deep-Sea Res. Part II: Topical Studies in Oceanography, Submarine Canyons: Complex Deep-Sea Environments Unravelled by Multidisciplinary Research 104, 267–290. https://doi.org/10.1016/j.dsr2.2013.06.015.

Derviche, P., Menegotto, A., Lana, P., 2022. Carbon budget trends in octocorals: a literature review with data reassessment and a conceptual framework to understand their resilience to environmental changes. Mar. Biol. 169, 159. https://doi.org/10.1007/s00227-022-04146-4.

Dominguez-Carrió, C., Sanchez-Vidal, A., Estournel, C., Corbera, G., Riera, J.L., Orejas, C., Canals, M., Gili, J.-M., 2020. Seafloor litter sorting in different domains of Cap de Creus continental shelf and submarine canyon (NW Mediterranean Sea). Mar. Pollut. Bull. 161, 111744. https://doi.org/10.1016/j.marpolbul.2020.111744.

Directive, S.F., 2013. Guidance on monitoring of marine litter in European seas. Publications Office, LU. https://publications.jrc.ec.europa.eu/repository/handle/JRC83985.

Dominguez-Carrió, C., Riera, J.L., Robert, K., Zabala, M., Requena, S., Gori, A., Orejas, C., Lo Iacono, C., Estournel, C., Corbera, G., Ambroso, S., Uriz, M.J., López-González, P.J., Sardá, R., Gili, J.M., 2022. Diversity, structure and spatial distribution of megabenthic communities in Cap de Creus continental shelf and submarine canyon (NW Mediterranean). Prog. Oceanogr. 208, 1–28. https://doi.org/10.1016/j.pocean.2022.102877.

Durán, R., Canals, M., Lastras, G., Micallef, A., Amblas, D., Pedrosa-Pàmies, R., Sanz, J.L., 2013. Sediment dynamics and post-glacial evolution of the continental shelf around the Blanes submarine canyon head (NW Mediterranean). Progress in Oceanography, Integrated study of a deep submarine canyon and adjacent open slopes in the Western Mediterranean Sea: an essential habitat 118, 28–46. https://doi.org/10.1016/j.pocean.2013.07.031.

D'Onghia, G., 2019. 30 cold-water corals as shelter, feeding and life-history critical habitats for fish species: ecological interactions and fishing impact. In: Orejas, C., Jiménez, C. (Eds.), Mediterranean Cold-Water Corals: Past, Present and Future: Understanding the Deep-Sea Realms of Coral, Coral Reefs of the World. Springer International Publishing, Cham, pp. 335–356. https://doi.org/10.1007/978-3-319-91608-8_30.

Eigaard, O.R., Bastardie, F., Hintzen, N.T., Buhl-Mortensen, L., Buhl-Mortensen, P., Catarino, R., Dinesen, G.E., Egekvist, J., Fock, H.O., Geitner, K., Gerritsen, H.D., González, M.M., Jonsson, P., Kavadas, S., Laffargue, P., Lundy, M., Gonzalez-Mirelis, G., Nielsen, J.R., Papadopoulou, N., Posen, P.E., Pulcinella, J., Russo, T., Sala, A., Silva, C., Smith, C.J., Vanelslander, B., Rijnsdorp, A.D., 2017. The footprint of bottom trawling in European waters: distribution, intensity, and seabed integrity. ICES (Int. Counc. Explor. Sea) J. Mar. Sci. 74, 847–865. https://doi.org/10.1093/icesjms/fsw194.

Elsler, L.G., Oostdijk, M., Levin, L.A., Satterthwaite, E.V., Pinsky, M.L., Crespo, G.O., Wisz, M.S., 2022. Protecting ocean carbon through biodiversity and climate governance. Front. Mar. Sci. 9, 880424. https://doi.org/10.3389/fmars.2022.880424.

Enrichetti, F., Dominguez-Carrió, C., Toma, M., Bavestrello, G., Betti, F., Canese, S., Bo, M., 2019. Megabenthic communities of the Ligurian deep continental shelf and shelf break (NW Mediterranean Sea). PLoS One 14, e0223949. https://doi.org/10.1371/journal.pone.0223949.

Evans, J., Aguilar, R., Alvarez, H., Borg, J.A., Garcia, S., Knittweis, L., Schembri, P.J., 2016. Recent evidence that the deep sea around Malta is a biodiversity hotspot. Presented at the Congrès de la Commission Internationale pour l'Exploitation Scientifique de la Mer Méditerranée 41, 463.

Evans, J.S., Murphy, M.A., Ram, K., 2021. Package 'spatialEco. ' R CRAN Project.

Fabri, M.-C., Dugornay, O., de la Bernardie, X., Guerin, C., Sanchez, P., Arnaubec, A., Autin, T., Piasco, R., Puig, P., 2022. 3D-Representations for studying deep-sea coral habitats in the Lacaze-Duthiers Canyon, from geological settings to individual specimens. Deep Sea Res. Oceanogr. Res. Pap. 187, 103831. https://doi.org/10.1016/J.DSR.2022.103831.

Fabri, M.-C., Pedel, L., Beuck, L., Galgani, F., Hebbeln, D., Freiwald, A., 2014. Megafauna of vulnerable marine ecosystems in French mediterranean submarine canyons: Spatial distribution and anthropogenic impacts. Deep-Sea Research Part II: Topical Studies in Oceanography, Submarine Canyons: Complex Deep-Sea Environments Unravelled by Multidisciplinary Research 104, 184–207. https://doi.org/10.1016/j.dsr2.2013.06.016.

Fernandez-Arcaya, U., Ramirez-Llodra, E., Aguzzi, J., Allcock, A.L., Davies, J.S., Dissanayake, A., Harris, P., Howell, K., Huvenne, V.A.I., Macmillan-Lawler, M., Martín, J., Menot, L., Nizinski, M., Puig, P., Rowden, A.A., Sanchez, F., Van den Beld, I.M.J., 2017. Ecological role of submarine canyonsand need for canyon conservation: a review. Front. Mar. Sci. 4, 5. https://doi.org/10.3389/fmars.2017.00005.

Flexas, M.M., Boyer, D.L., Espino, M., Puigdefàbregas, J., Rubio, A., Company, J.B., 2008. Circulation over a submarine canyon in the NW Mediterranean. J. Geophys. Res.: Oceans 113, C12. https://doi.org/10.1029/2006JC003998.

Font, J., Garcialadona, E., Gorriz, E., 1994. The seasonality of mesoscale motion in the northern current of the western mediterranean - several years of evidence. Oceanol. Acta 18, 207–219. http://hdl.handle.net/10261/194235.

Food and Agriculture Organization (FAO), 2009. International Guidelines for the Management of Deep-Sea Fisheries in the High Seas. FAO, Rome, Italy.

Food and Agriculture Organization (FAO), 2016. Vulnerable marine ecosystems: processes and practices in the high seas. In: Thompson, A., Sanders, J., Tandstad, M., Carocci, F., Fuller, J. (Eds.), FAO Fisheries and Aquaculture Technical Paper No. 595. Rome, Italy.

Försterra, G., Häussermann, V., 2003. First report on large scleractinian (Cnidaria: anthozoa) accumulations in cold-temperate shallow water of south Chilean fjords. Zool. Verhandel. 345, 117–128.

Försterra, G., Häussermann, V., Laudien, J., 2017. Animal forests in the Chilean fjords: discoveries, perspectives, and threats in shallow and deep waters. In: Rossi, S., Bramanti, L., Gori, A., Orejas, C. (Eds.), Marine Animal Forests: the Ecology of Benthic Biodiversity Hotspots. Springer International Publishing, Cham, pp. 277–313. https://doi.org/10.1007/978-3-319-21012-4_3.

Fosså, J.H., Skjoldal, H.R., 2009. Conservation of cold-water coral reefs in Norway. In: Grafton, R.Q., Hilborn, R., Squires, D., Tait, M., Williams, M. (Eds.), An Evolution towards Scientific Consensus for a Sustainable Ocean Future. npj Ocean Sustainability1, pp. 1–7. https://doi.org/10.1038/s44183-022-00007-1. Handbook of Marine Fisheries and Management. 215-230.Gaill, F., Brodie Rudolph, T., Lebleu, L., Allemand, D., Blasiak, R., Cheung, W.W.L., Claudet, J., Gerhardinger, L.C., Le Bris, N., Levin, L., Pörtner, H.-O., Visbeck, M., Zivian, A., Bahurel, P., Bopp, L., Bowler, C., Chlous, F., Cury, P., Gascuel, D., Goyet, S., Hilmi, N., Ménard, F., Micheli, F., Mullineaux, L., Parmentier, R., Sicre, M.-A., Speich, S., Thébaud, O., Thiele, T., Bowler, M., Charvis, P., Cuvelier, R., Houllier, F., Palazot, S., Staub, F., Poivre d'Arvor, O., 2022.

Gaill, F., Brodie Rudolph, T., Lebleu, L., Allemand, D., Blasiak, R., Cheung, W.W.L., Claudet, J., Gerhardinger, L.C., Le Bris, N., Levin, L., Pörtner, H.-O., Visbeck, M., Zivian, A., Bahurel, P., Bopp, L., Bowler, C., Chlous, F., Cury, P., Gascuel, D., Goyet, S., Hilmi, N., Ménard, F., Micheli, F., Mullineaux, L., Parmentier, R., Sicre, M.-A., Speich, S., Thébaud, O., Thiele, T., Bowler, M., Charvis, P., Cuvelier, R., Houllier, F., Palazot, S., Staub, F., Poivre d'Arvor, O., 2022. An evolution towards scientific consensus for a sustainable ocean future. npj Ocean Sustain. 1, 1–7. https://doi.org/10.1038/s44183-022-00007-1.

General Fisheries Commission for the Mediterranean (GFCM), 2018. Report of the Second Meeting of the Working Groups on Vulnerable Marine Ecosystems (WGVME). FAO, Rome, Italy.

Giusti, M., Canese, S., Fourt, M., Bo, M., Innocenti, C., Goujard, A., Daniel, B., Angeletti, L., Taviani, M., Aquilina, L., Tunesi, L., 2019. Coral forests and derelict fishing gears in submarine canyon systems of the Ligurian Sea. Prog. Oceanogr. 178, 102186. https://doi.org/10.1016/j.pocean.2019.102186.

Gorelli, G., Sardà, F., Company, J.B., 2016. Fishing effort increase and resource status of the deep-sea red shrimp Aristeus antennatus (Risso 1816) in the Northwest Mediterranean Sea since the 1950s. Reviews in Fisheries Science & Aquaculture 24, 192–202. https://doi.org/10.1080/23308249.2015.1119799.

Gori, A., Rossi, S., Berganzo, E., Pretus, J.L., Dale, M.R., Gili, J.-M., 2011. Spatial distribution patterns of the gorgonians eunicella singularis, paramuricea clavata, and Leptogorgia sarmentosa (Cape of Creus, northwestern Mediterranean Sea). Mar. Biol. 158, 143–158. https://doi.org/10.1007/s00227-010-1548-8.

Gori, A., Orejas, C., Madurell, T., Bramanti, L., Martins, M., Quintanilla, E., Marti-Puig, P., Lo Iacono, C., Puig, P., Requena, S., Greenacre, M., Gili, J.M., 2013. Bathymetrical distribution and size structure of cold-water coral populations in the Cap de Creus and Lacaze-Duthiers canyons (northwestern Mediterranean). Biogeosciences 10, 2049–2060. https://doi.org/10.5194/bg-10-2049-2013.

Gori, A., Wienberg, C., Grinyó, J., Taviani, M., Hebbeln, D., Lo Iacono, C., Freiwald, A., Orejas, C., 2023. Life and death of cold-water corals across the Mediterranean Sea. In: Cordes, E., Mienis, F. (Eds.), Cold-Water Coral Reefs of the World. Springer International Publishing, Cham, pp. 171–197. https://doi.org/10.1007/978-3-031-40897-7_7.

Grady, L., Albrecht, J., Beazley, L., Braga Henriques, A., Cárdenas, P., Carreiro-Silva, M., Colaco, A., Fomin, K., Golding, N., Howell, K., Ingels, J., Kazanidis, G., Kenchington, E., Manushyn, I., Menot, L., Metaxas, A., Buhl-Mortensen, P., Olafsdottir, S., Orejas, C., Watling, L., 2020. ICES/NAFO joint working group on deep-water ecology (WGDEC). ICES Scientific Reports. https://doi.org/10.17895/ices.pub.6095.

Grange, K.R., Singleton, R.I., Richardson, J.R., Hill, P.J., Main, W. deL., 1981. Shallow rock-wall biological associations of some southern fiords of New Zealand. N. Z. J. Zool 8, 209–227. https://doi.org/10.1080/03014223.1981.10427963.

Grehan, A., Unnithan, V., Wheeler, A., Monteys, X., Beck, T., Wilson, M., Guinan, J., Foubert, A., Klages, M., 2004. Evidence of major fisheries impact on cold-water corals in the deep waters off the Porcupine Bank, west coast of Ireland: are interim management measures required? 2004 ICES Annual Science Conference, Vigo, Spain. CM 2004/AA:07. https://doi.org/10.17895/ices.pub.25349143.

Grinyó, J., Gori, A., Greenacre, M., Requena, S., Canepa, A., Lo Iacono, C., Ambroso, S., Purroy, A., Gili, J.-M., 2018. Megabenthic assemblages in the continental shelf edge and upper slope of the Menorca Channel, Western Mediterranean Sea. Prog. Oceanogr. 162, 40–51. https://doi.org/10.1016/j.pocean.2018.02.002.

Grinyó, J., Lo Iacono, C., Pierdomenico, M., Conlon, S., Corbera, G., Gràcia, E., 2020. Evidences of human impact on megabenthic assemblages of bathyal sediments in the Alboran Sea (western Mediterranean). Deep Sea Res. Oceanogr. Res. Pap. 165, 103369. https://doi.org/10.1016/j.dsr.2020.103369.

Grinyó, J., Chevaldonné, P., Schohn, T., Le Bris, N., 2021. Megabenthic assemblages on bathyal escarpments off the west Corsican margin (Western Mediterranean). Deep

Sea Res. Oceanogr. Res. Pap. 171, 103475. https://doi.org/10.1016/j.dsr.2021.103475.
Guilloux, E.L., Hall-Spencer, J.M., Söffker, M.K., Olu, K., 2010. Association between the squat lobster Gastroptychus formosus and cold-water corals in the North Atlantic. J. Mar. Biol. Assoc. U. K. 90, 1363–1369. https://doi.org/10.1017/S0025315410000524.
Hall-Spencer, J., Stehfest, K., 2009. Background Document for Lophelia Pertusa Reefs. OSPAR Commission.
Harris, P.T., Baker, E.K., 2020. GeoHab Atlas of seafloor geomorphic features and benthic habitats–synthesis and lessons learned. In: Harris, P.T., Baker, E.K. (Eds.), Seafloor Geomorphology as Benthic Habitat. Elsevier, pp. 969–990. https://doi.org/10.1016/b978-0-12-814960-7.00060-9.
Harris, P.T., Whiteway, T., 2011. Global distribution of large submarine canyons: geomorphic differences between active and passive continental margins. Mar. Geol. 285, 69–86. https://doi.org/10.1016/j.margeo.2011.05.008.
Henry, L.A., Roberts, J., 2017. Global biodiversity in cold-water coral reef ecosystems. In: Rossi, S., Bramanti, L., Gori, A., Orejas, C. (Eds.), Marine Animal Forests. Springer, Cham, pp. 235–256. https://doi.org/10.1007/978-3-319-21012-4_6.
Hernandez, I., Davies, J.S., Huvenne, V.A.I., Dissanayake, A., 2022. Marine litter in submarine canyons: a systematic review and critical synthesis. Front. Mar. Sci. 9, 965612. https://doi.org/10.3389/fmars.2022.965612.
Huvenne, V.A.I., Davies, J.S., 2014. Towards a new and integrated approach to submarine canyon research. Deep-Sea Res. Part II: Topical Studies in Oceanography, Submarine Canyons: Complex Deep-Sea Environments Unravelled by Multidisciplinary Research 104, 1–5. https://doi.org/10.1016/j.dsr2.2013.09.012.
Huvenne, V.A.I., Tyler, P.A., Masson, D.G., Fisher, E.H., Hauton, C., Hühnerbach, V., Bas, T.P., Wolff, G.A., 2011. A picture on the wall: innovative mapping reveals cold-water coral refuge in submarine canyon. PLoS One 6, 1–9. https://doi.org/10.1371/journal.pone.0028755.
Ingels, J., Vanreusel, A., Romano, C., Coenjaerts, J., Mar Flexas, M., Zúñiga, D., Martin, D., 2013. Spatial and temporal infaunal dynamics of the Blanes submarine canyon-slope system (NW Mediterranean); changes in nematode standing stocks, feeding types and gender-life stage ratios. Progress in Oceanography, Integrated study of a deep submarine canyon and adjacent open slopes in the Western Mediterranean Sea: an essential habitat 118, 159–174. https://doi.org/10.1016/j.pocean.2013.07.021.
Jorda, G., Flexas, M.M., Espino, M., Calafat, A., 2013. Deep flow variability in a deeply incised Mediterranean submarine valley (Blanes canyon). Progress in Oceanography, Integrated study of a deep submarine canyon and adjacent open slopes in the Western Mediterranean Sea: an essential habitat 118, 47–60. https://doi.org/10.1016/j.pocean.2013.07.024.
Keller, N.B., Os' kina, N.S., 2008. Habitat temperature ranges of azooxantellate scleractinian corals in the world ocean. Oceanology 48, 77–84. https://doi.org/10.1134/S0001437008010098.
Kelley, D.E., Richards, C., Layton, C., 2022. oce: an R package for Oceanographic Analysis. J. Open Source Softw. 7, 3594. https://doi.org/10.21105/joss.03594.
Khripounoff, A., Caprais, J.C., Le Bruchec, J., Rodier, P., Noel, P., Cathalot, C., 2014. Deep cold-water coral ecosystems in the Brittany submarine canyons (Northeast Atlantic): hydrodynamics, particle supply, respiration, and carbon cycling. Limnol. Oceanogr. 59, 87–98. https://doi.org/10.4319/lo.2014.59.1.0087.
Kiriakoulakis, K., Blackbird, S., Ingels, J., Vanreusel, A., Wolff, G.A., 2011. Organic geochemistry of submarine canyons: the Portuguese Margin. Deep-Sea Res. Part II: Topical Studies in Oceanography, The Geology, Geochemistry, and Biology of Submarine Canyons West of Portugal 58, 2477–2488. https://doi.org/10.1016/j.dsr2.2011.04.010.
Larsson, A.I., van Oevelen, D., Purser, A., Thomsen, L., 2013. Tolerance to long-term exposure of suspended benthic sediments and drill cuttings in the cold-water coral Lophelia pertusa. Mar. Pollut. Bull. 70, 176–188. https://doi.org/10.1016/j.marpolbul.2013.02.033.
Lartaud, F., Pareige, S., de Rafelis, M., Feuillassier, L., Bideau, M., Peru, E., Romans, P., Alcala, F., Le Bris, N., 2013. A new approach for assessing cold-water coral growth in situ using fluorescent calcein staining. Aquat. Living Resour. 26, 187–196. https://doi.org/10.1051/alr/2012029.
Lartaud, F., Meistertzheim, A.L., Peru, E., Le Bris, N., 2017. In situ growth experiments of reef-building cold-water corals: the good, the bad and the ugly. Deep Sea Res. Oceanogr. Res. Pap. 121, 70–78. https://doi.org/10.1016/j.dsr.2017.01.004.
Lastras, G., Canals, M., Amblas, D., Lavoie, C., Church, I., De Mol, B., Duran, R., Calafat, A.M., Hughes-Clarke, J.E., Smith, C.J., Heussner, S., 2011. Understanding sediment dynamics of two large submarine valleys from seafloor data: Blanes and La Fonera canyons, northwestern Mediterranean Sea. Mar. Geol. 280, 20–39. https://doi.org/10.1016/j.margeo.2010.11.005.
Lastras, G., Canals, M., Ballesteros, E., Gili, J.M., Sanchez-Vidal, A., 2016. Cold-water corals and anthropogenic impacts in la Fonera submarine canyon head, Northwestern Mediterranean Sea. PLoS One 11, 1–36. https://doi.org/10.1371/journal.pone.0155729.
Levin, L.A., Cimoli, L., Gjerde, K., Harden-Davies, H., Heimbach, P., LaScala-Gruenewald, D., Pachiadaki, M., Pillar, H.R., Smith, L.M., Stocks, K., 2022. Designing, generating, and translating deep-ocean observations for and with international policy makers. ICES (Int. Counc. Explor. Sea) J. Mar. Sci. 79, 1992–1995. https://doi.org/10.1093/icesjms/fsac143.
Lo Iacono, C., Robert, K., Gonzalez-Villanueva, R., Gori, A., Gili, J.M., Orejas, C., 2018. Predicting cold-water coral distribution in the Cap de Creus Canyon (NW Mediterranean): Implications for marine conservation planning. Progress in Oceanography, Bridging the gap between the shallow and deep oceans: The key role of submarine canyons 169, 169–180. https://doi.org/10.1016/j.pocean.2018.02.012.
Lopez-Fernandez, P., Bianchelli, S., Pusceddu, A., Calafat, A., Danovaro, R., Canals, M., 2013a. Bioavailable compounds in sinking particulate organic matter, Blanes Canyon, NW Mediterranean Sea: effects of a large storm and sea surface biological processes. Progress in Oceanography, Integrated study of a deep submarine canyon and adjacent open slopes in the Western Mediterranean Sea: an essential habitat 118, 108–121. https://doi.org/10.1016/j.pocean.2013.07.022.
Lopez-Fernandez, P., Calafat, A., Sanchez-Vidal, A., Canals, M., Mar Flexas, M., Cateura, J., Company, J.B., 2013b. Multiple drivers of particle fluxes in the Blanes submarine canyon and southern open slope: results of a year round experiment. Progress in Oceanography, Integrated study of a deep submarine canyon and adjacent open slopes in the Western Mediterranean Sea: an essential habitat 118, 95–107. https://doi.org/10.1016/j.pocean.2013.07.029.
Maier, S.R., Bannister, R.J., Oevelen, D. van, Kutti, T., 2019. Seasonal controls on the diet, metabolic activity, tissue reserves and growth of the cold-water coral Lophelia pertusa. Coral Reefs 39, 173–187. https://doi.org/10.1007/S00338-019-01886-6.
Maier, S.R., Jantzen, C., Laudien, J., Häussermann, V., Försterra, G., Cornils, A., Niggemann, J., Dittmar, T., Richter, C., 2021. The carbon and nitrogen budget of Desmophyllum dianthus—a voracious cold-water coral thriving in an acidified Patagonian fjord. PeerJ 9, e12609. https://doi.org/10.7717/peerj.12609.
Maier, S.R., Brooke, S., De Clippele, L.H., de Froe, E., van der Kaaden, A.-S., Kutti, T., Mienis, F., van Oevelen, D., 2023. On the paradox of thriving cold-water coral reefs in the food-limited deep sea. Biol. Rev. 98 (5), 1768–1795. https://doi.org/10.1111/brv.12976.
Martín, J., Puig, P., Masqué, P., Palanques, A., Sánchez-Gómez, A., 2014a. Impact of bottom trawling on deep-sea sediment properties along the flanks of a submarine canyon. PLoS One 9, e104536. https://doi.org/10.1371/journal.pone.0104536.
Martín, J., Puig, P., Palanques, A., Ribó, M., 2014b. Trawling-induced daily sediment resuspension in the flank of a Mediterranean submarine canyon. Deep-Sea Res. Part II: Topical Studies in Oceanography, Submarine Canyons: Complex Deep-Sea Environments Unravelled by Multidisciplinary Research 104, 174–183. https://doi.org/10.1016/j.dsr2.2013.05.036.
Mastrototaro, F., Chimienti, G., Montesanto, F., Perry, A.L., García, S., Alvarez, H., Blanco, J., Aguilar, R., 2019. Finding of the macrophagous deep-sea ascidian dicopia antirrhinum Monniot, 1972 (Chordata: tunicata) in the tyrrhenian sea and updating of its distribution. The European Zoological Journal 86, 181–188. https://doi.org/10.1080/24750263.2019.1616838.
Matos, F.L., Company, J.B., Cunha, M.R., 2021. Mediterranean seascape suitability for Lophelia pertusa: living on the edge. Deep Sea Res. Oceanogr. Res. Pap. 170, 103496. https://doi.org/10.1016/j.dsr.2021.103496.
Matos, F.L., Aguzzi, J., Company, J.B., Cunha, M.R., 2024. Gone with the stream: functional connectivity of a cold-water coral at basin scale. Limnol. Oceanogr. 69, 217–231. https://doi.org/10.1002/lno.12444.
McClain, C.R., Barry, J.P., 2010. Habitat heterogeneity, disturbance, and productivity work in concert to regulate biodiversity in deep submarine canyons. Ecology 91, 964–976. https://doi.org/10.1890/09-0087.1.
Mecho, A., Billett, D.S., Ramírez-Llodra, E., Aguzzi, J., Tyler, P.A., 2014. First records, rediscovery and compilation of deep-sea echinoderms in the middle and lower continental slope of the Mediterranean Sea. Sci. Mar. 78 (2), 281–302. https://doi.org/10.3989/scimar.03983.30C.
Mienis, F., de Stigter, H.C., White, M., Duineveld, G., de Haas, H., van Weering, T.C.E., 2007. Hydrodynamic controls on cold-water coral growth and carbonate-mound development at the SW and SE Rockall Trough Margin, NE Atlantic Ocean. Deep Sea Res. Oceanogr. Res. Pap. 54, 1655–1674. https://doi.org/10.1016/j.dsr.2007.05.013.
Millot, C., 1999. Circulation in the western Mediterranean Sea. J. Mar. Syst. 20, 423–442. https://doi.org/10.1016/S0924-7963(98)00078-5.
Moccia, D., Cau, A., Bramanti, L., Carugati, L., Canese, S., Follesa, M.C., Cannas, R., 2021. Spatial distribution and habitat characterization of marine animal forest assemblages along nine submarine canyons of Eastern Sardinia (central Mediterranean Sea). Deep Sea Res. Oceanogr. Res. Pap. 167, 103422. https://doi.org/10.1016/j.dsr.2020.103422.
Mortensen, P.B., Buhl-Mortensen, L., 2005. Deep-water corals and their habitats in the Gully, a submarine canyon off Atlantic Canada. In: Freiwald, A., Roberts, J.M. (Eds.), Cold-Water Corals and Ecosystems. Erlangen Earth Conference Series. Springer, Berlin, Heidelberg, pp. 247–277. https://doi.org/10.1007/3-540-27673-4_12.
Mouchi, V., Chapron, L., Peru, E., Pruski, A.M., Meistertzheim, A.-L., Vétion, G., Galand, P.E., Lartaud, F., 2019. Long-term aquaria study suggests species-specific responses of two cold-water corals to macro-and microplastics exposure. Environmental Pollution 253, 322–329. https://doi.org/10.1016/j.envpol.2019.07.024.
Naumann, M.S., Orejas, C., Ferrier-Pagès, C., 2014. Species-specific physiological response by the cold-water corals lophelia pertusa and Madrepora oculata to variations within their natural temperature range. Deep-sea research Part II: topical studies in oceanography, biology and geology of deep-sea coral ecosystems. Proceedings of the Fifth International Symposium on Deep Sea Corals 99, 36–41. https://doi.org/10.1016/j.dsr2.2013.05.025.
Oksanen, J., Blanchet, F.G., Friendly, M., Kindt, R., Legendre, P., McGlinn, D., Minchin, P.R., O'Hara, R.B., Simpson, G.L., Solymos, P., 2022. Vegan: community ecology package. R package version 2, 5–7, 2020.
Orejas, C., Jiménez, C. (Eds.), 2019. Mediterranean Cold-Water Corals: Past, Present and Future. Springer.
Orejas, C., Gori, A., Iacono, C.L., Puig, P., Gili, J.-M., Dale, M.R.T., 2009. Cold-water corals in the Cap de Creus canyon, northwestern Mediterranean: spatial distribution, density and anthropogenic impact. Mar. Ecol. Prog. Ser. 397, 37–51. https://doi.org/10.3354/meps08314.

Otero, M.M., Numa, C., Bo, M., Orejas, C., Garrabou, J., Cerrano, C., Kružić, P., Antoniadou, C., Aguilar, R., Kipson, S., Linares, C., Terrón-Sigler, A., Brossard, J., Kersting, D., Casado-Amezúa, P., García, S., Goffredo, S., Ocaña, Ó., Caroselli, E., Maldonado, M., Bavestrello, G., Cattaneo-Vietti, R., 2017. Overview of the conservation status of Mediterranean anthozoans. International Union for Conservation of Nature and Natural Resources. IUCN. https://doi.org/10.2305/IUCN.CH.2017.RA.2.en.

Palanques, A., García-Ladona, E., Gomis, D., Martín, J., Marcos, M., Pascual, A., Puig, P., Gili, J.-M., Emelianov, M., Monserrat, S., 2005. General patterns of circulation, sediment fluxes and ecology of the Palamós (La Fonera) submarine canyon, northwestern Mediterranean. Progress in Oceanography, Mediterranean physical oceanography and biogeochemical cycles: Mediterranean general circulation and climate variability 66, 89–119. https://doi.org/10.1016/j.pocean.2004.07.016.

Palanques, A., Puig, P., Martín, J., Durán, R., Cabrera, C., Paradis, S., 2024. Direct and deferred sediment-transport events and seafloor disturbance induced by trawling in submarine canyons. Sci. Total Environ. 947, 174470. https://doi.org/10.1016/j.scitotenv.2024.174470.

Paradis, S., Puig, P., Sanchez-Vidal, A., Masqué, P., Garcia-Orellana, J., Calafat, A., Canals, M., 2018. Spatial distribution of sedimentation-rate increases in Blanes Canyon caused by technification of bottom trawling fleet. Progress in Oceanography, Bridging the gap between the shallow and deep oceans: The key role of submarine canyons 169, 241–252. https://doi.org/10.1016/j.pocean.2018.07.001.

Paradis, S., Lo Iacono, C., Masqué, P., Puig, P., Palanques, A., Russo, T., 2021. Evidence of large increases in sedimentation rates due to fish trawling in submarine canyons of the Gulf of Palermo (SW Mediterranean). Mar. Pollut. Bull. 172, 112861. https://doi.org/10.1016/j.marpolbul.2021.112861.

Paradis, S., Arjona-Camas, M., Goñi, M., Palanques, A., Masque, P., Puig, P., 2022. Contrasting particle fluxes and composition in a submarine canyon affected by natural sediment transport events and bottom trawling. Front. Mar. Sci. 9, 1017052. https://doi.org/10.3389/fmars.2022.1017052.

Pasqual, C., Lee, C., Goñi, M., Tesi, T., Sanchez-Vidal, A., Calafat, A., Canals, M., Heussner, S., 2011. Use of organic biomarkers to trace the transport of marine and terrigenous organic matter through the southwestern canyons of the Gulf of Lion. Mar. Chem. 126, 1–12. https://doi.org/10.1016/j.marchem.2011.03.001.

Pearman, T.R.R., Robert, K., Callaway, A., Hall, R.A., Mienis, F., Huvenne, V.A.I., 2023. Spatial and temporal environmental heterogeneity induced by internal tides influences faunal patterns on vertical walls within a submarine canyon. Front. Mar. Sci. 10, 1091855. https://doi.org/10.3389/fmars.2023.1091855.

Pedrosa-Pàmies, R., Sanchez-Vidal, A., Calafat, A., Canals, M., Durán, R., 2013. Impact of storm-induced remobilization on grain size distribution and organic carbon content in sediments from the Blanes Canyon area, NW Mediterranean Sea. Progress in Oceanography, Integrated study of a deep submarine canyon and adjacent open slopes in the Western Mediterranean Sea: an essential habitat 118, 122–136. https://doi.org/10.1016/j.pocean.2013.07.023.

Pereira, J.M., Carreiro-Silva, M., Sire de Vilar, A., Godinho, A., Lewis, C., Pham, C.K., 2024. Cold-water octocoral interactions with microplastics under laboratory conditions. Deep Sea Res. Oceanogr. Res. Pap. 213, 104400. https://doi.org/10.1016/j.dsr.2024.104400.

Pham, C.K., Ramirez-Llodra, E., Alt, C.H.S., Amaro, T., Bergmann, M., Canals, M., Company, J.B., Davies, J., Duineveld, G., Galgani, F., Howell, K.L., Huvenne, V.A.I., Isidro, E., Jones, D.O.B., Lastras, G., Morato, T., Gomes-Pereira, J.N., Purser, A., Stewart, H., Tojeira, I., Tubau, X., Van Rooij, D., Tyler, P.A., 2014. Marine litter distribution and density in European seas, from the shelves to deep basins. PLoS One 9, e95839. https://doi.org/10.1371/journal.pone.0095839.

Pierdomenico, M., Cardone, F., Carluccio, A., Casalbore, D., Chiocci, F., Maiorano, P., D'Onghia, G., 2019. Megafauna distribution along active submarine canyons of the central Mediterranean: relationships with environmental variables. Progress in Oceanography, Ecology and functioning of Mediterranean submarine canyons 171, 49–69. https://doi.org/10.1016/j.pocean.2018.12.015.

Poos, M.S., Jackson, D.A., 2012. Addressing the removal of rare species in multivariate bioassessments: the impact of methodological choices. Ecol. Indic. 18, 82–90. https://doi.org/10.1016/j.ecolind.2011.10.008.

Puig, P., Gili, J.-M., 2019. 27 submarine canyons in the mediterranean: a shelter for cold-water corals. In: Orejas, C., Jiménez, C. (Eds.), Mediterranean Cold-Water Corals: Past, Present and Future: Understanding the Deep-Sea Realms of Coral, Coral Reefs of the World. Springer International Publishing, Cham, pp. 285–289. https://doi.org/10.1007/978-3-319-91608-8_27.

Puig, P., Palanques, A., Orange, D.L., Lastras, G., Canals, M., 2008. Dense shelf water cascades and sedimentary furrow formation in the Cap de Creus Canyon, northwestern Mediterranean Sea. Continental Shelf Research, Sediment Dynamics in the Gulf of Lions; the Impact of Extreme Events 28, 2017–2030. https://doi.org/10.1016/j.csr.2008.05.002.

Puig, P., Canals, M., Company, J.B., Martín, J., Amblas, D., Lastras, G., Palanques, A., Calafat, A.M., 2012. Ploughing the deep sea floor. Nature 489, 286–289. https://doi.org/10.1038/nature11410.

Puig, P., Madron, X.D. de, Salat, J., Schroeder, K., Martín, J., Karageorgis, A.P., Palanques, A., Roullier, F., Lopez-Jurado, J.L., Emelianov, M., Moutin, T., Houpert, L., 2013. Thick bottom nepheloid layers in the western Mediterranean generated by deep dense shelf water cascading. Prog. Oceanogr. 111, 1–23. https://doi.org/10.1016/j.pocean.2012.10.003.

Puig, P., Palanques, A., Martín, J., 2014. Contemporary sediment-transport processes in submarine canyons. Ann. Rev. Mar. Sci 6, 53–77. https://doi.org/10.1146/annurev-marine-010213-135037.

Quattrini, A.M., Nizinski, M.S., Chaytor, J.D., Demopoulos, A.W.J., Roark, E.B., France, S.C., Moore, J.A., Heyl, T., Auster, P.J., Kinlan, B., Ruppel, C., Elliott, K.P., Kennedy, B.R.C., Lobecker, E., Skarke, A., Shank, T.M., 2015. Exploration of the canyon-incised continental margin of the northeastern United States reveals dynamic habitats and diverse communities. PLoS One 10, e0139904. https://doi.org/10.1371/journal.pone.0139904.

R Core Team, 2022. R: A Language and Environment for Statistical Computing. R Foundation for Statistical Computing, Vienna, Austria. https://www.R-project.org/.

Ragnarsson, S.Á., Burgos, J.M., Kutti, T., van den Beld, I., Egilsdóttir, H., Arnaud-Haond, S., Grehan, A., 2017. The impact of anthropogenic activity on cold-water corals. In: Rossi, S., Bramanti, L., Gori, A., Orejas, C. (Eds.), Marine Animal Forests: the Ecology of Benthic Biodiversity Hotspots. Springer International Publishing, Cham, pp. 989–1023. https://doi.org/10.1007/978-3-319-21012-4_27.

Rakka, M., Maier, S.R., Van Oevelen, D., Godinho, A., Bilan, M., Orejas, C., Carreiro-Silva, M., 2021. Contrasting metabolic strategies of two co-occurring deep-sea octocorals. Sci. Rep. 11, 1–12. https://doi.org/10.1038/s41598-021-90134-5.

Ramirez-Llodra, E., Company, J.B., Sardà, F., Rotllant, G., 2010. Megabenthic diversity patterns and community structure of the Blanes submarine canyon and adjacent slope in the Northwestern Mediterranean: a human overprint? Mar. Ecol. 31, 167–182. https://doi.org/10.1111/j.1439-0485.2009.00336.x.

Robert, K., Jones, D.O.B., Tyler, P.A., Van Rooij, D., Huvenne, V.A.I., 2015. Finding the hotspots within a biodiversity hotspot: fine-scale biological predictions within a submarine canyon using high-resolution acoustic mapping techniques. Mar. Ecol. 36, 1256–1276. https://doi.org/10.1111/maec.12228.

Robert, K., Jones, D.O.B., Georgiopoulou, A., Huvenne, V.A.I., 2019. Cold-water coral assemblages on vertical walls from the Northeast Atlantic. Divers. Distrib. 26 (3), 284–298. https://doi.org/10.1111/ddi.13011.

Roberts, D.W., Roberts, M.D.W., 2016. Package 'labdsv. ' Ordination and multivariate 775, 1–68.

Román, S., Lins, L., Ingels, J., Romano, C., Martin, D., Vanreusel, A., 2019. Role of spatial scales and environmental drivers in shaping nematode communities in the Blanes Canyon and its adjacent slope. Deep Sea Res. Oceanogr. Res. Pap. 146, 62–78. https://doi.org/10.1016/j.dsr.2019.03.002.

Rueda, J.L., Urra, J., Aguilar, R., Angeletti, L., Bo, M., García-Ruiz, C., González-Duarte, M.M., López, E., Madurell, T., Maldonado, M., Mateo-Ramírez, Á., Megina, C., Moreira, J., Moya, F., Ramalho, L.V., Rosso, A., Sitjà, C., Taviani, M., 2019. 29 cold-water coral associated fauna in the Mediterranean Sea and adjacent areas. In: Orejas, C., Jiménez, C. (Eds.), Mediterranean Cold-Water Corals: Past, Present and Future: Understanding the Deep-Sea Realms of Coral, Coral Reefs of the World. Springer International Publishing, Cham, pp. 295–333. https://doi.org/10.1007/978-3-319-91608-8_29.

Rueda, J.L., Gofas, S., Aguilar, R., de la Torriente, A., García Raso, J.E., Lo Iacono, C., Luque, Á.A., Marina, P., Mateo-Ramírez, Á., Moya-Urbano, E., Moreno, D., Navarro-Barranco, C., Salas, C., Sánchez-Tocino, L., Templado, J., Urra, J., 2021. Benthic fauna of littoral and deep-sea habitats of the alboran sea: a hotspot of biodiversity. In: Báez, J.C., Vázquez, J.T., Camiñas, J.A., Malouli Idrissi, M. (Eds.), Alboran Sea - Ecosystems and Marine Resources. Springer International Publishing, Cham, pp. 285–358. https://doi.org/10.1007/978-3-030-65516-7_9.

Sanchez-Vidal, A., Canals, M., Calafat, A.M., Lastras, G., Pedrosa-Pàmies, R., Menéndez, M., Medina, R., Company, J.B., Hereu, B., Romero, J., Alcoverro, T., 2012. Impacts on the deep-sea ecosystem by a Severe coastal storm. PLoS One 7, e30395. https://doi.org/10.1371/journal.pone.0030395.

Santín, A., Grinyó, J., Ambroso, S., Uriz, M.J., Gori, A., Dominguez-Carrió, C., Gili, J.M., 2018. Sponge assemblages on the deep mediterranean continental shelf and slope (menorca channel, western Mediterranean Sea). Deep Sea Res. Oceanogr. Res. Pap. 131, 75–86. https://doi.org/10.1016/j.dsr.2017.11.003.

Santín, A., Grinyó, J., Ambroso, S., Uriz, M.J., Dominguez-Carrió, C., Gili, J.M., 2019. Distribution patterns and demographic trends of demosponges at the menorca channel (northwestern Mediterranean Sea). Prog. Oceanogr. 173, 9–25. https://doi.org/10.1016/j.pocean.2019.02.002.

Santín, A., Grinyó, J., Bilan, M., Ambroso, S., Puig, P., 2020. First report of the carnivorous sponge Lycopodina hypogea (Cladorhizidae) associated with marine debris, and its possible implications on deep-sea connectivity. Mar. Pollut. Bull. 159, 111501. https://doi.org/10.1016/j.marpolbul.2020.111501.

Santín, A., Grinyó, J., Uriz, M.J., Lo Iacono, C., Gili, J.M., Puig, P., 2021a. Mediterranean coral provinces as a sponge diversity reservoir: is there a mediterranean cold-water coral sponge fauna? Front. Mar. Sci. 8, 662899. https://doi.org/10.3389/fmars.2021.662899.

Santín, A., Uriz, M.-J., Cristobo, J., Xavier, J.R., Ríos, P., 2021b. Unique spicules may confound species differentiation: taxonomy and biogeography of Melonanchora Carter, 1874 and two new related genera (Myxillidae: poecilosclerida) from the Okhotsk Sea. PeerJ 9, e12515. https://doi.org/10.7717/peerj.12515.

Sartoretto, S., Zibrowius, H., 2018. Note on new records of living Scleractinia and Gorgonaria between 1700 and 2200 m depth in the western Mediterranean Sea. Mar. Biodivers. 48, 689–694. https://doi.org/10.1007/s12526-017-0829-6.

Stampar, S.N., Morandini, A.C., Branco, L.C., da Silveira, F.L., Migotto, A.E., 2015. Drifting in the oceans: isarachnanthus nocturnus (Cnidaria, Ceriantharia, Arachnactidae), an anthozoan with an extended planktonic stage. Mar. Biol. 162, 2161–2169. https://doi.org/10.1007/s00227-015-2747-0.

Taviani, M., Freiwald, A., Zibrowius, H., 2005. Deep coral growth in the Mediterranean Sea: an overview. In: Freiwald, A., Roberts, J.M. (Eds.), Cold-Water Corals and Ecosystems. Erlangen Earth Conference Series. Springer, Berlin, Heidelberg, pp. 137–156. https://doi.org/10.1007/3-540-27673-4_7.

Taviani, M., Angeletti, L., Cardone, F., Montagna, P., Danovaro, R., 2019. A unique and threatened deep water coral-bivalve biotope new to the Mediterranean Sea offshore the Naples megalopolis. Sci. Rep. 9, 3411. https://doi.org/10.1038/s41598-019-39655-8.

Tubau, X., Canals, M., Lastras, G., Rayo, X., Rivera, J., Amblas, D., 2015. Marine litter on the floor of deep submarine canyons of the Northwestern Mediterranean Sea: the

role of hydrodynamic processes. Prog. Oceanogr. 134, 379–403. https://doi.org/10.1016/j.pocean.2015.03.013.
Tursi, A., Mastrototaro, F., Matarrese, A., Maiorano, P., D'onghia, G., 2004. Biodiversity of the white coral reefs in the ionian sea (central mediterranean). Chem. Ecol. 20, 107–116. https://doi.org/10.1080/02757540310001629170.
UNGA, 2007. Resolution 61/105 sustainable fisheries, including through the 1995 agreement for the implementation of the provisions of the united nations convention on the law of the sea of 10 december 1982 relating to the conservation and management of straddling fish stocks and highly migratory fish stocks, and related instruments. UNGA A/RES/61/105. https://docs.un.org/en/A/RES/61/105.
van den Beld, I.M.J., Bourillet, J.-F., Arnaud-Haond, S., de Chambure, L., Davies, J.S., Guillaumont, B., Olu, K., Menot, L., 2017. Cold-water coral habitats in submarine canyons of the Bay of Biscay. Front. Mar. Sci. 4, 118. https://doi.org/10.3389/fmars.2017.00118.
Venables, W.N., Ripley, B.D., 2002. Modern Applied Statistics with S, fourth ed. Springer, New York https://www.stats.ox.ac.uk/pub/MASS4/.
Vetter, E.W., Smith, C.R., De Leo, F.C., 2010. Hawaiian hotspots: enhanced megafaunal abundance and diversity in submarine canyons on the oceanic islands of Hawaii. Mar. Ecol. 31, 183–199. https://doi.org/10.1111/j.1439-0485.2009.00351.x.
Wickham, H., 2016. ggplot2: Elegant Graphics for Data Analysis. Springer-Verlag, New York. https://ggplot2.tidyverse.org.
Wilson, M.F.J., O'Connell, B., Brown, C., Guinan, J.C., Grehan, A.J., 2007. Multiscale terrain analysis of multibeam bathymetry data for habitat mapping on the continental slope. Mar. Geod. 30, 3–35. https://doi.org/10.1080/01490410701295962.
Wright, D.J., Lundblad, E.R., Larkin, E.M., Rinehart, R.W., Murphy, J., Cary-Kothera, L., Draganov, K., 2005. ArcGIS Benthic Terrain Modeler. Oregon State University, Corvallis, OR, USA.
Yamamuro, M., Kayanne, H., 1995. Rapid direct determination of organic carbon and nitrogen in carbonate-bearing sediments with a Yanaco MT-5 CHN analyzer. Limnol. Oceanogr. 40, 1001–1005. https://doi.org/10.4319/lo.1995.40.5.1001.
Yentsch, C.S., Menzel, D.W., 1963. A method for the determination of phytoplankton chlorophyll and phaeophytin by fluorescence. Deep Sea Res. Oceanogr. Abstr. 10, 221–231. https://doi.org/10.1016/0011-7471(63)90358-9.
Zabala, M., Maluquer, P., Harmelin, J.-G., 1993. Epibiotic bryozoans on deep-water seleractinian corals from the Catalonia slope (western Mediterranean, Spain, France). Sci. Mar. 57, 65–78. https://hdl.handle.net/2445/32438.
Zeileis, A., Grothendieck, G., 2005. Zoo: S3 Infrastructure for Regular and Irregular Time Series arXiv preprint math/0505527.
Zúñiga, D., Flexas, M.M., Sanchez-Vidal, A., Coenjaerts, J., Calafat, A., Jordà, G., García-Orellana, J., Puigdefàbregas, J., Canals, M., Espino, M., Sardà, F., Company, J.B., 2009. Particle fluxes dynamics in Blanes submarine canyon (Northwestern Mediterranean). Prog. Oceanogr. 82, 239–251. https://doi.org/10.1016/j.pocean.2009.07.002.